



UNIVERSITÉ
CAEN
NORMANDIE



Normandie Université



From transport properties to the nuclear equation of state

An experimental survey in the Fermi energy domain

Olivier LOPEZ (lopezo@lpccaen.in2p3.fr)

*Laboratoire de Physique Corpusculaire de Caen
Normandie Université , ENSICAEN, CNRS/IN2P3*



Outlines

1. From the use of low energy nuclear reactions (dissipative)
2. The nuclear equation of state
 - Phase transitions
 - Empirical parameters
 - Evaluations & uncertainties
3. Panorama of nuclear reactions from B_{coul} up to 100 MeV/nucleon
 - Basic considerations
 - Reaction mechanisms
 - Toward the production of exotic nuclei
4. Path to equilibrium : transport properties in nuclear medium
 - Energy dissipation
 - Isospin transport
5. Improving our knowledge for EOS
6. Experimental tools and some related instrumentation

Motivations

**Why using nuclear reactions
@ low energy ?**

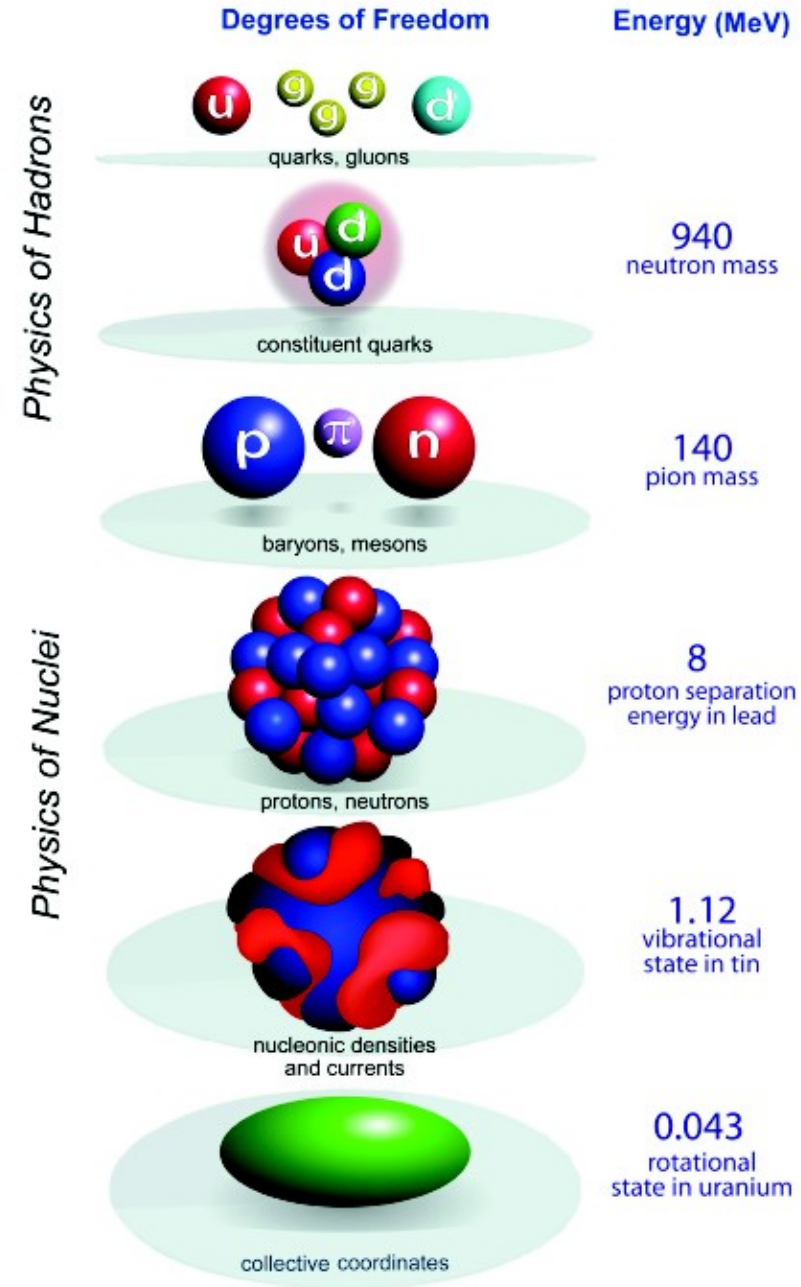
Energy scales in the subatomic world

Depending on scale/energy, systems are described by different **degrees of freedom** and are associated to **different (quasi-)particles**

De Broglie equation (spatial resolution) :

$$\lambda = \hbar / p$$

E_{inc} (MeV)	λ (fm)
1	8
10	1.5
100	0.5



Energy scales in the subatomic world

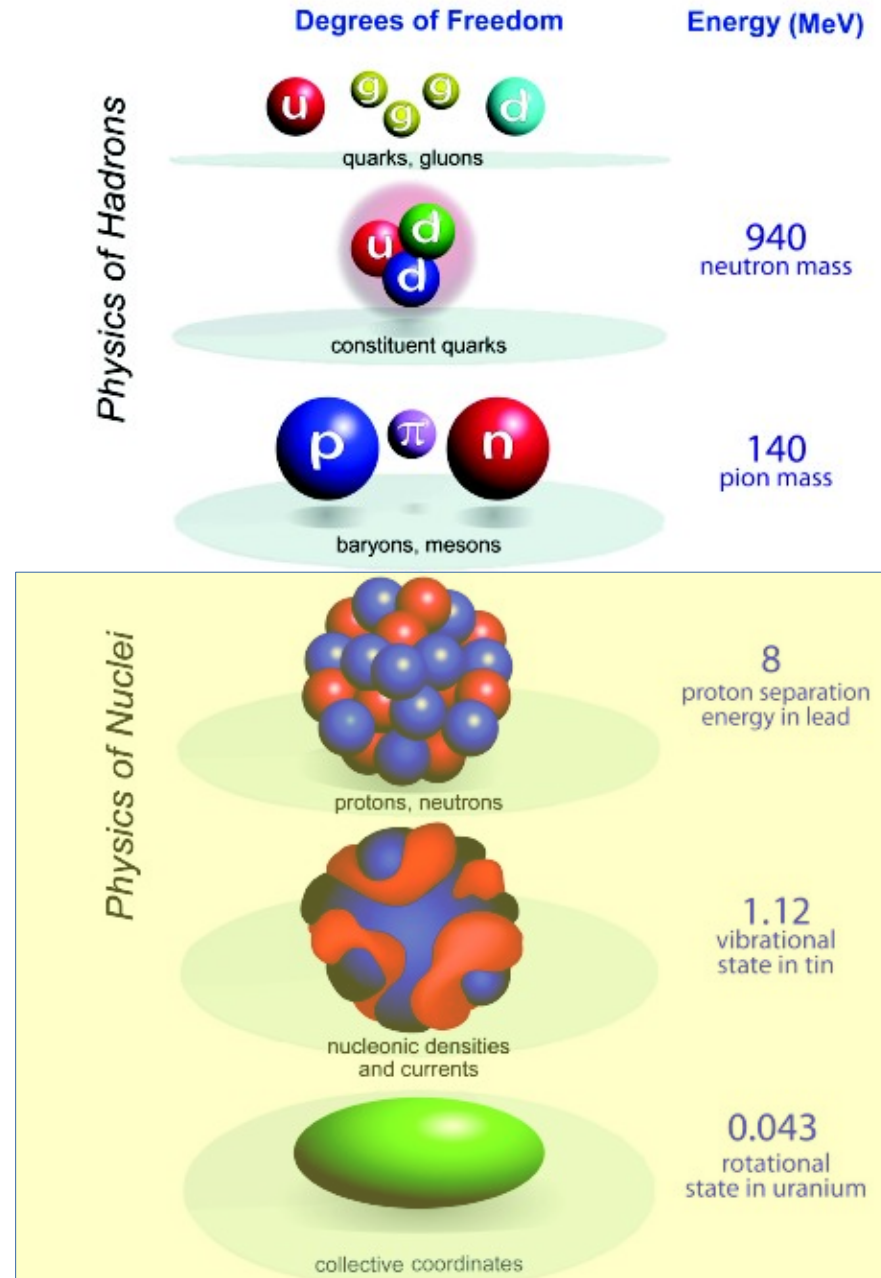
Depending on scale/energy, systems are described by different **degrees of freedom** and are associated to **different phenomena**

Nuclear physics at low E = nuclear degrees of freedom

- nucleus
- collective phenomena
- excited states
- bulk and surface properties in continuum states

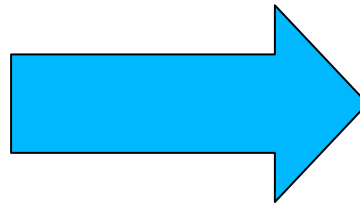
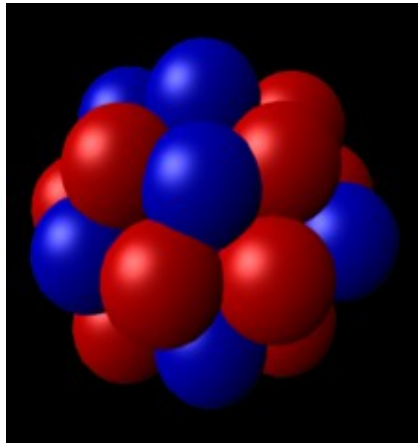
Nuclear reactions

$E_{inc} = 5 - 100 \text{ MeV/nucleon}$



From nuclei to compact stars

nucleus



Supernova / neutron star

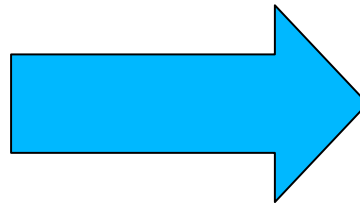
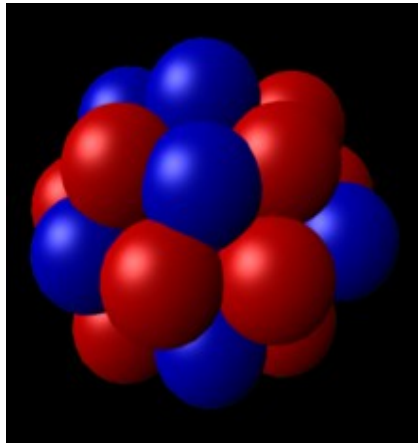


Nucleosynthesis above iron element

From nuclei to compact stars

Under pressure !

nucleus



Supernova / neutron star



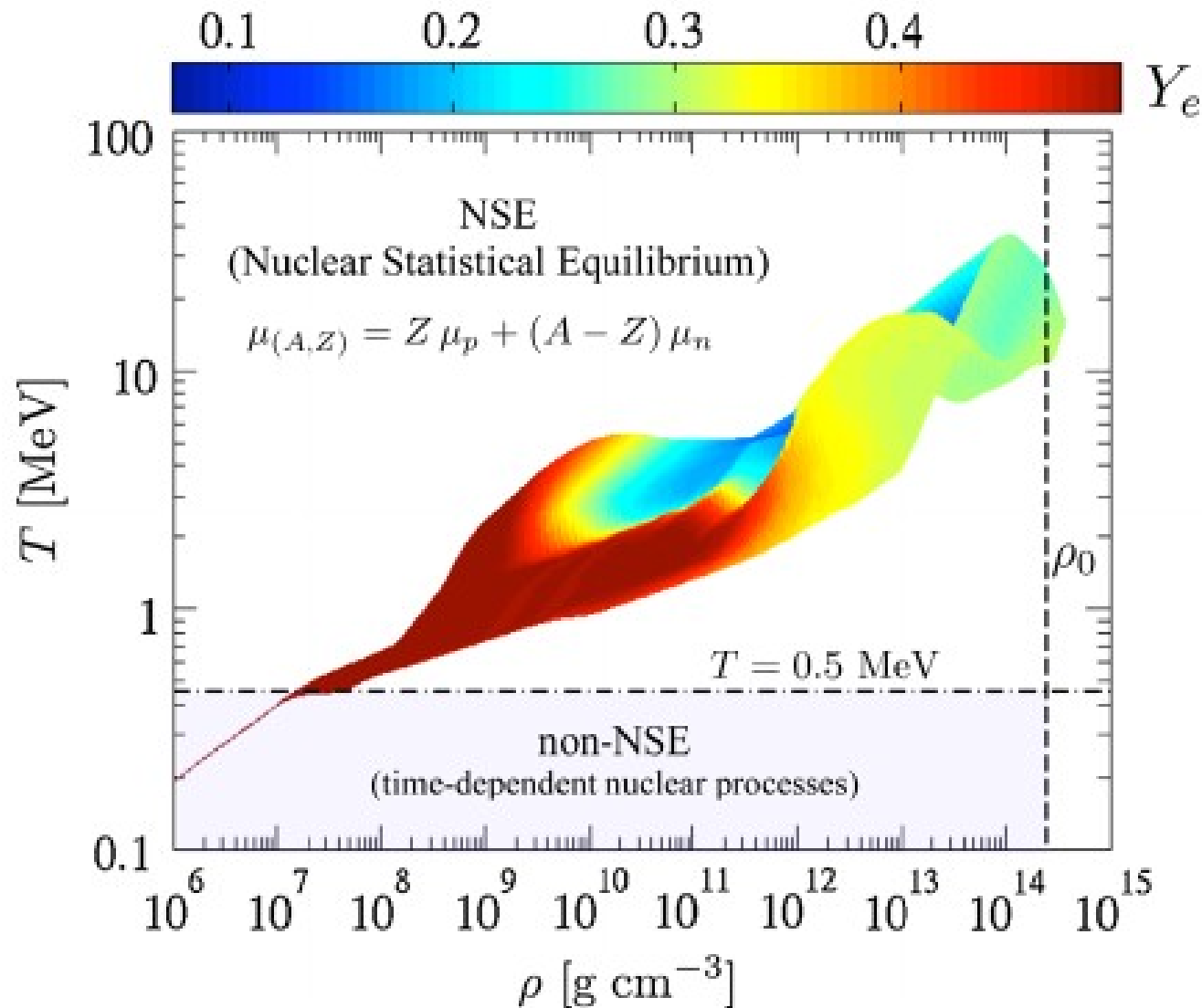
Nucleosynthesis above iron element

Core Collapse of Supernova : x 10,000,000,000 Sun luminosity ...

NS is governed by the nuclear Equation of State $E(\rho, T, \delta)$

Domain in the plane (ρ, T)

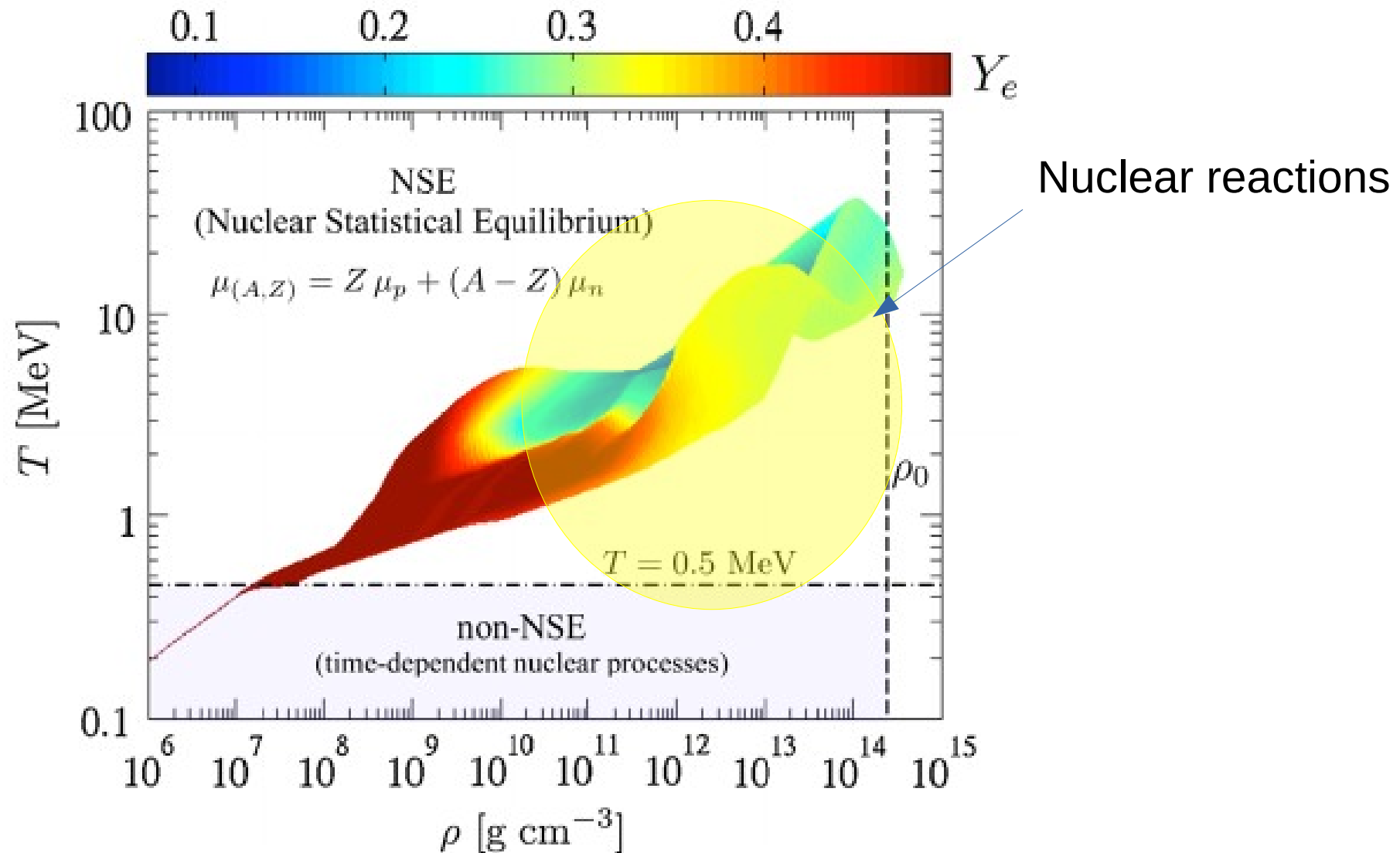
Temperatures and densities reached during a CCSN simulation within 1s post-bounce



M. Oertel *et al.*, Rev. Mod. Phys. 89, Vol. 1 (2017)

Domain in the plane (ρ, T)

Temperatures and densities reached during a CCSN simulation within 1s post-bounce



M. Oertel *et al.*, Rev. Mod. Phys. 89, Vol. 1 (2017)

(Some of the) Key questions in LE Nuclear Physics

How can we build the atomic nucleus starting from **QCD first principles** and the strong interaction?

Effective interactions and ab-initio models

Nucleus as a **many-body quantum system** : how can we explain and predict the **observed regularities** : magic numbers, collective excitations (GR), deformation, pairing, ...?

(No core) shell model and approaches beyond the Mean-Field

How can we describe nuclear matter at very different scales as in nuclei (microscopic) and in compact stars and binary NS mergers (macroscopic)?

Equation of State of nuclear matter / phase transitions



The nuclear Equation of state

Equation of State of nuclear matter

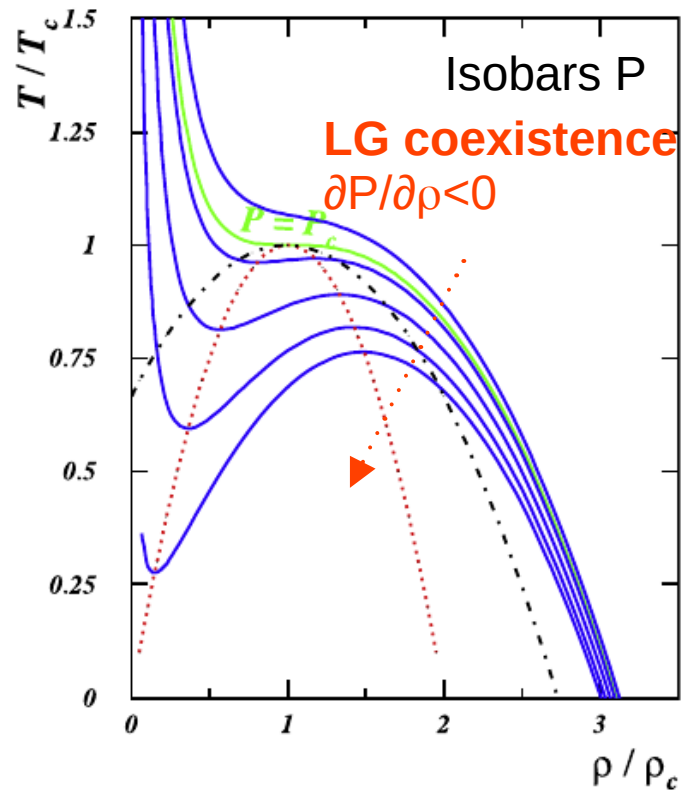
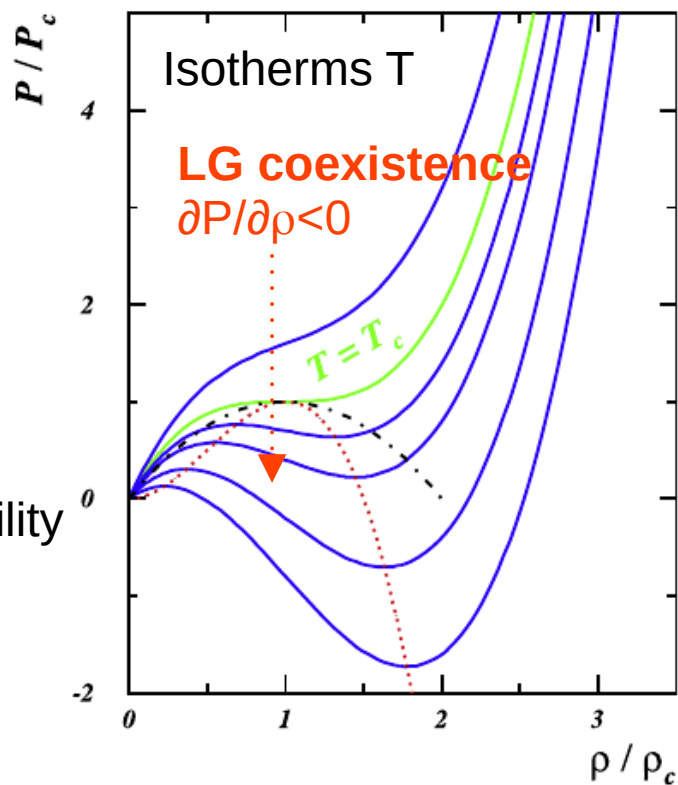
$$E \text{ (or } P) = f(\rho, T, \delta)$$

Thermodynamical relation between state variables

Equation of State of nuclear matter

$$E \text{ (or } P) = f(\rho, T, \delta)$$

Thermodynamical relation between state variables



Skyrme HF
at finite T

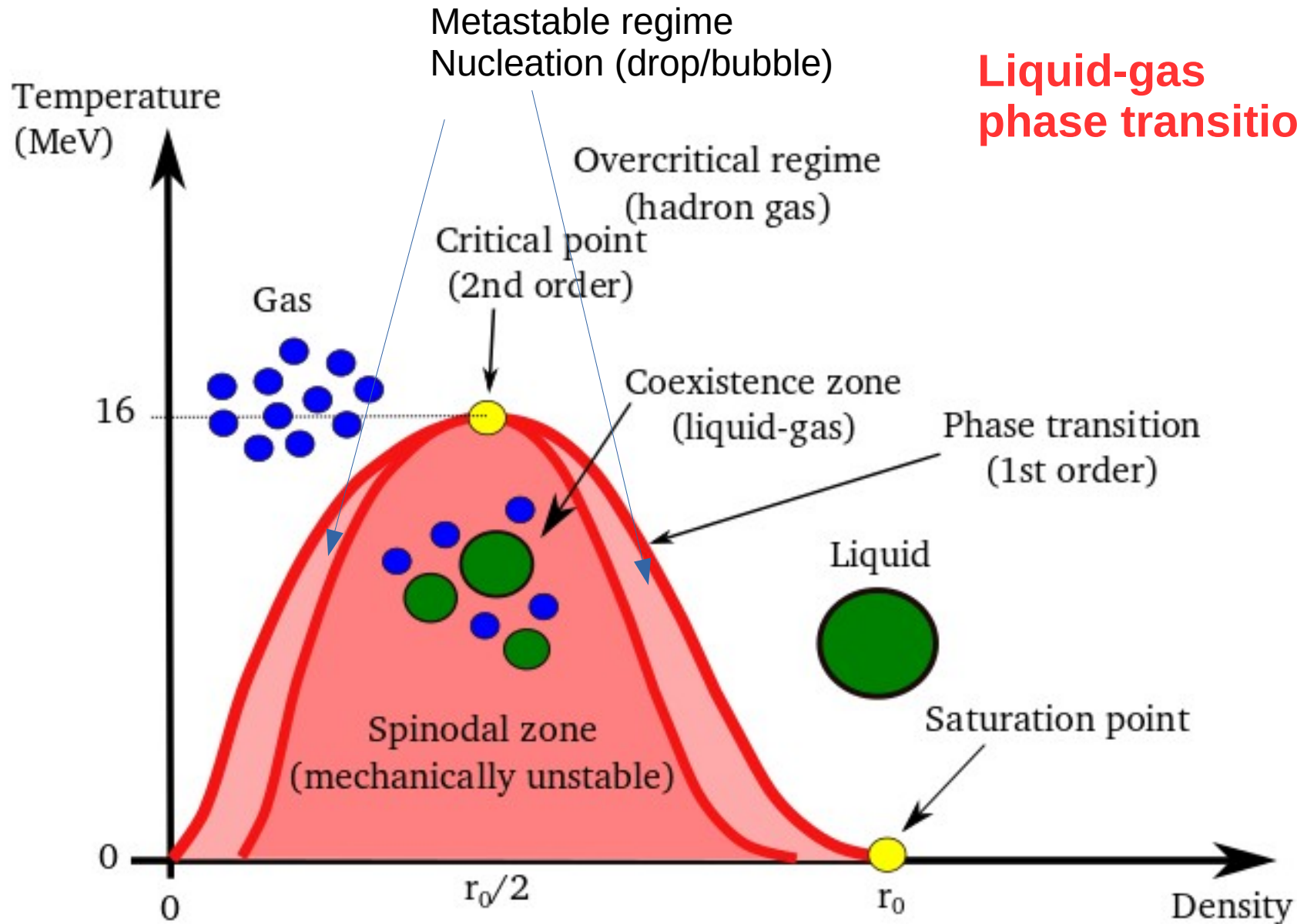
B. Borderie,
J. Phys. G:
Nucl. Part.
Phys. 28 (2002)
R217

Pressure : $P(\rho) = \rho^2 (\partial E/\partial \rho)_\rho$

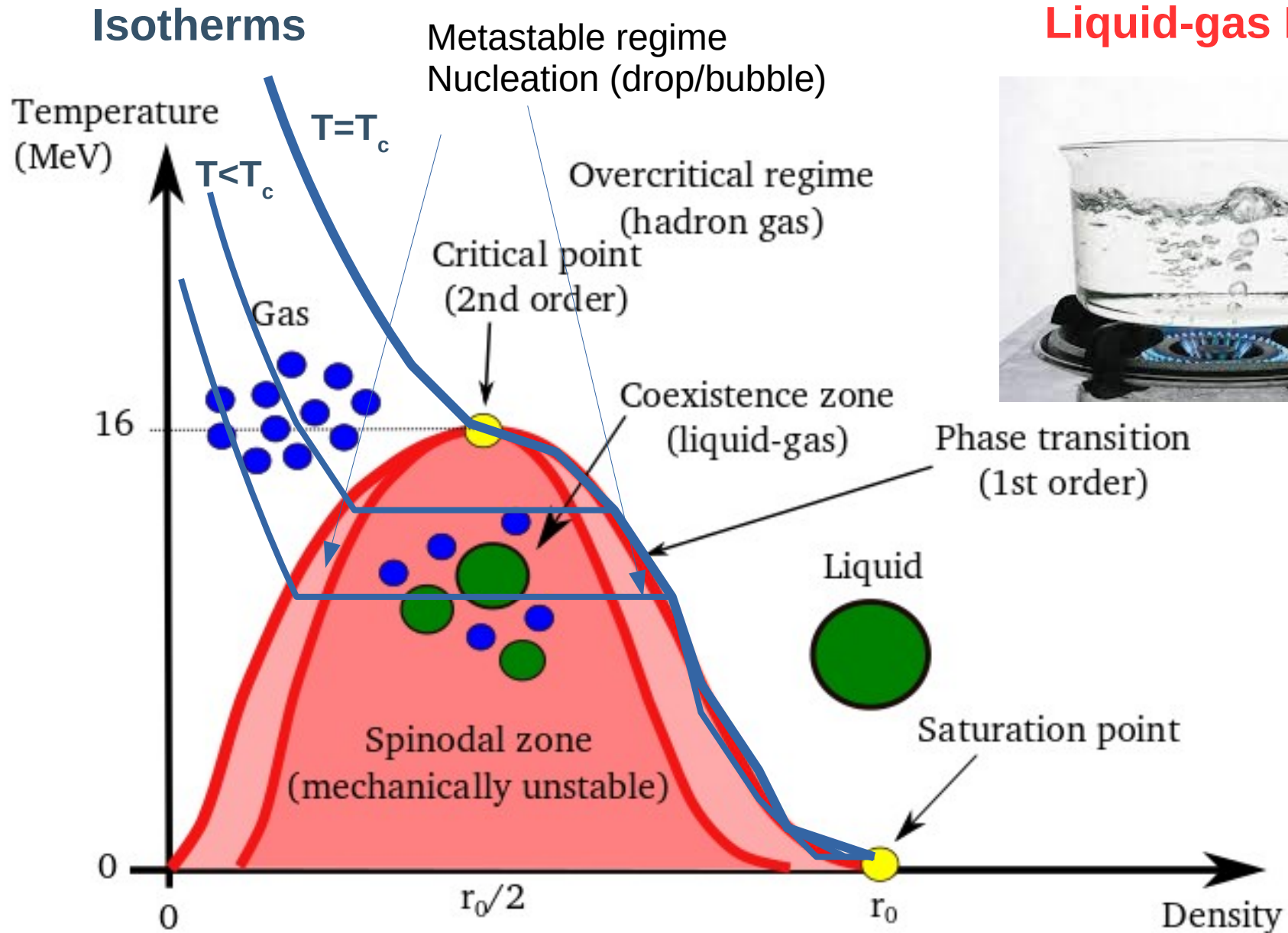
P_c, T_c, ρ_c : **critical point** of the liquid-gas phase transition with $T_c = 16-18 \text{ MeV}$, $\rho_c = 0.3-0.5 \rho_{sat}$

Spinodal decomposition : Mean-Field instabilities

Liquid-gas
phase transition



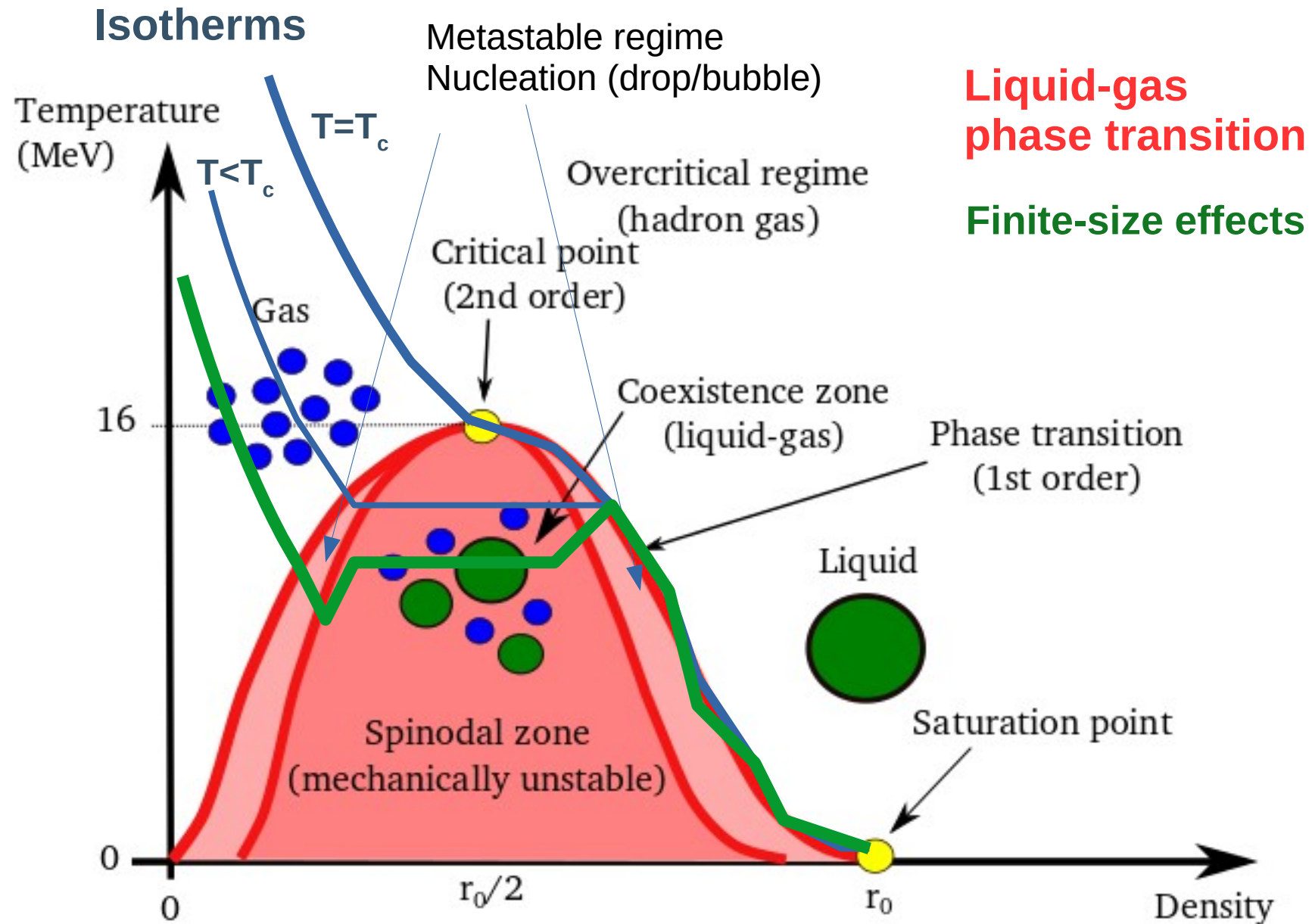
Spinodal decomposition : Mean-Field instabilities



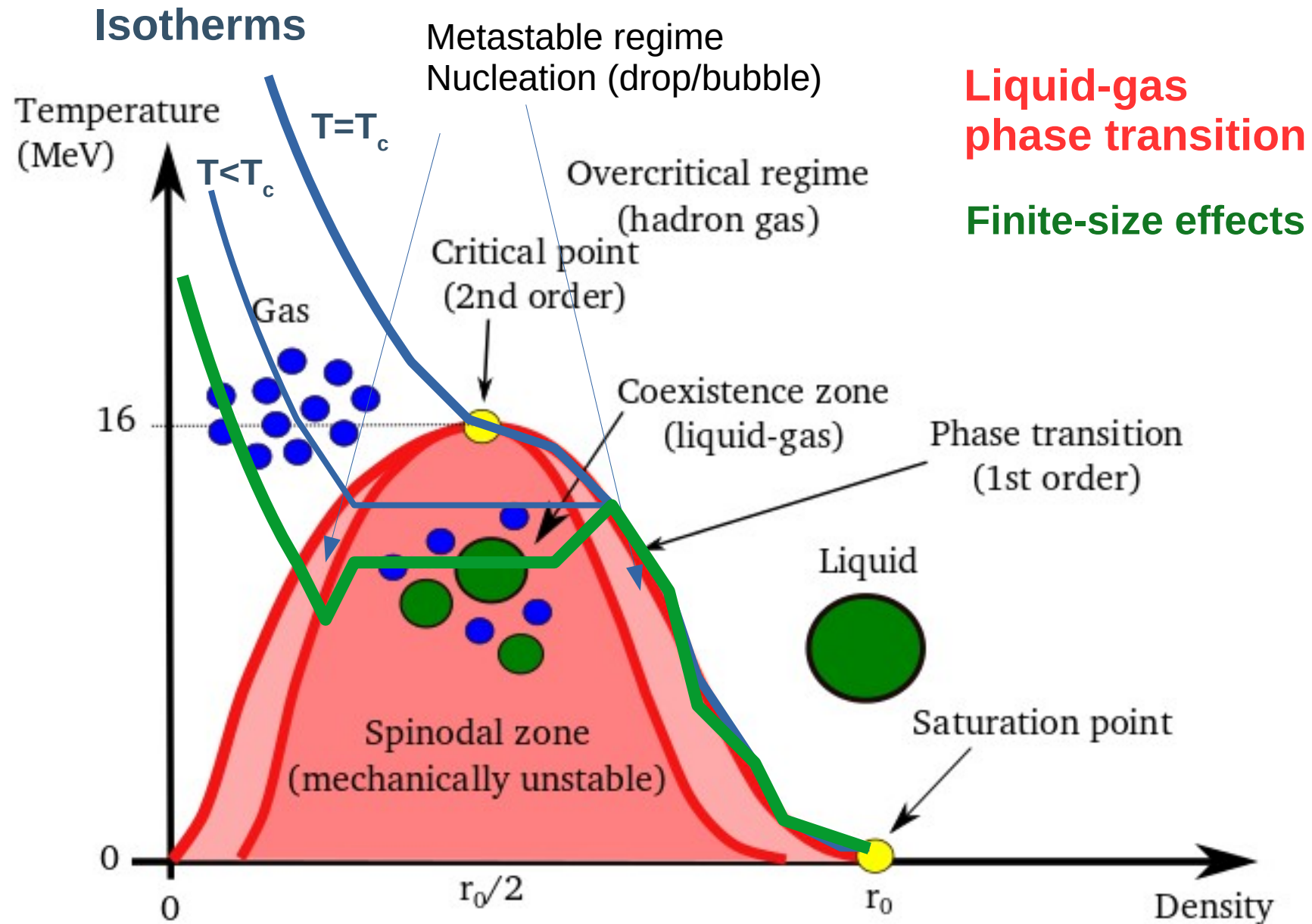
Liquid-gas PT



Spinodal decomposition : Mean-Field instabilities



Spinodal decomposition : Mean-Field instabilities



Liquid-gas phase transition

Finite-size effects



Multifragmentation !

Equation of State in nuclei

$$E = f(\rho, T, \delta)$$

$$\delta = (N-Z)/A$$

Astrophysical context (NS)

Nuclear matter :
Bulk properties

Extensive systems
(volume, size)

Pure **neutron matter** ($\delta=1$)

Equation of State in nuclei

$$E = f(\rho, T, \delta)$$

$$\delta = (N-Z)/A$$

Astrophysical context (NS)

Nuclear matter :
Bulk properties

Extensive systems
(volume, size)

Pure **neutron matter** ($\delta=1$)

Terrestrial Labs

Nuclei :
Finite-size effects

Non-extensive systems
(surface, Coulomb)

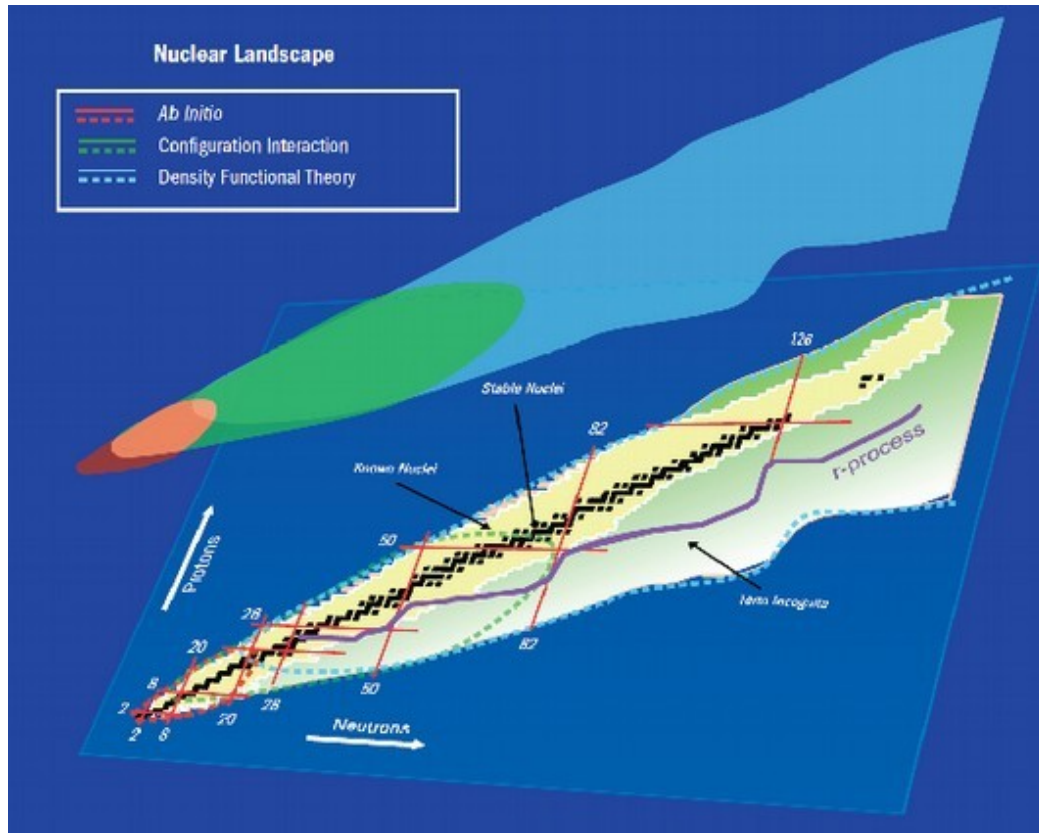
Asymmetric NM
($|\delta| \sim 0-0.4$, E_{sym})

Phase Diagram and Phase Transitions in finite systems

EoS in Nuclear Physics

Energy-density functionals modelization is probably the best possible framework to understand the properties of medium and heavy nuclei.

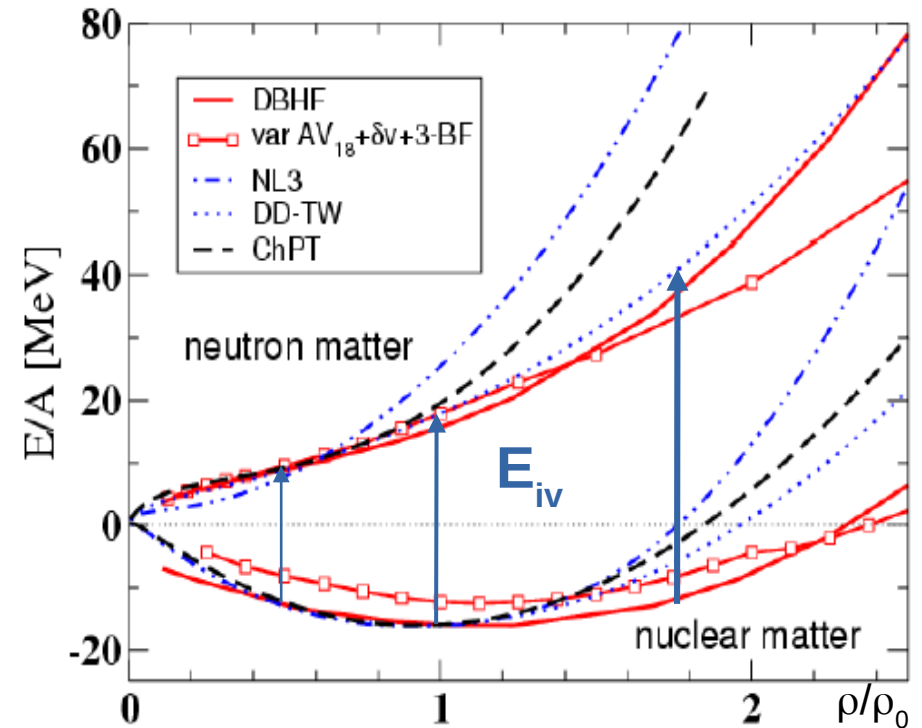
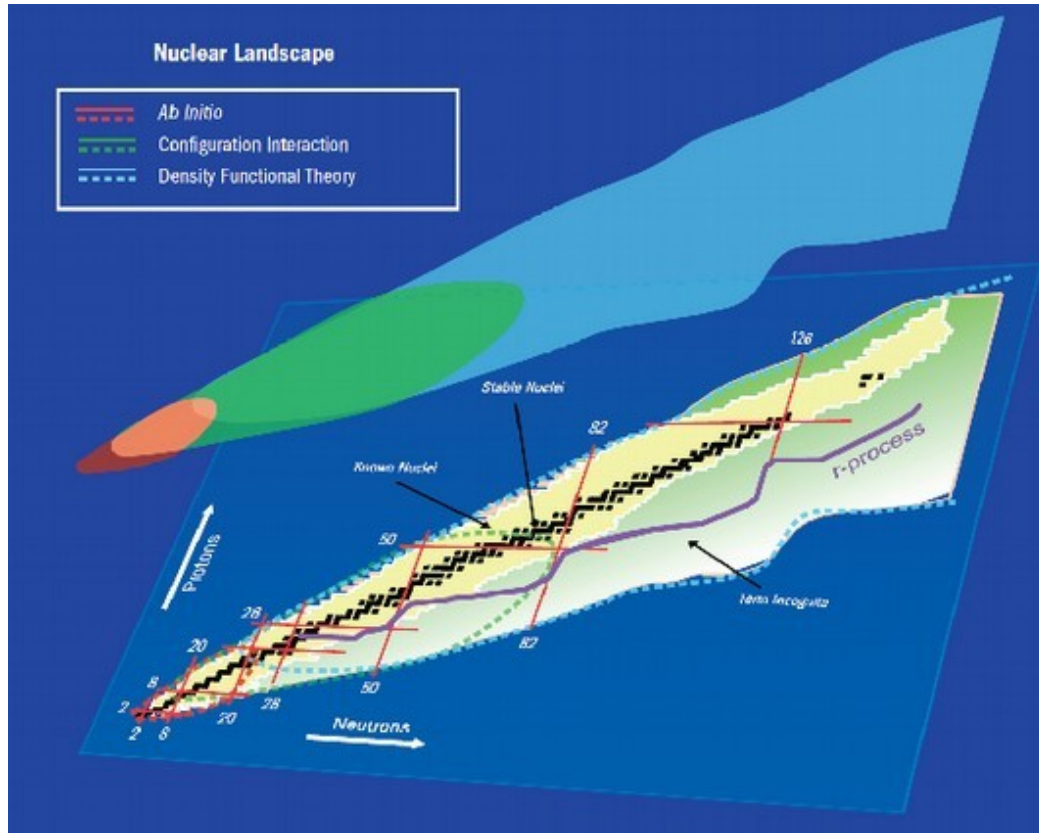
Energy-Density Functionals
(HK theorem) : $H_{eff} = E[\rho]$



EoS in Nuclear Physics

Energy-density functionals modelization is probably the best possible framework to understand the structure of medium and heavy nuclei.

Energy-Density Functionals
(HK theorem) : $H_{eff} = E[\rho]$



Direct link to *EOS* and Symmetry Energy (isovector term)

$$E_{iv} \text{ (aka } S) = E(\rho, \delta=1) - E(\rho, \delta=0)$$

EOS density and isospin dependence

Energy per nucleon in the parabolic (2nd order) approximation is the sum of isoscalar (ρ) and isovector (δ) terms:

Isospin ratio : $\delta=(N-Z)/A$
 $\rho_{\text{sat}} \approx 0.17 \text{ fm}^{-3}$

$$E(\rho, \delta) = E_0(\rho) + S(\rho) \cdot \delta^2 + O(\delta^4)$$

EOS density and isospin dependence

Energy per nucleon in the parabolic (2nd order) approximation is the sum of isoscalar (ρ) and isovector (δ) terms:

$$\begin{aligned} \text{Isospin ratio : } \delta &= (N-Z)/A \\ \rho_{\text{sat}} &\approx 0.17 \text{ fm}^{-3} \end{aligned}$$

$$E(\rho, \delta) \approx E_0(\rho) + S(\rho) \cdot \delta^2 + O(\delta^4)$$

Each term (isoscalar and isovector) can be decomposed in **Taylor expansion** (up to the fourth order) in $\chi = (\rho - \rho_0)/3\rho_0$:

$$E_0(\rho) = E_{\text{sat}}(\rho_0) + 1/2 K_0 \chi^2 + 1/3 ! Q_0 \chi^3 + 1/4 ! Z_0 \chi^4 + O(\delta^5)$$

E_{sat} is the **saturation energy** at $\rho = \rho_0$

K_0 is the **compressibility** (curvature) around ρ_0

Q_0 and Z_0 are the **cubic** and **quartic** terms needed for $\rho \gg \rho_0$

EOS density and isospin dependence

Energy per nucleon in the parabolic (2nd order) approximation is the sum of isoscalar (ρ) and isovector (δ) terms:

$$\text{Isospin ratio : } \delta = (N-Z)/A \\ \rho_{\text{sat}} \approx 0.17 \text{ fm}^{-3}$$

$$E(\rho, \delta) \approx E_0(\rho) + S(\rho) \cdot \delta^2 + O(\delta^4)$$

Each term (isoscalar and isovector) can be decomposed in **Taylor expansion** (here up to the fourth order) in $\chi = (\rho - \rho_0)/3\rho_0$:

$$E_0(\rho) = E_{\text{sat}}(\rho_{\text{sat}}) + 1/2 K_{\text{sat}} \chi^2 + 1/3 ! Q_{\text{sat}} \chi^3 + 1/4 ! Z_{\text{sat}} \chi^4 + O(\chi^5)$$

$$S(\rho) = J + L\chi + 1/2 K_{\text{sym}} \chi^2 + 1/3 ! Q_{\text{sym}} \chi^3 + 1/4 ! Z_{\text{sym}} \chi^4 + O(\chi^5)$$

E_{sat} is the **saturation energy** at $\rho = \rho_{\text{sat}}$

K_{sat} is the **compressibility** (curvature) around ρ_{sat}

Q_{sat} and Z_{sat} are the **cubic** and **quartic** terms needed for ρ far from ρ_{sat}

J is the **symmetry energy** at $\rho = \rho_{\text{sat}}$

L_{sym} is the **slope** (conn. to P) of the symmetry energy around ρ_{sat}

K_{sym} is the **curvature** of the symmetry energy

Q_{sym} and Z_{sym} are the **cubic** and **quartic** terms needed for ρ far from ρ_{sat}

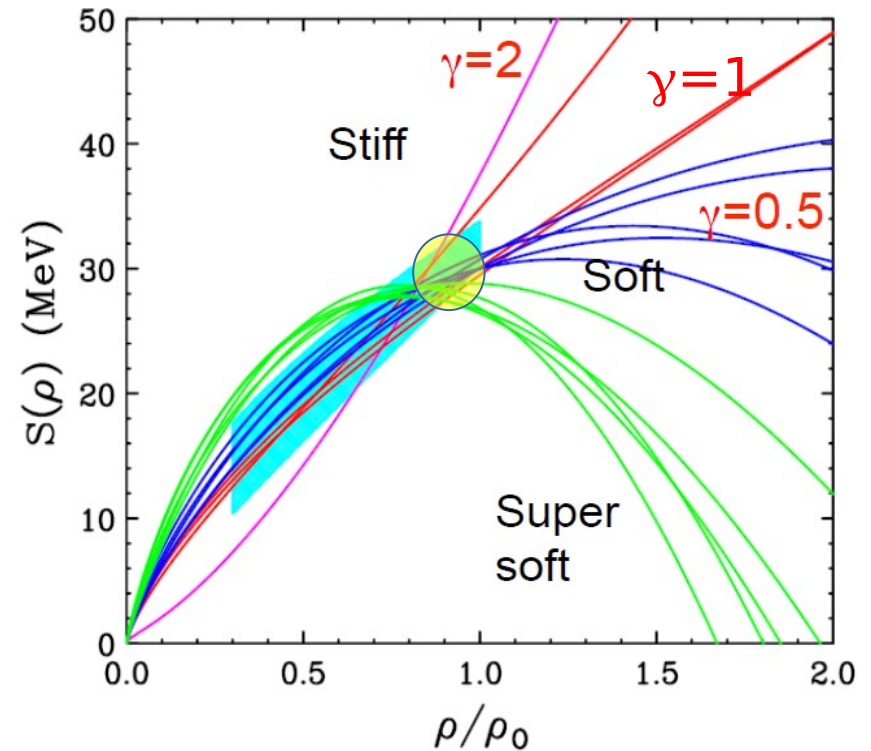
Symmetry Energy and Density Dependence

$$E/A(\rho, \delta) = E/A(\rho, 0) + \delta^2 \cdot S(\rho)$$

$$\delta = (\rho_n - \rho_p) / (\rho_n + \rho_p) = (N - Z) / A$$

- Constraints for **Astrophysics** (NS) and for laboratory experiments
- Needed for **transport models** and nuclear matter studies (Thermodyn.)
- Link to the **NN interaction** (isovector) in the nuclear medium

M.B. Tsang, Prog. Part.Nucl.Phys. 66, 400 (2011)
Brown, Phys. Rev. Lett. 85, 5296 (2001)



$$S(\rho) = S_k(\rho/\rho_0)^{2/3} + S_i(\rho/\rho_0)^\gamma$$

Kinetic (FG) Potential (int.)

Symmetry Energy and Density Dependence

$$E/A(\rho, \delta) = E/A(\rho, 0) + \delta^2 \cdot S(\rho)$$

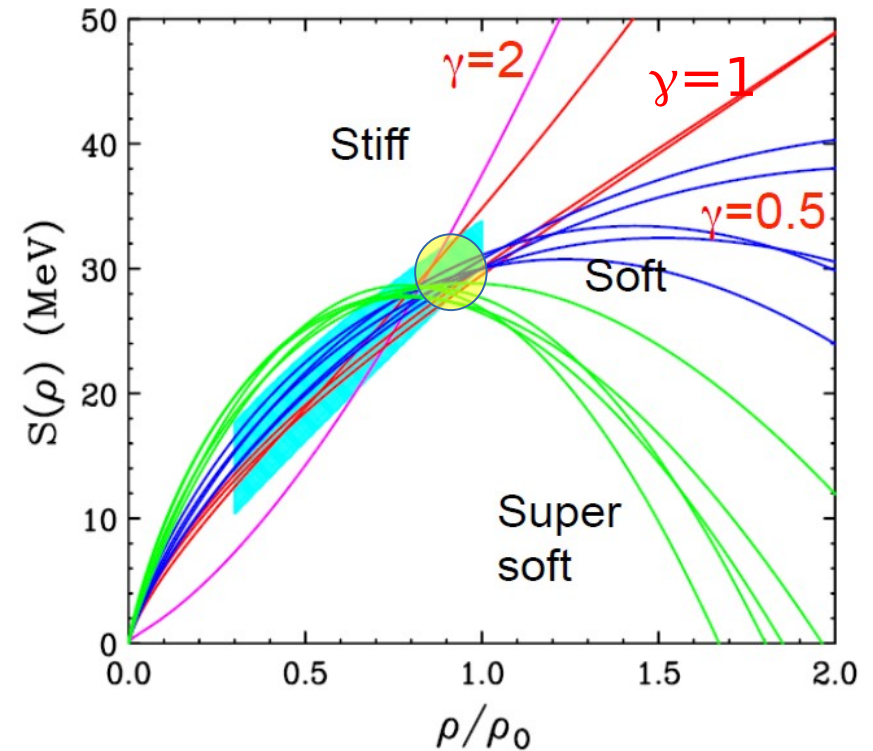
$$\delta = (\rho_n - \rho_p) / (\rho_n + \rho_p) = (N - Z) / A$$

- Constraints for **Astrophysics** (NS) and for laboratory experiments
- Needed for **transport models** and nuclear matter studies (Thermodyn.)
- Link to the **NN interaction** (isovector) in the nuclear medium

Density dependence of SE

Poorly constrained ...
Need experimental data !

M.B. Tsang, Prog. Part.Nucl.Phys. 66, 400 (2011)
Brown, Phys. Rev. Lett. 85, 5296 (2001)



$$S(\rho) = S_k(\rho/\rho_0)^{2/3} + S_i(\rho/\rho_0)^\gamma$$

Kinetic (FG) Potential (int.)

Symmetry Energy and density Dependence

$$E/A(\rho, \delta) = E/A(\rho, 0) + \delta^2 \cdot S(\rho)$$

$$\delta = (\rho_n - \rho_p) / (\rho_n + \rho_p) = (N - Z) / A$$

- Constraints for **Astrophysics** (NS) and for laboratory experiments
- Needed for **transport models** and nuclear matter studies (Thermodyn.)
- Link to the **NN interaction** (isovector) in the nuclear medium

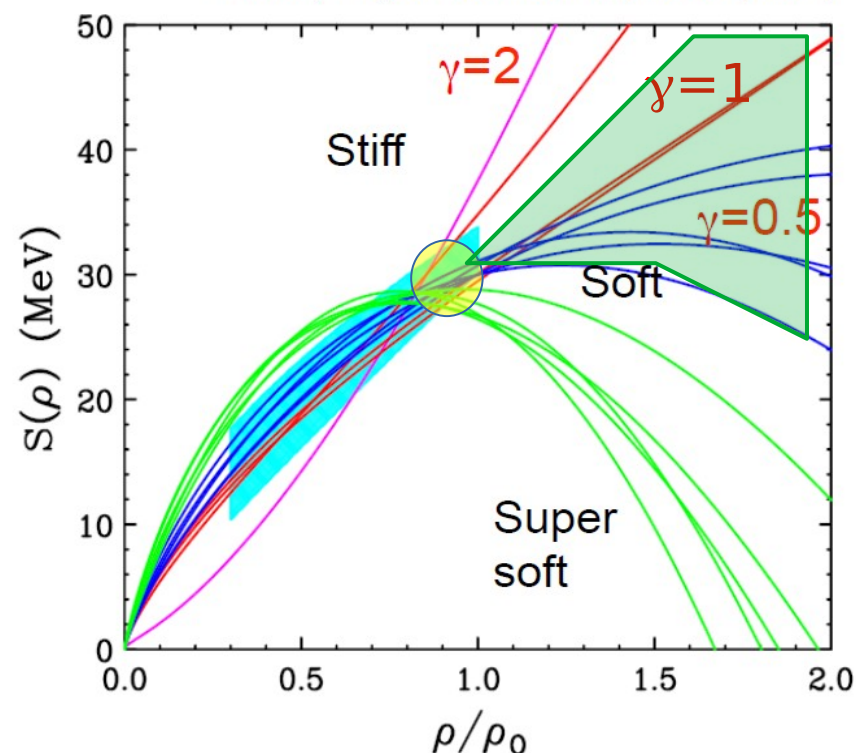
Density dependence of SE

From Asy-EOS : $\gamma = 0.8 \pm 0.25$

P. Russotto, *et al.*, Phys. Rev. C 94 , 034608 (2016).

**Poorly constrained ...
Need experimental data !**

M.B. Tsang, Prog. Part.Nucl.Phys. 66, 400 (2011)
Brown, Phys. Rev. Lett. 85, 5296 (2001)



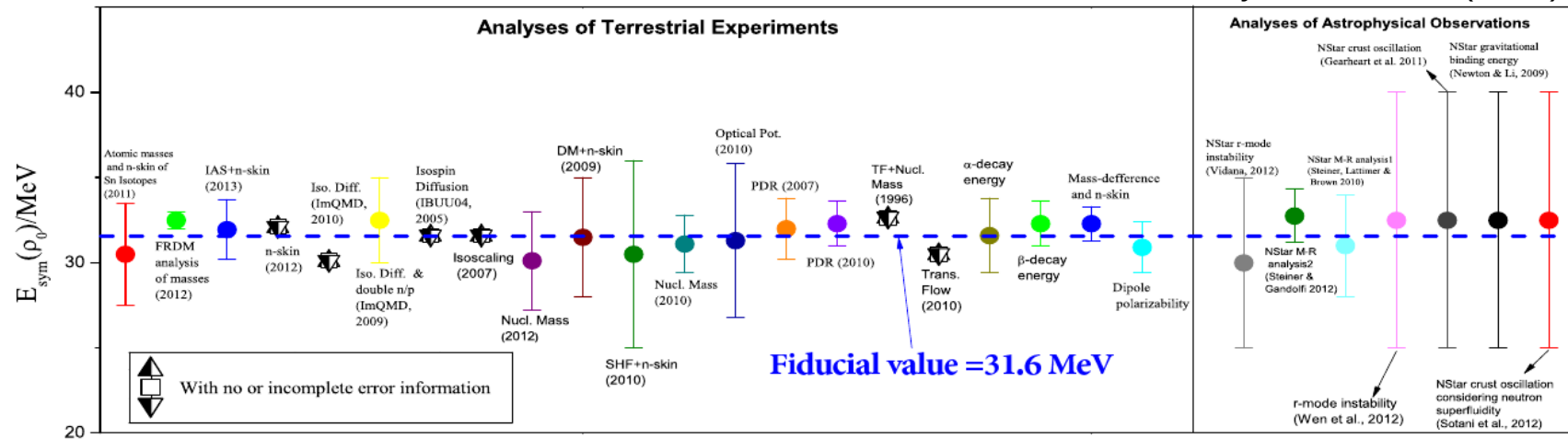
$$S(\rho) = S_k(\rho/\rho_0)^{2/3} + S_i(\rho/\rho_0)^\gamma$$

Kinetic (FG) Potential (int.)

Symmetry Energy around ρ_{sat} (I)

Evaluations for E_{sym} , slope L , curvature K_{sym} , ...

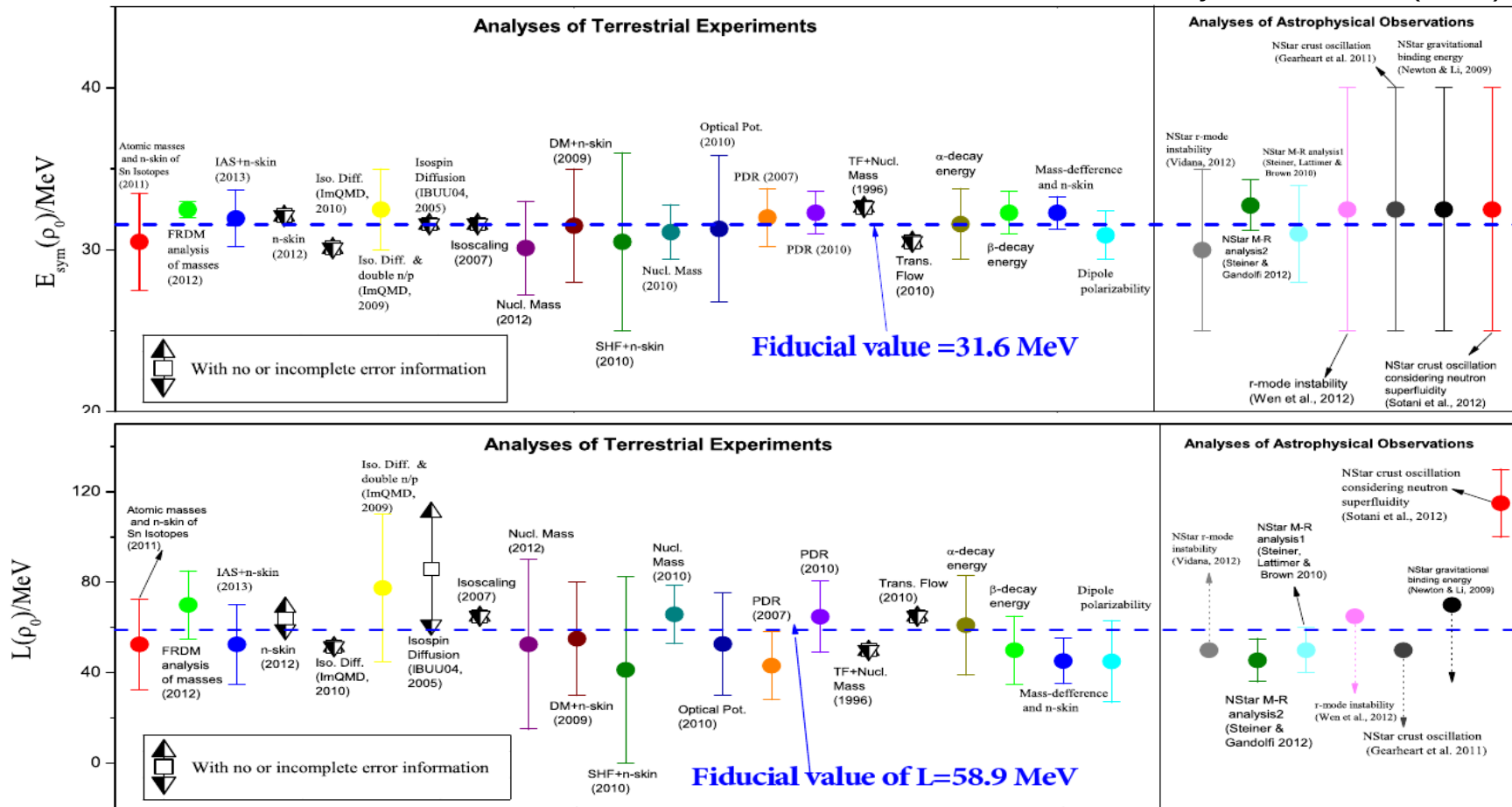
B.A. Li and X. Han, Phys. Lett. B727 (2018) 276



Symmetry Energy around ρ_{sat} (I)

Evaluations for E_{sym} , slope L , curvature K_{sym} , ...

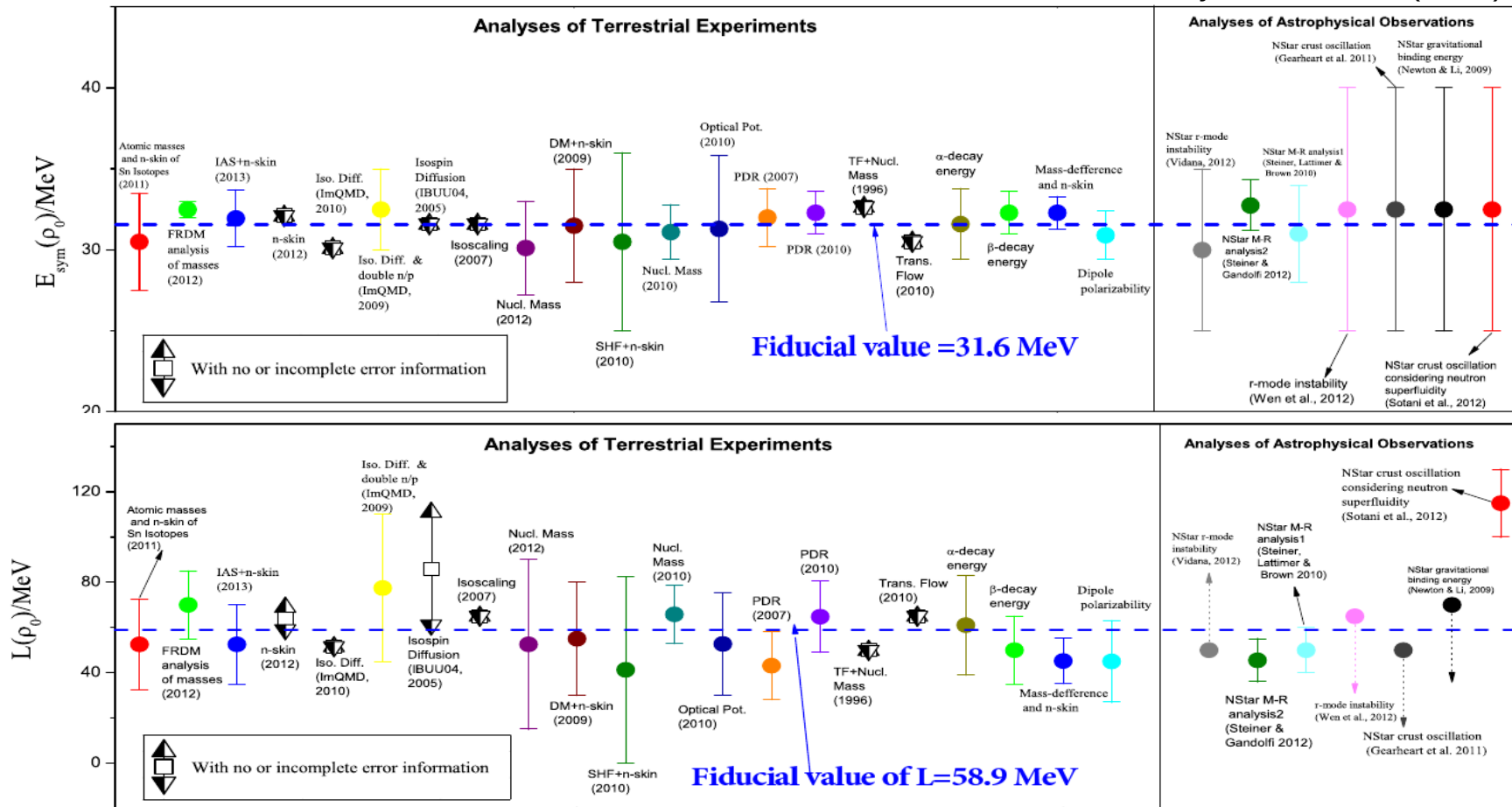
B.A. Li and X. Han, Phys. Lett. B727 (2018) 276



Symmetry Energy around ρ_{sat} (I)

Evaluations for E_{sym} , slope L , curvature K_{sym} , ...

B.A. Li and X. Han, Phys. Lett. B727 (2018) 276



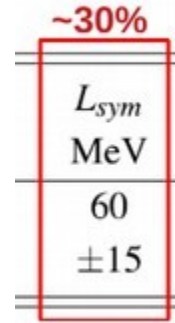
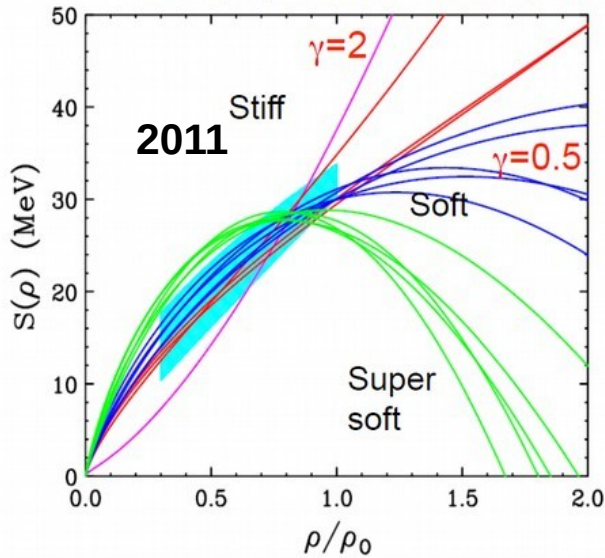
P_α	E_{sat} MeV	E_{sym} MeV	ρ_0 fm^{-3}	L_{sym} MeV	K_{sat} MeV	K_{sym} MeV	Q_{sat} MeV	Q_{sym} MeV	Z_{sat} MeV	Z_{sym} MeV
$\langle P_\alpha \rangle$	-15.8	32	0.155	60	230	-100	300	0	-500	-500
σ_{P_α}	± 0.3	± 2	± 0.005	± 15	± 20	± 100	± 400	± 400	± 1000	± 1000

J. margueron et al., PRC 97, 025805 (2018)



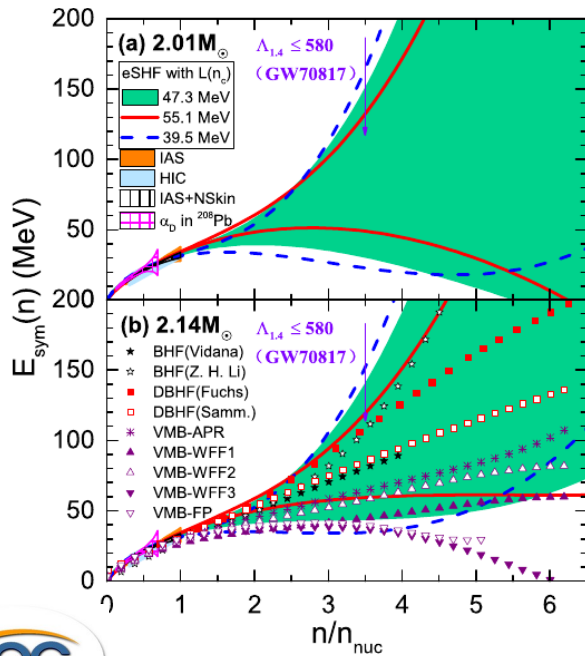
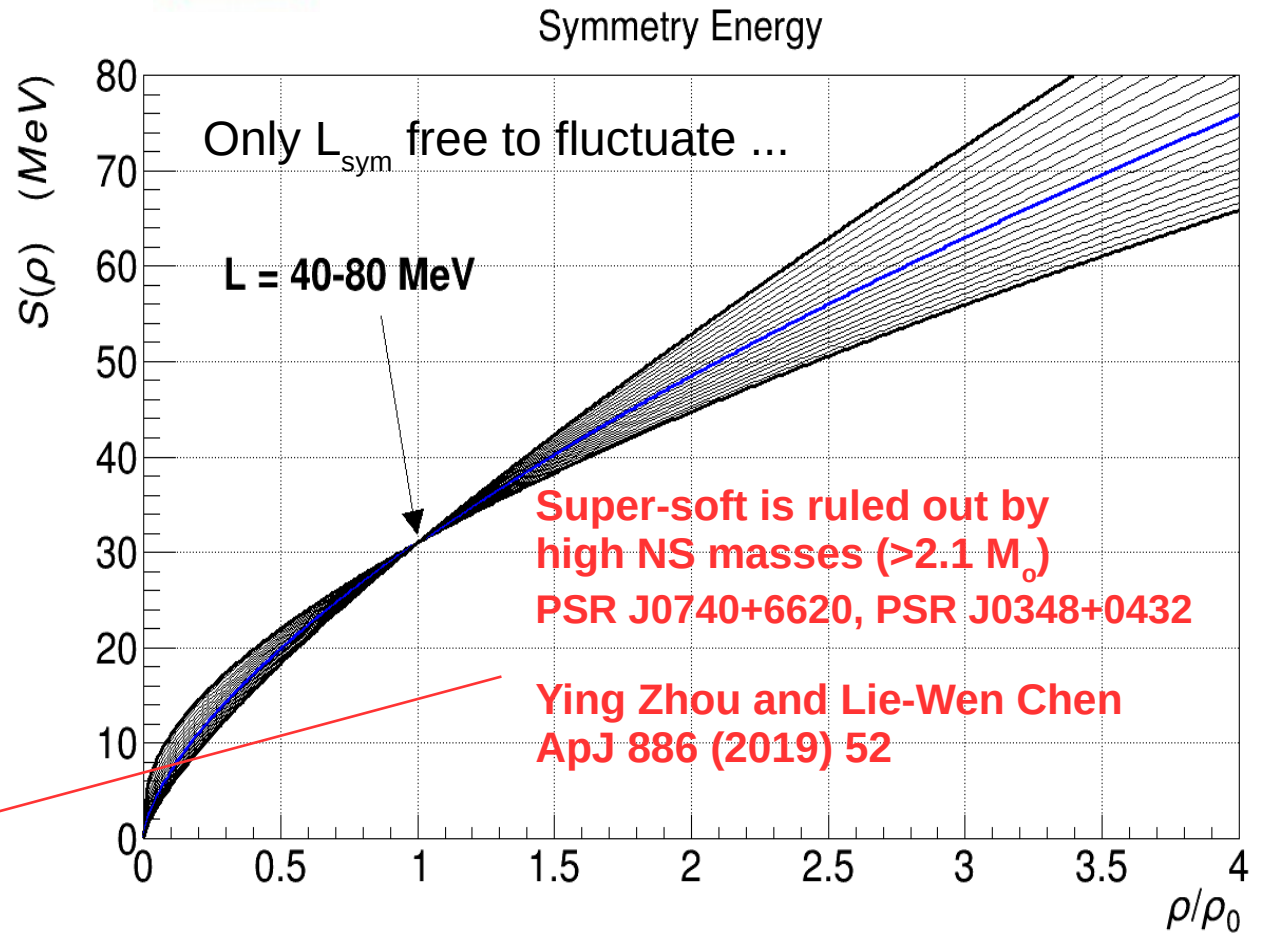
Symmetry Energy around ρ_{sat} (II)

M.B. Tsang, Prog. Part.Nucl.Phys. 66, 400 (2011)
Brown, Phys. Rev. Lett. 85, 5296 (2001)



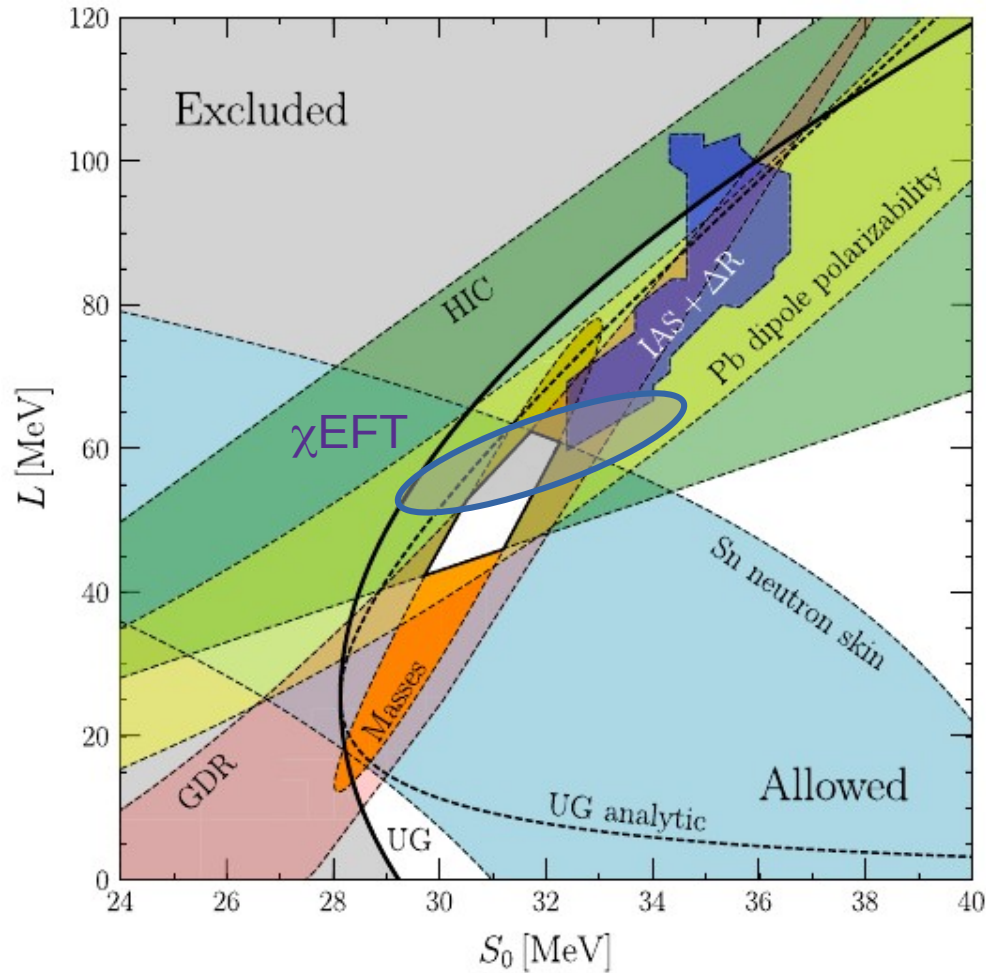
Uncertainties can be reduced but **covariance analysis / Bayesian Inference** is mandatory

$$S(\rho) = S_k(\rho/\rho_0)^{2/3} + S_i(\rho/\rho_0)^\gamma$$

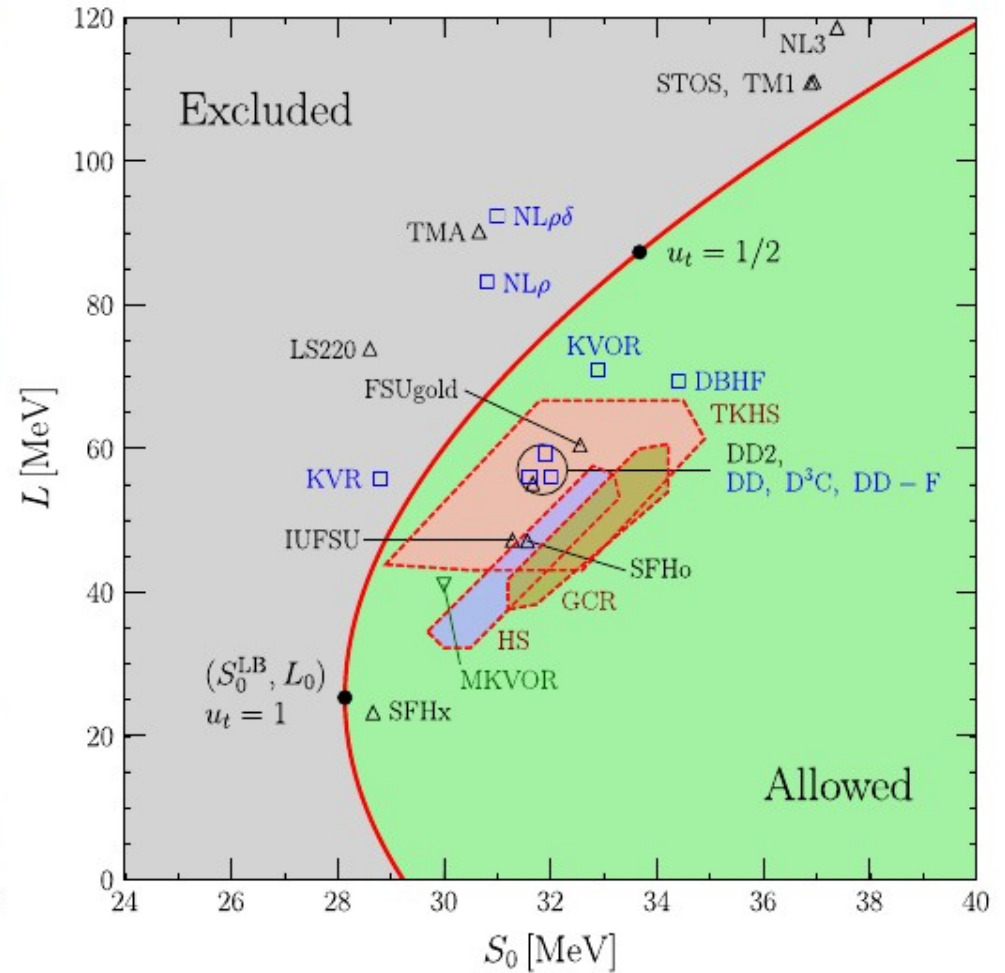


Symmetry Energy around ρ_{sat} (III)

Experimental constraints



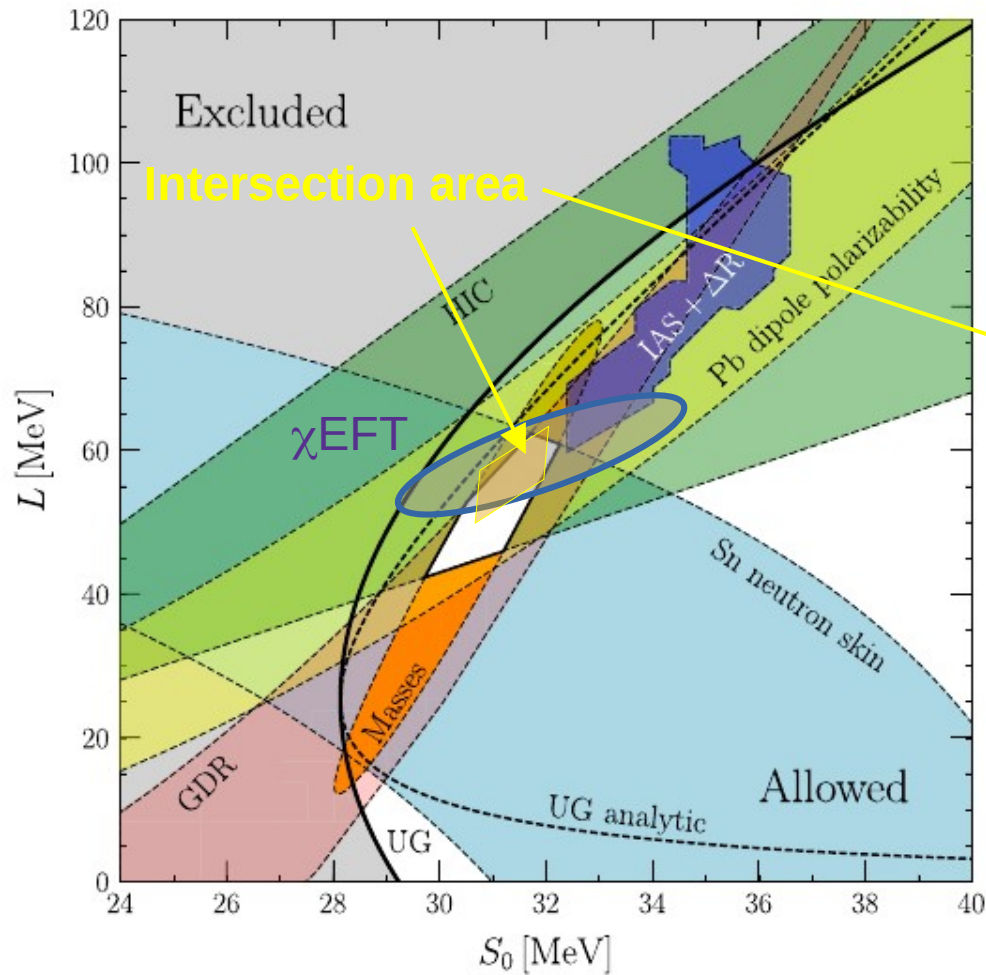
Model predictions



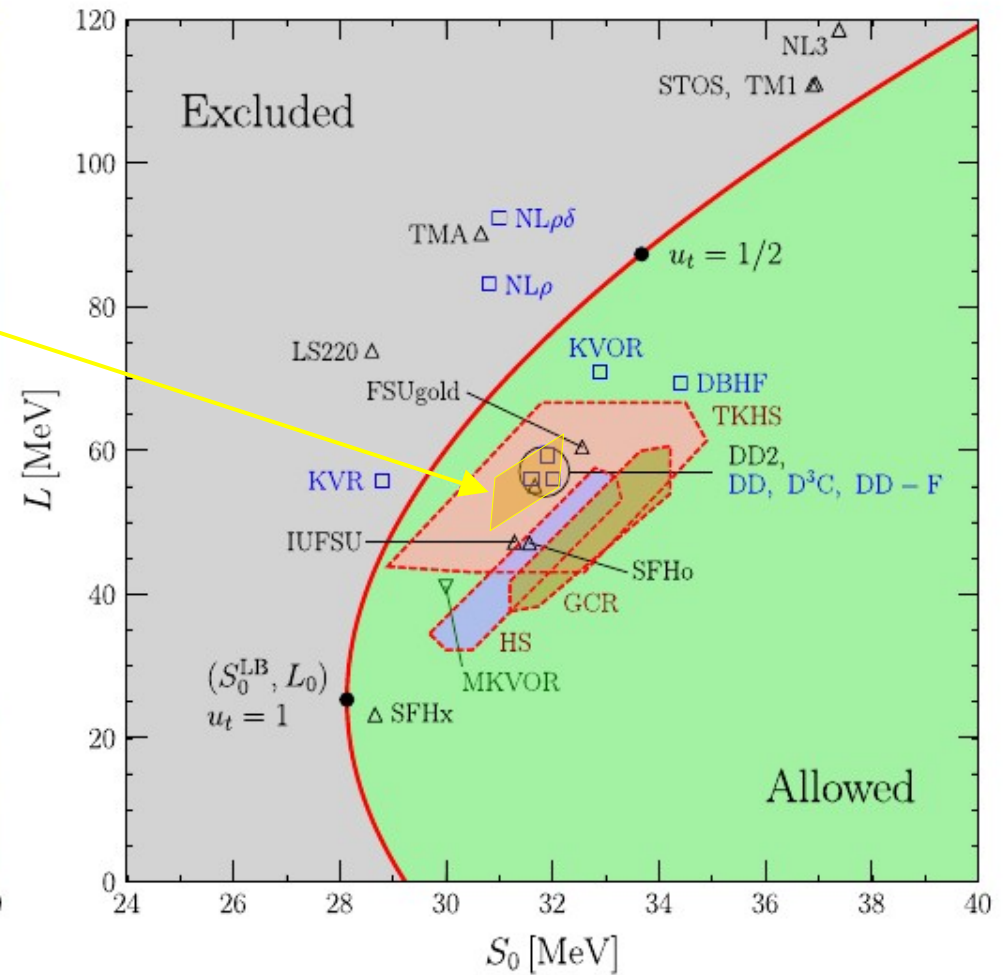
I. Tews *et al.*, *Astroph. J.* **848** (2017) 105
 C. Drischler *et al.*, *PRL* **125** (2020) 202702

Symmetry Energy around ρ_0

Experimental constraints



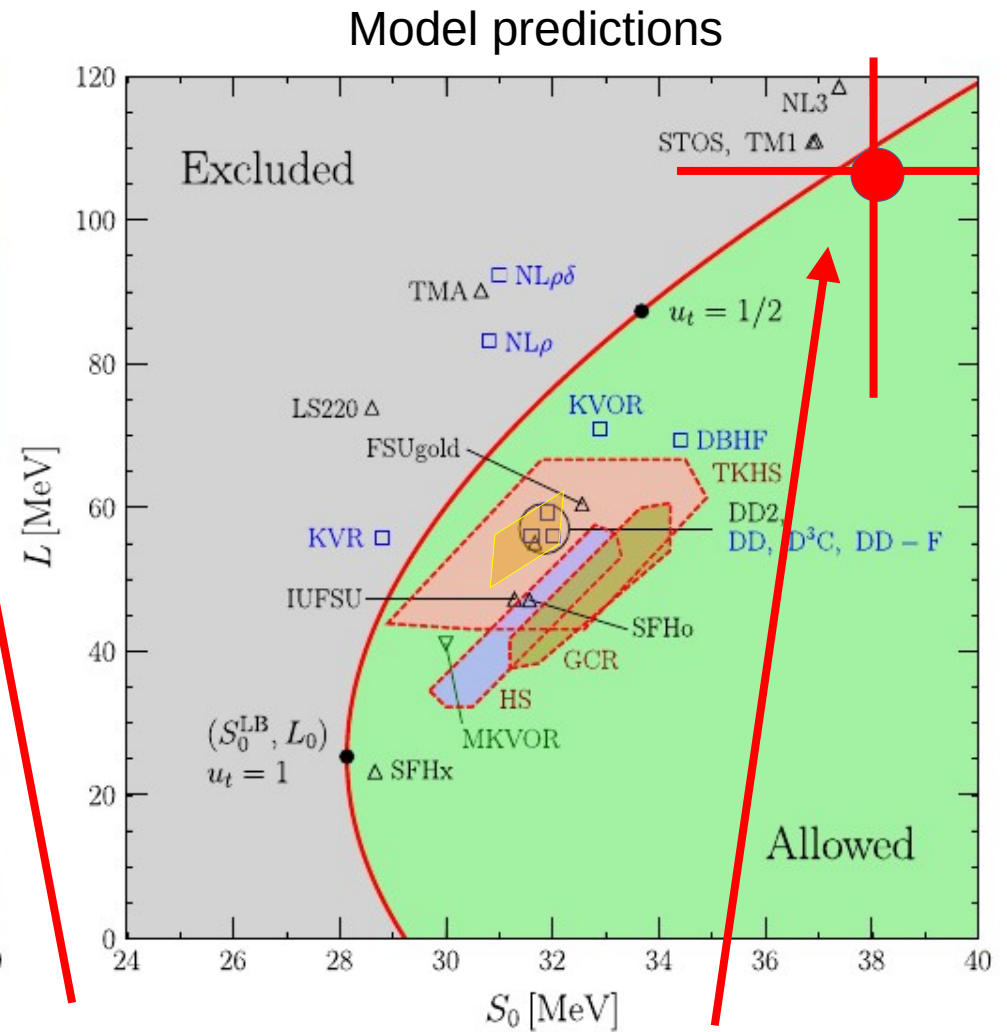
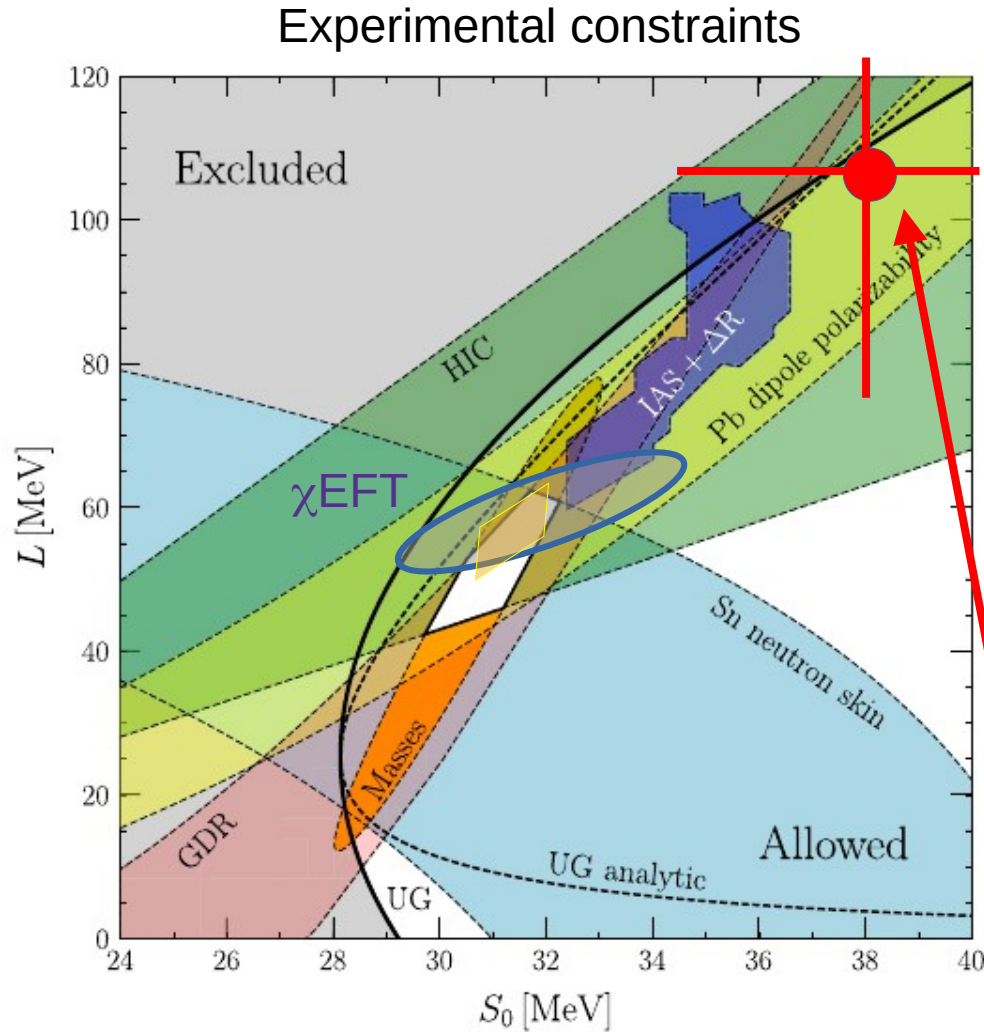
Model predictions



I. Tews *et al.*, *Astroph. J.* **848** (2017) 105
 C. Drischler *et al.*, *PRL* **125** (2020) 202702

Symmetry Energy around ρ_0 : newcomer in 2021

Tension between PREX-2 and other experimental / theoretical evaluations

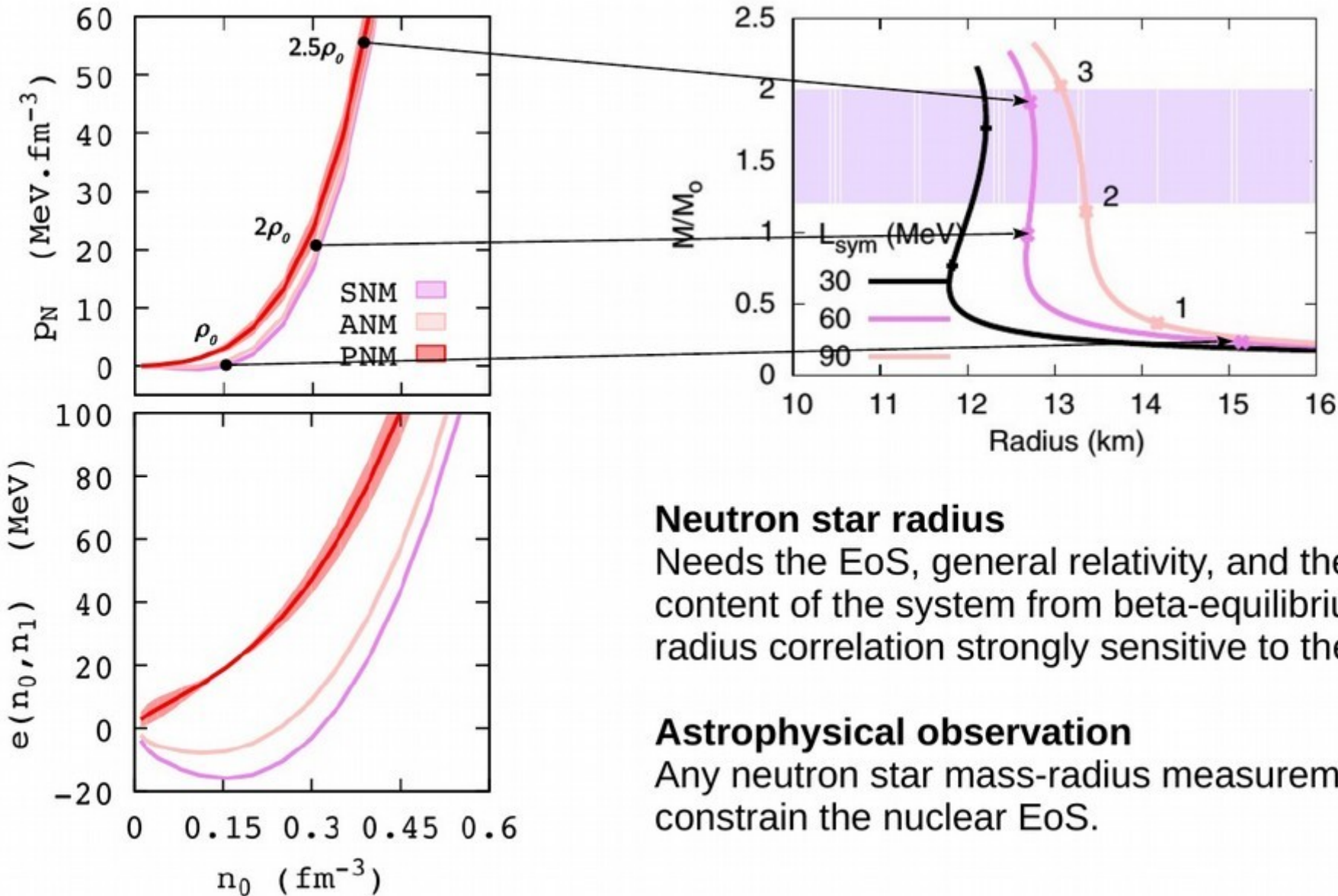


I. Tews *et al.*, *Astroph. J.* **848** (2017) 105
 C. Drischler *et al.*, *PRL* **125** (2020) 202702

PREX-2, B. T. Reed *et al.*, *PRL* **126** (2021) 172503
 $S_0 = 38.1 \pm 4.7$ MeV
 $L_{sym} = 106 \pm 37$ MeV

→ See Chirangi Mondal's poster

Constraints on Neutron Stars



Neutron star radius

Needs the EoS, general relativity, and the spin content of the system from beta-equilibrium. Mass-radius correlation strongly sensitive to the EoS.

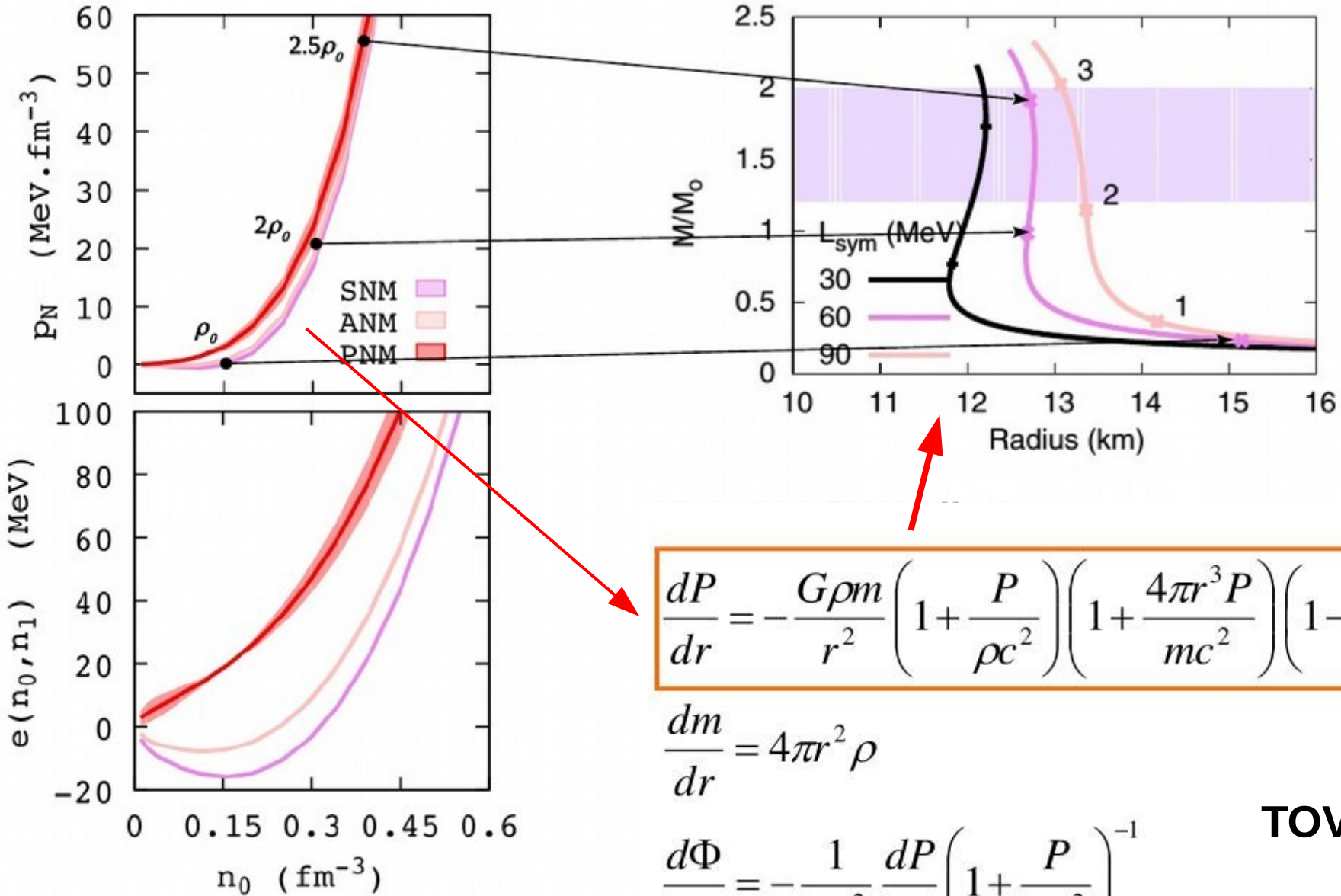
Astrophysical observation

Any neutron star mass-radius measurement would constrain the nuclear EoS.

Also tidal deformability provide a strong constraint
See B. Giacomazzo's lecture

Margueron PRC **97** (2018) 025805
Margueron PRC **97** (2018) 025806

Constraints on Neutron Stars



$$\frac{dP}{dr} = -\frac{G\rho m}{r^2} \left(1 + \frac{P}{\rho c^2}\right) \left(1 + \frac{4\pi r^3 P}{mc^2}\right) \left(1 - \frac{2Gm}{rc^2}\right)^{-1}$$

$$\frac{dm}{dr} = 4\pi r^2 \rho$$

$$\frac{d\Phi}{dr} = -\frac{1}{\rho c^2} \frac{dP}{dr} \left(1 + \frac{P}{\rho c^2}\right)^{-1}$$

$$P = P(\rho)$$

TOV eqs.

Margueron PRC **97** (2018) 025805
 Margueron PRC **97** (2018) 025806

Nuclear reactions at low incident energy

Terrestrial experiments

At GANIL (Caen, Normandy, France), many teams study heavy ions induced nuclear reactions to investigate stable and exotic nuclei properties



lpc
caen
Laboratoire de physique corpusculaire

GANIL/SPIRAL1

CSS1/CSS2/CIME :

Stable beams (He-U) $E_{inc} = 5 - 100 \text{ MeV/nucl.}$

Radioactive beams $E_{inc} = 5 - 15 \text{ MeV/nucl.}$



Terrestrial experiments

At GANIL (Caen, Normandy, France), one studies heavy ions induced reactions at low energy to investigate stable and exotic nuclei properties.



SPIRAL2

New SC-LINAC :

Intense p,d and HI beams

$E_{inc} = 5 - 20 \text{ MeV/nucl.}$

GANIL/SPIRAL1

CSS1/CSS2/CIME :

Stable beams (He-U) $E_{inc} = 5 - 100 \text{ MeV/nucl.}$

Radioactive beams $E_{inc} = 5 - 15 \text{ MeV/nucl.}$



SPIRAL2

L'ACCÉLÉRATEUR LINÉAIRE SUPRACONDUCTEUR

délivre des faisceaux de particules de très grande intensité : le nombre de collisions entre les particules accélérées et les noyaux de la cible de matière est ainsi plus important.

GANIL

LES SALLES D'EXPÉRIENCES renferment des systèmes de détection et de mesure très sophistiqués, permettant d'étudier les propriétés de noyaux très exotiques.



SPIRAL2

LES SOURCES D'IONS DE SPIRAL2

permettent de produire un large éventail de particules, dont de très légères comme les deutons ou les protons.

GANIL

L'ENSEMBLE ACCÉLÉRATEUR,

composé de cinq cyclotrons, accélère des faisceaux d'ions allant du carbone-12 à l'uranium-238 à différentes énergies adaptées aux types d'expériences réalisées. Les ions de carbone-12 peuvent par exemple atteindre 120 000 kilomètres par seconde, soit plus du tiers de la vitesse de la lumière.

GANIL

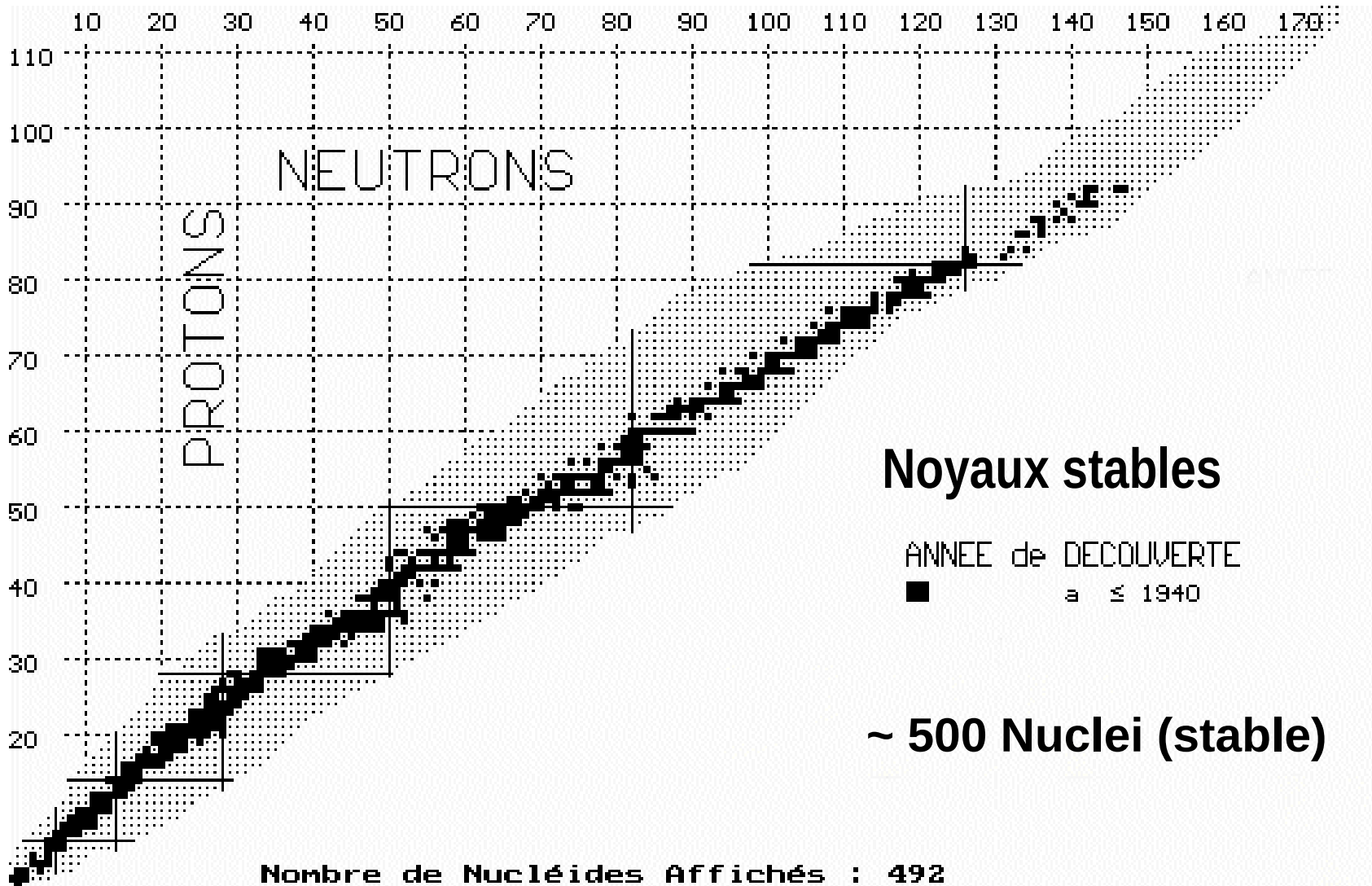
LES SOURCES

permettent de produire les ions stables ou radioactifs qui seront ensuite mis en faisceaux et accélérés.

Producing exotic nuclei

Towards the driplines

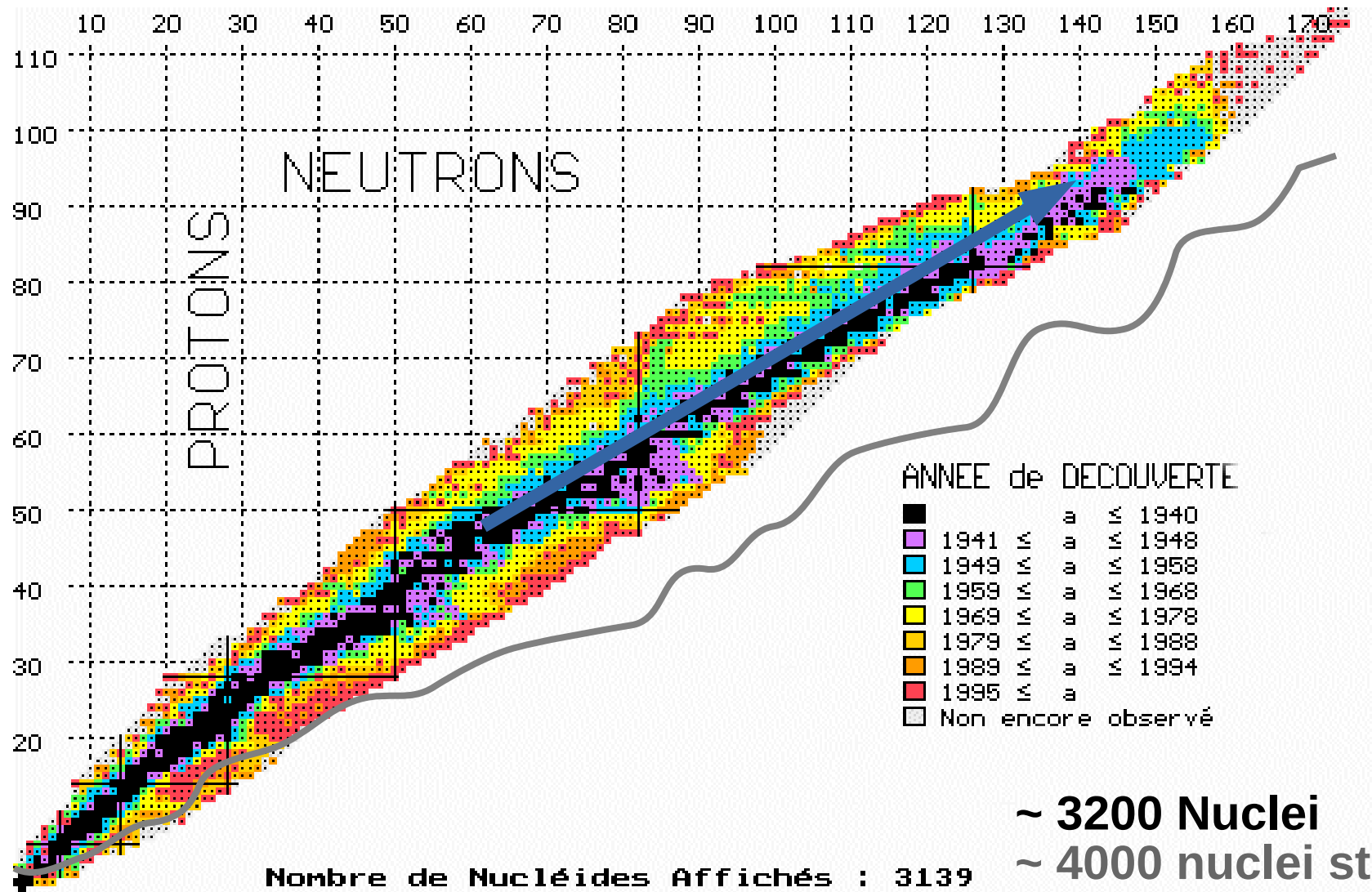
Discovered nuclei before WW II



Known Nuclei nowadays and future

Major outcomes of nuclear physics after 50's

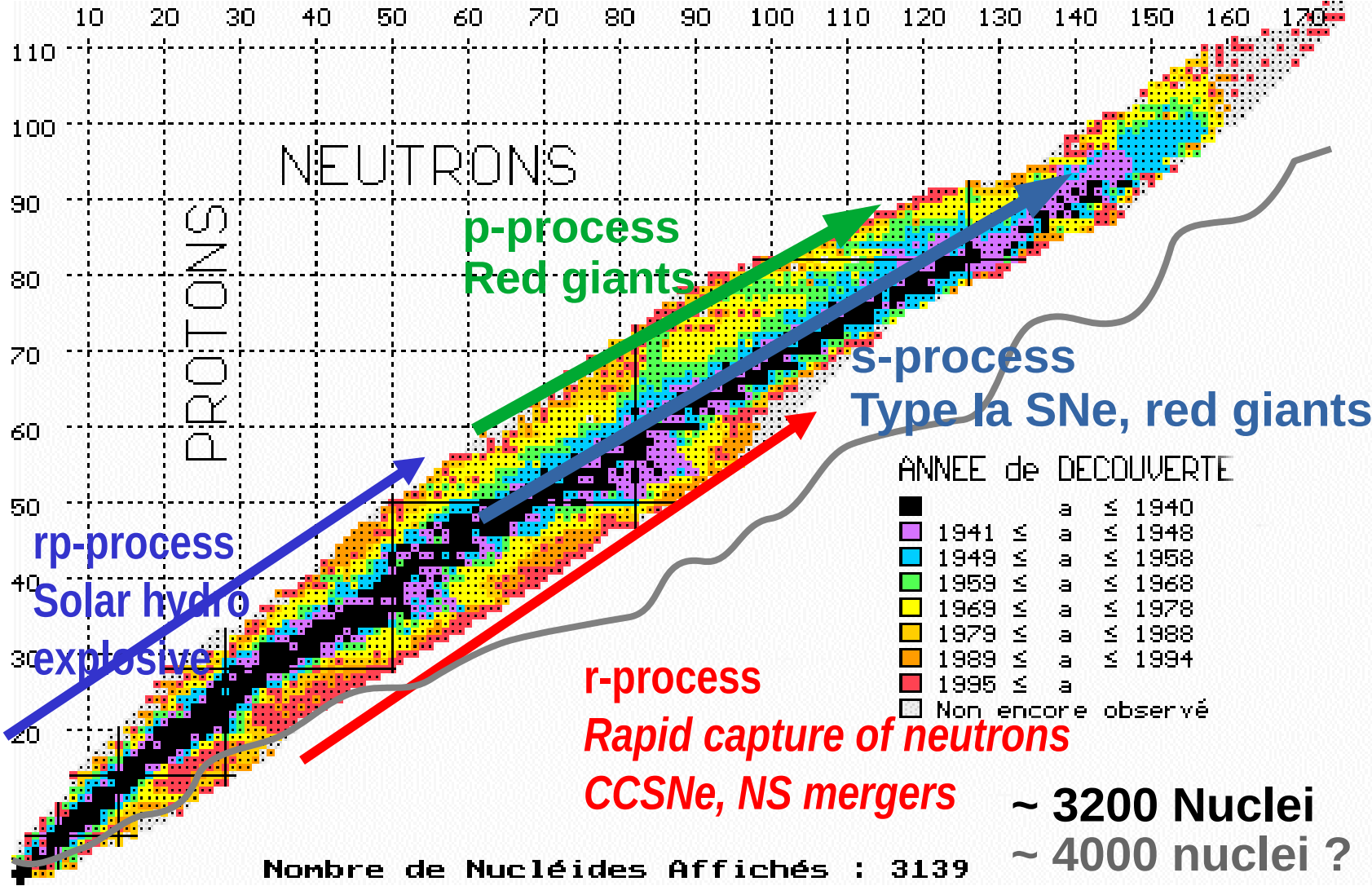
“Terra Incognita”



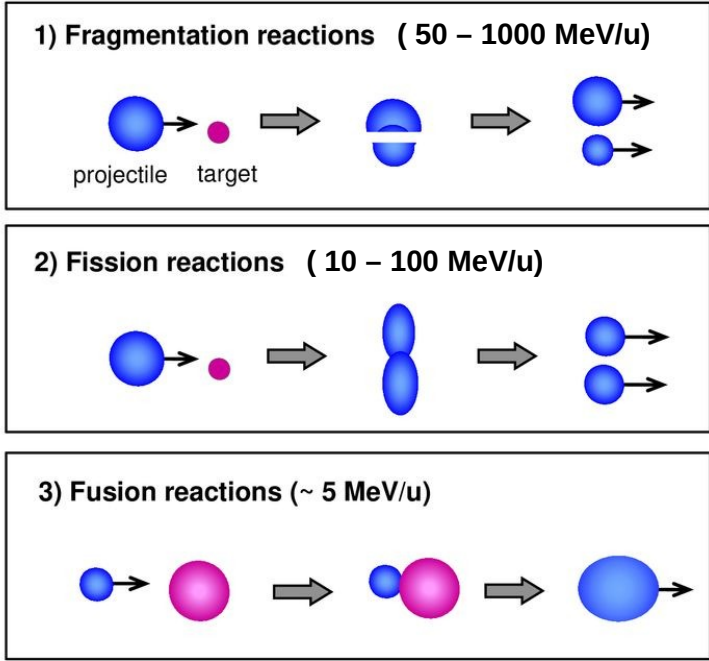
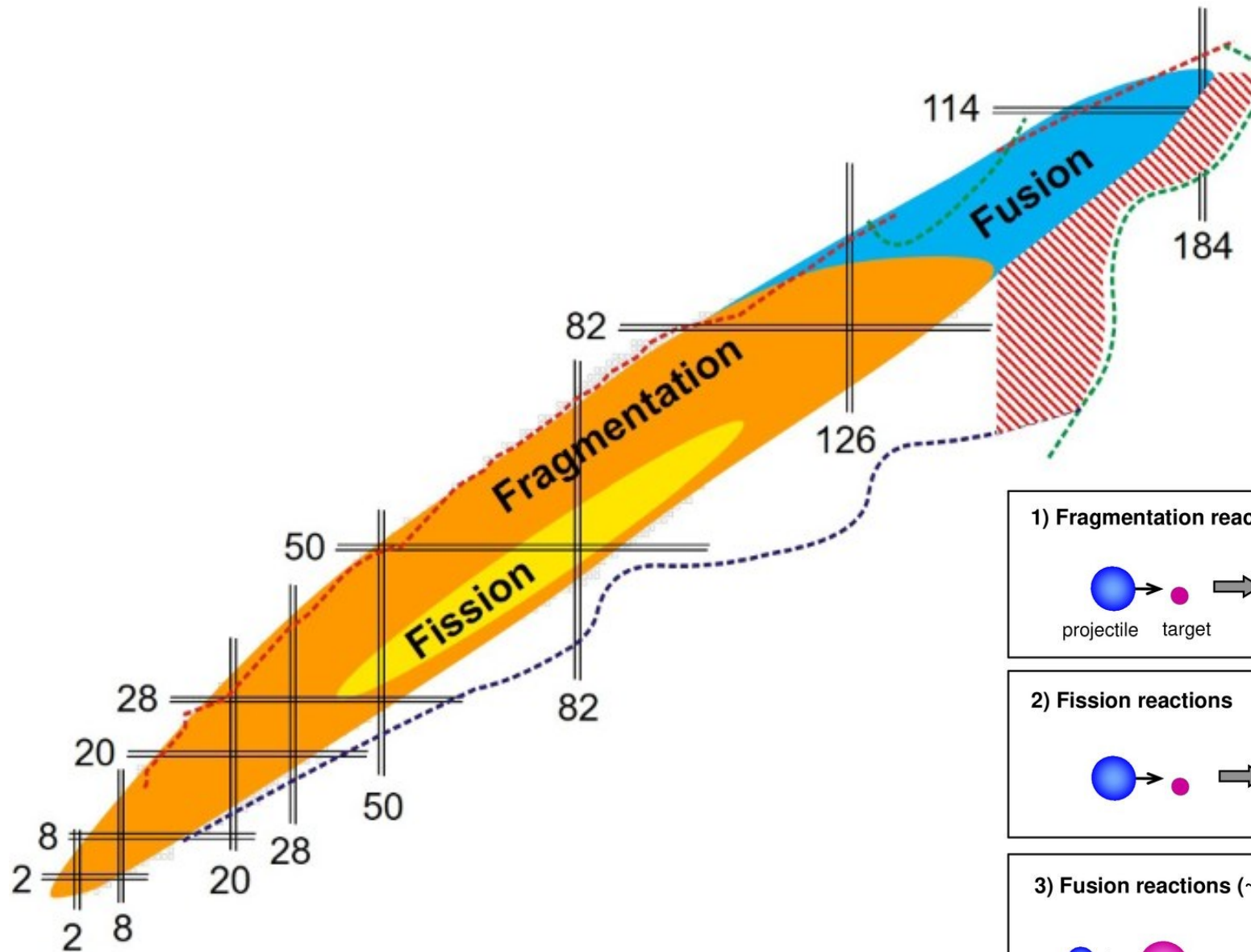
~ 3200 Nuclei
~ 4000 nuclei still
to discover ?

Known Nuclei nowadays and future

“Terra Incognita”



Production of exotic nuclei with HI beams



End of lecture I

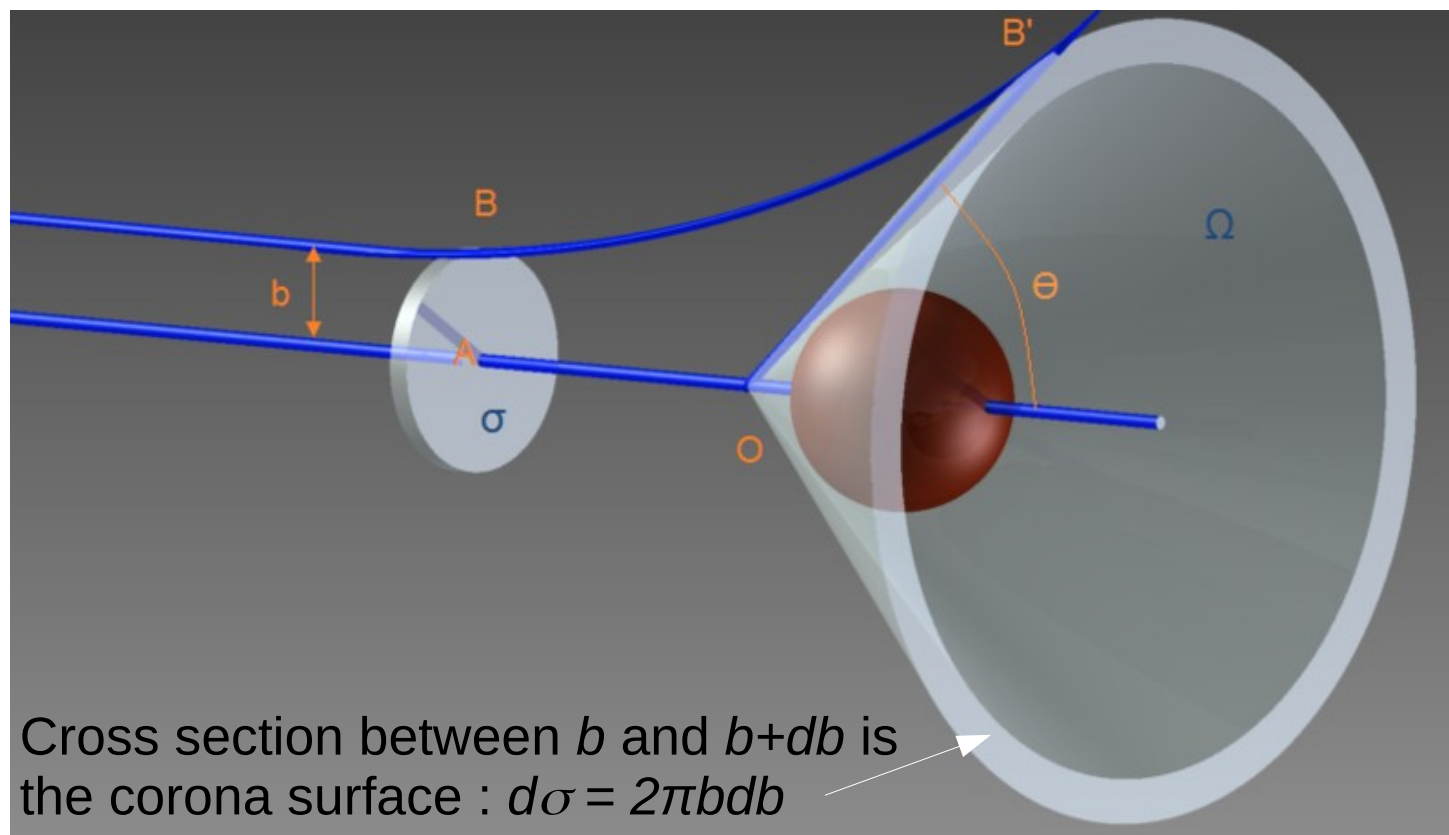
Outlines

1. From the use of low energy nuclear reactions (dissipative)
2. The nuclear equation of state
 - Phase transitions
 - Empirical parameters
 - Evaluations & uncertainties
3. Toward the production of exotic nuclei
4. Panorama of nuclear reactions from B_{coul} up to 100 MeV/nucleon
 - Basic considerations
 - Reaction mechanisms
5. Path to equilibrium : transport properties in nuclear medium
 - Energy dissipation
 - Isospin transport
6. Improving our knowledge for EOS
7. Experimental tools and some related instrumentation



Reaction mechanisms
from Coulomb barrier
up to relativistic energies

Cross section in classical Physics



Integrating over b , we get : $\sigma(b) = \pi b^2$

Unit is the barn (b), $1b = 10^{-28}m^2 = 10^{-24}cm^2$

For a typical nuclear reaction between H1, we have $b_{\text{grazing}} \approx 10 \text{ fm}$,
then $\sigma_{\text{nuc}} = 3,142 b = 3142 \text{ mb}$

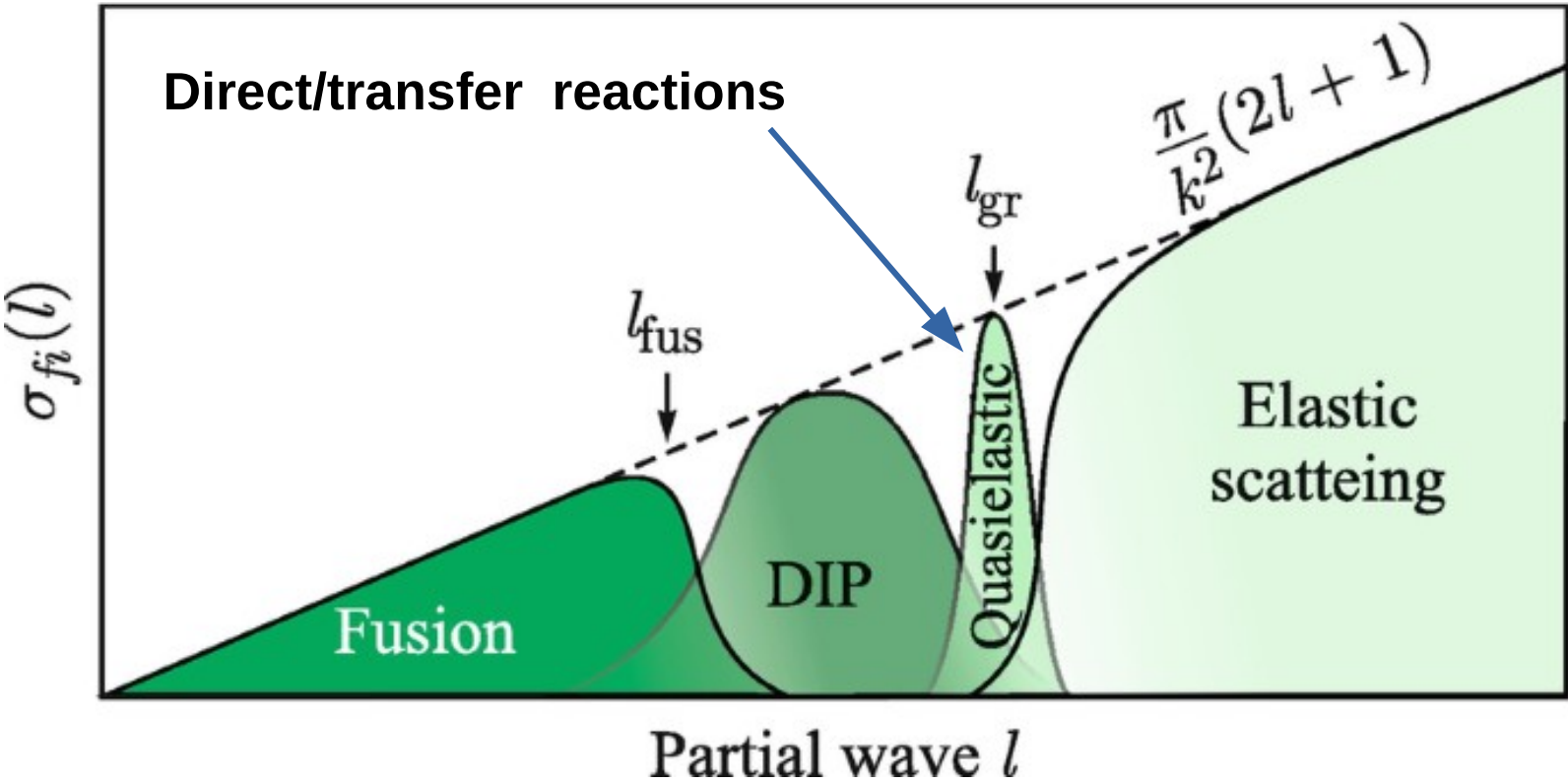
Cross section in Quantum Mechanics : partial waves

Total nuclear cross-section

$$\sigma_{nuc} = \pi b_{gr}^2 \approx \pi \ell_{gr} (\ell_{gr} + 1) \hbar^2 / \mu v$$

Classical ansatz :

$$|\ell| = \sqrt{l(l+1)} \hbar = \mu v b$$



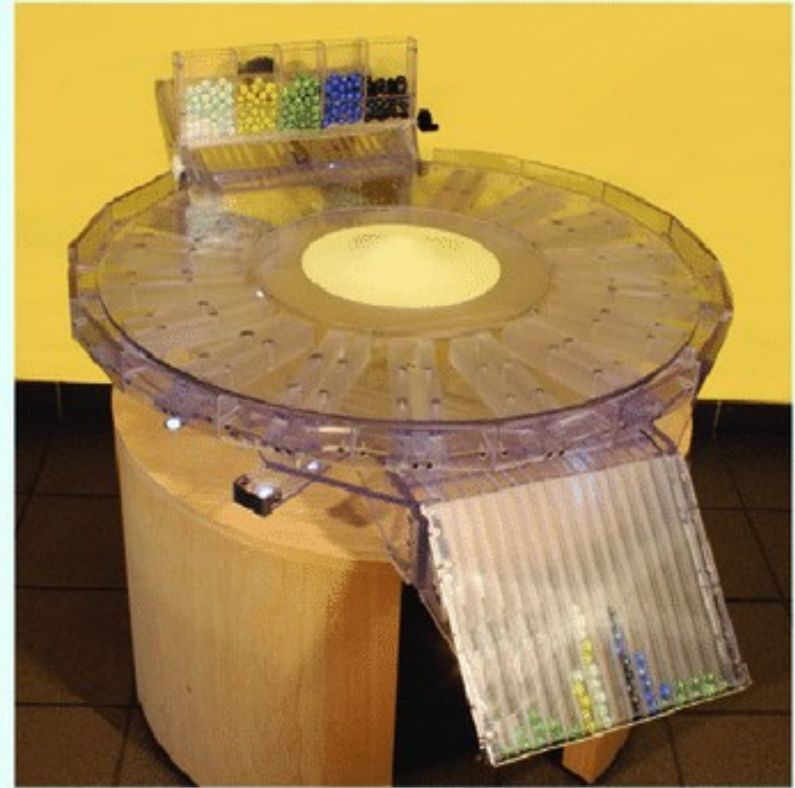
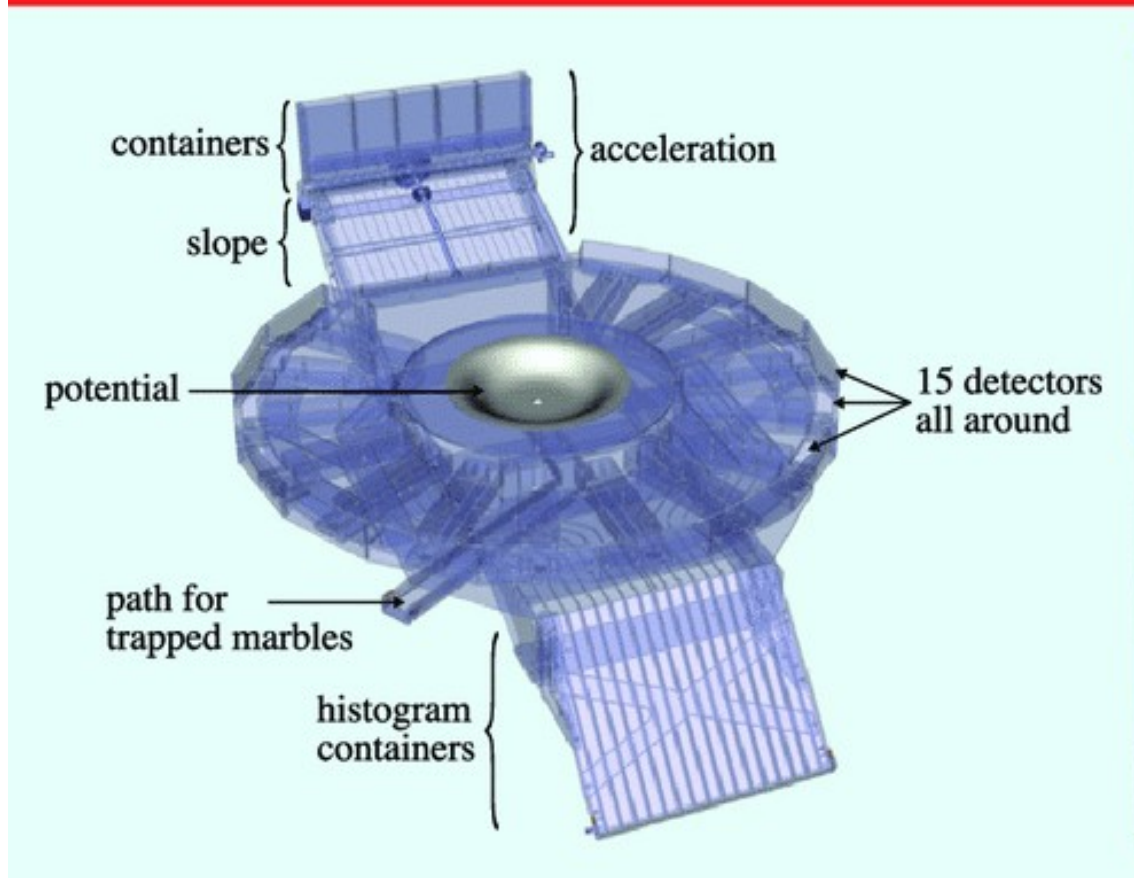
$$\sigma_r = \frac{\pi}{k^2} \sum_{\ell=0}^{\ell_{max}} (2\ell + 1)(1 - \eta_{\ell}^2)$$

η_{ℓ} is the **inelasticity coefficient** for partial wave ℓ
 $\eta_{\ell} = 0$ for **elastic** and $0 < \eta_{\ell} < 1$ for **absorption**



Rutherford scattering with marble balls : Billotron

<https://www.lpc-caen.in2p3.fr/grand-public-rencontrer/le-billotron/>



https://youtu.be/_KcK-jS2QQQ

A. Chapon, J. Gibelin, O. Lopez, D. Cussol, D. Dominique Durand, Ph. Desrues, H. Franck De Préaumont, Y. Lemièrè, J. Perronnel, and J.C. Steckmeyer. *The Billotron: a way to experimentally apprehend the subatomic world*. *Physics Education*, 50(4):453, 2015. doi: 10.1088/0031-9120/50/4/453. URL <http://hal.in2p3.fr/in2p3-01177619>.

➔ **Ask Julien Gibelin**

Cross section and event rate

Event rate E (s^{-1}) for a specific reaction cross section σ_r :

$$E_{\text{reac}} = \mathcal{F} \rho \mathcal{N} e \sigma_r / A$$

where :

- \mathcal{F} is the incident flux of particles per unit of time (s^{-1})
- ρ is the density of the target material (g.cm^{-3})
- e is the target thickness (cm)
- A is the molar mass of the target material (g.mol^{-1})
- $\mathcal{N} = 6.022.10^{23}$ is the Avogadro number
- σ_r is the reaction cross section (cm^{-2})

Cross section and event rate

Event rate E (s^{-1}) for a specific reaction cross section σ_r :

$$E_{\text{reac}} = \mathcal{F} \rho \mathcal{N} e \sigma_r / A$$

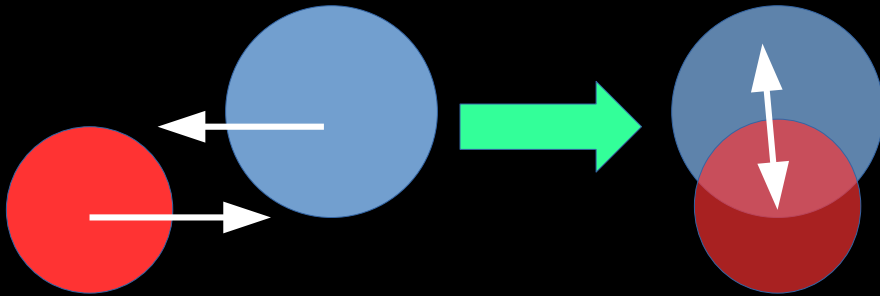
Thin target
 $e=300 \mu\text{m}$, Au

Reaction $\mathcal{F} = 10^9$ pps	Cross section	Event rate
Coulomb scattering	100 b	1000/s
Deep Inelastic/ Multi-nucleon Transfer	1 b	10/s
Central collision ($b < 1$ fm)	50 mb	1/mn
Fusion reaction for SHE	1 μb	1/month

Low energy reaction mechanisms

$B < E_{inc} < 15 \text{ MeV/nucleon}$

Composite system

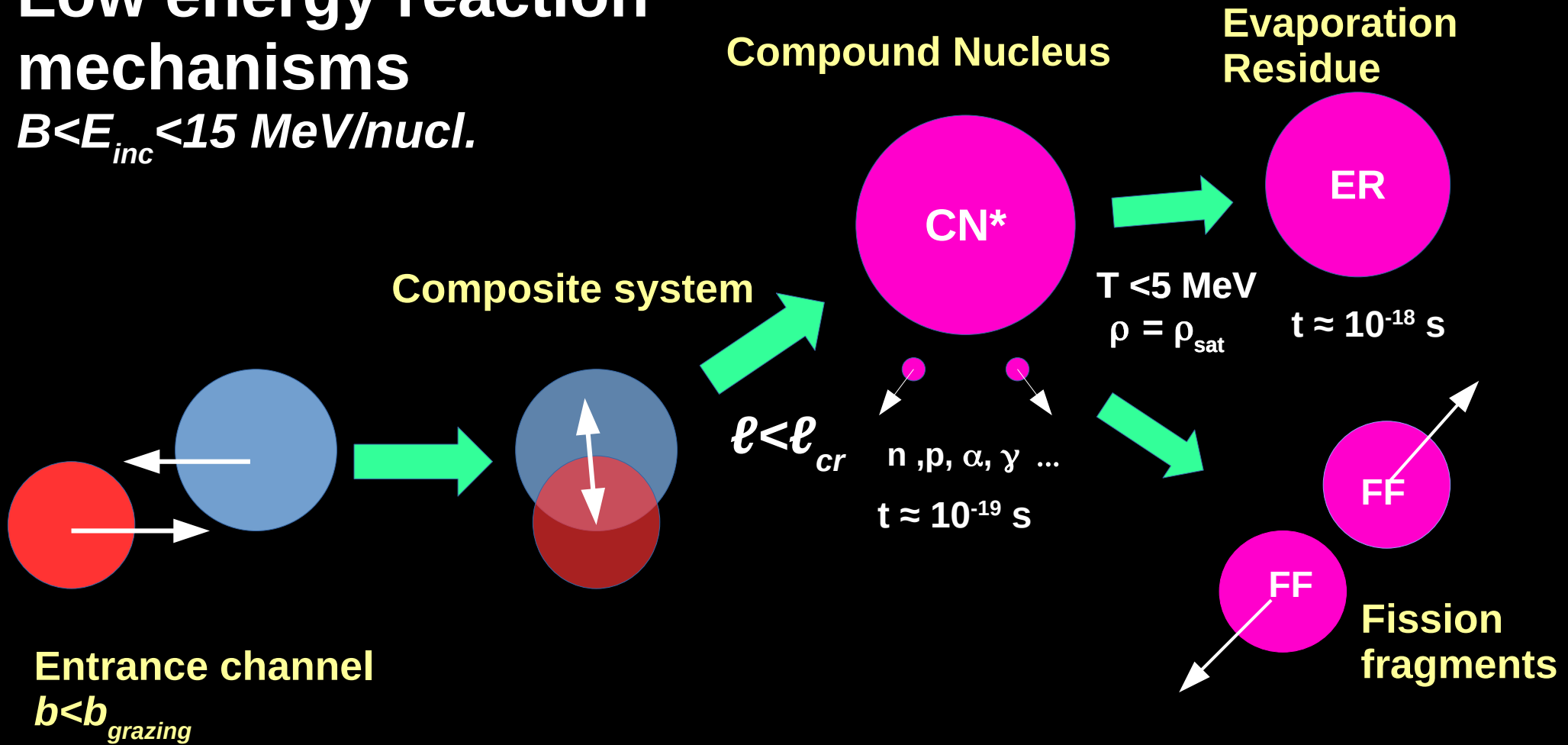


Entrance channel

$b < b_{grazing}$

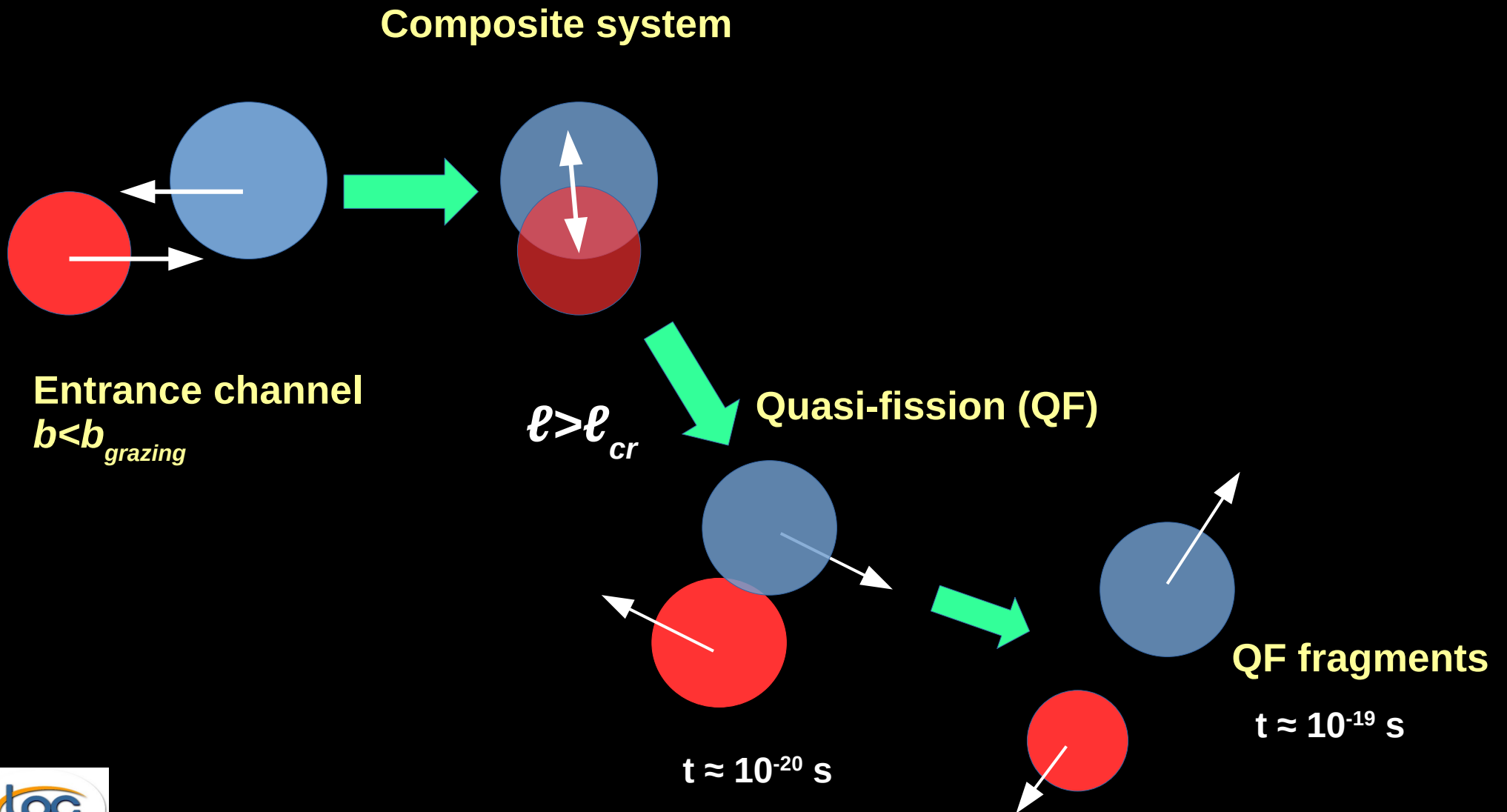
Low energy reaction mechanisms

$$B < E_{inc} < 15 \text{ MeV/nucl.}$$



Low energy reaction mechanisms

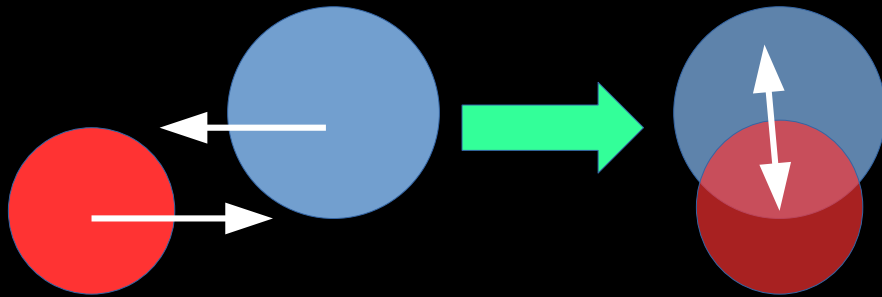
$B < E_{inc} < 15 \text{ MeV/nucl.}$



Fermi energy reaction mechanisms

$15 < E_{inc} < 40 \text{ MeV/nucl.}$

Composite system

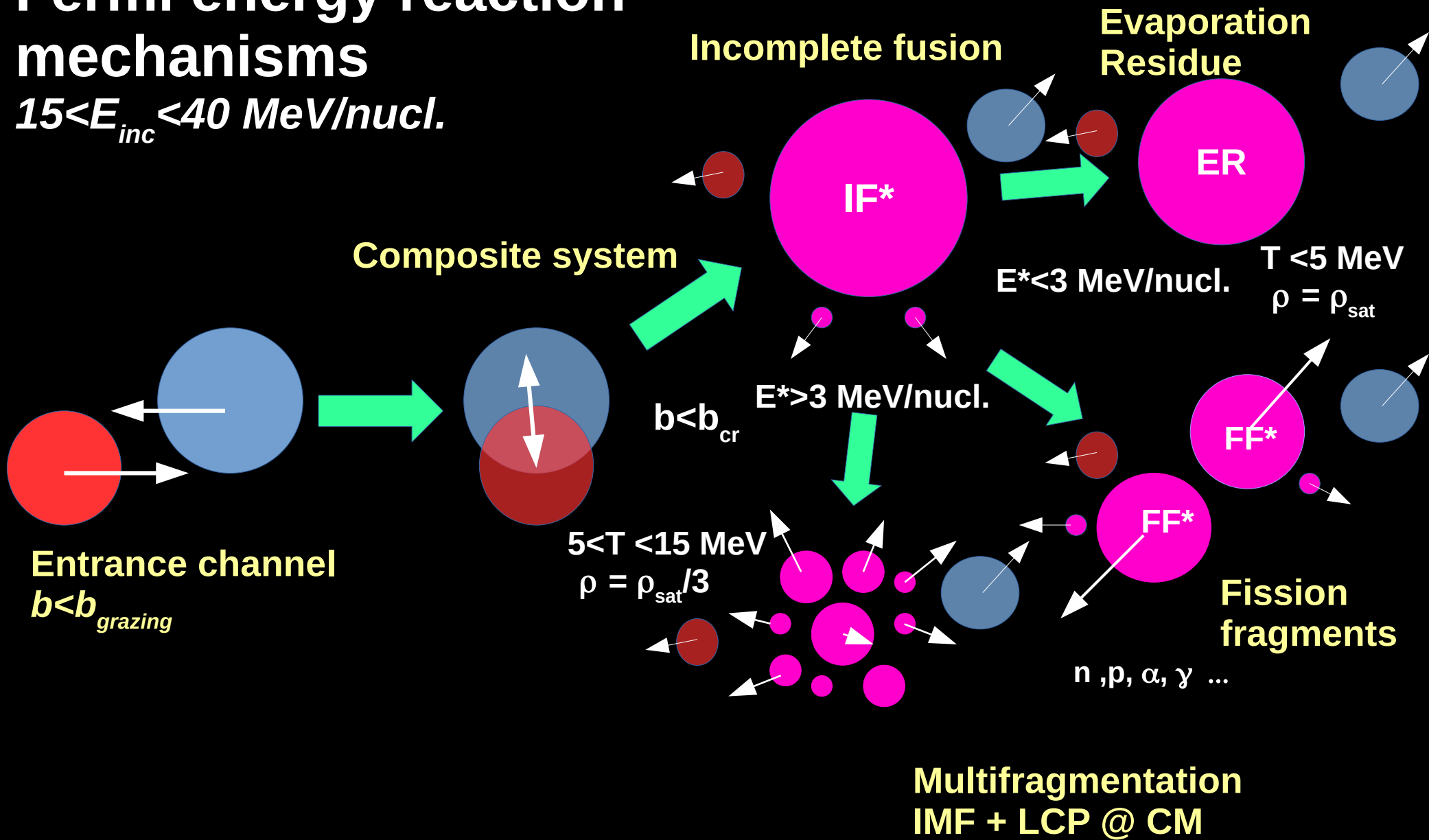


Entrance channel

$b < b_{grazing}$

Fermi energy reaction mechanisms

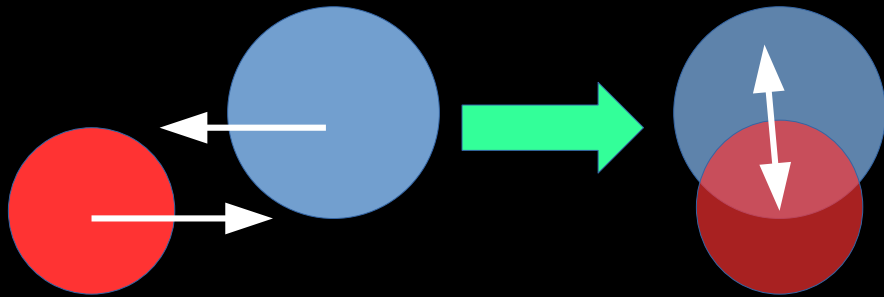
$15 < E_{inc} < 40 \text{ MeV/nucleon}$



Fermi energy reaction mechanisms

$15 < E_{inc} < 40 \text{ MeV/nucl.}$

Composite system

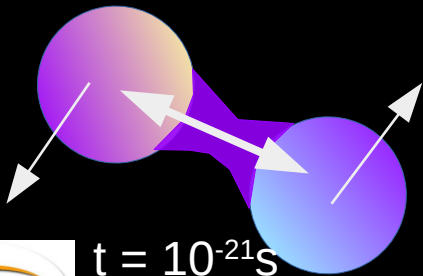


Entrance channel

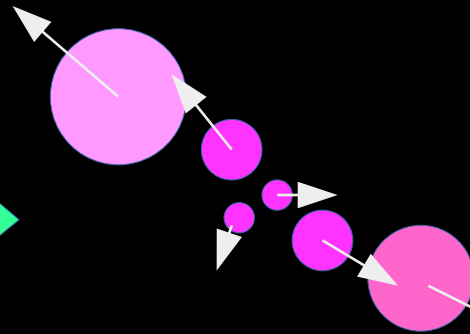
$b < b_{grazing}$

$b > b_{cr}$

Deep Inelastic scattering



$t = 10^{-21} \text{ s}$



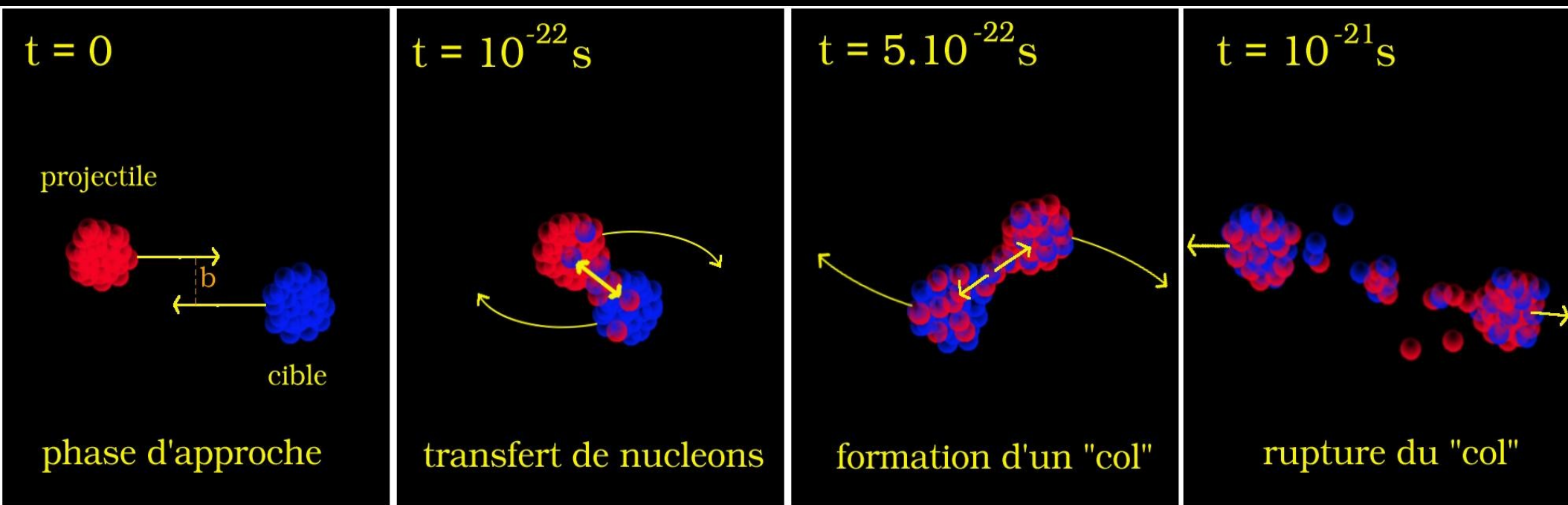
Neck emission
QP+QT+IMF @ mid-rapidity

$5 < T < 15 \text{ MeV}$

$\rho = \rho_{sat} / 10$

Deep Inelastic collisions ... toward the limits

« semi-peripheral » collision ($b=6$ fm)



Extreme rotation
 10^{23} rpm !

More diluted
 $\rho \ll \rho_0$

More n-rich
($N \ll Z$, $N \gg Z$)

Simulation Xe+Sn at 50 MeV/nucleon b=7 fm

Nuclear Collision Simulation

(Z=54,A=129) on (Z=50,A=119) @ E/A= 50MeV, b=4.0fm
HIPSE model - Phys. Rev. C69, 054604 (2004)
D. Lacroix (GANIL) and D. Durand (LPC Caen)

Simulation done by O. Lopez (lopezo@in2p3.fr)
Details at <http://www.lpc-caen.in2p3.fr>

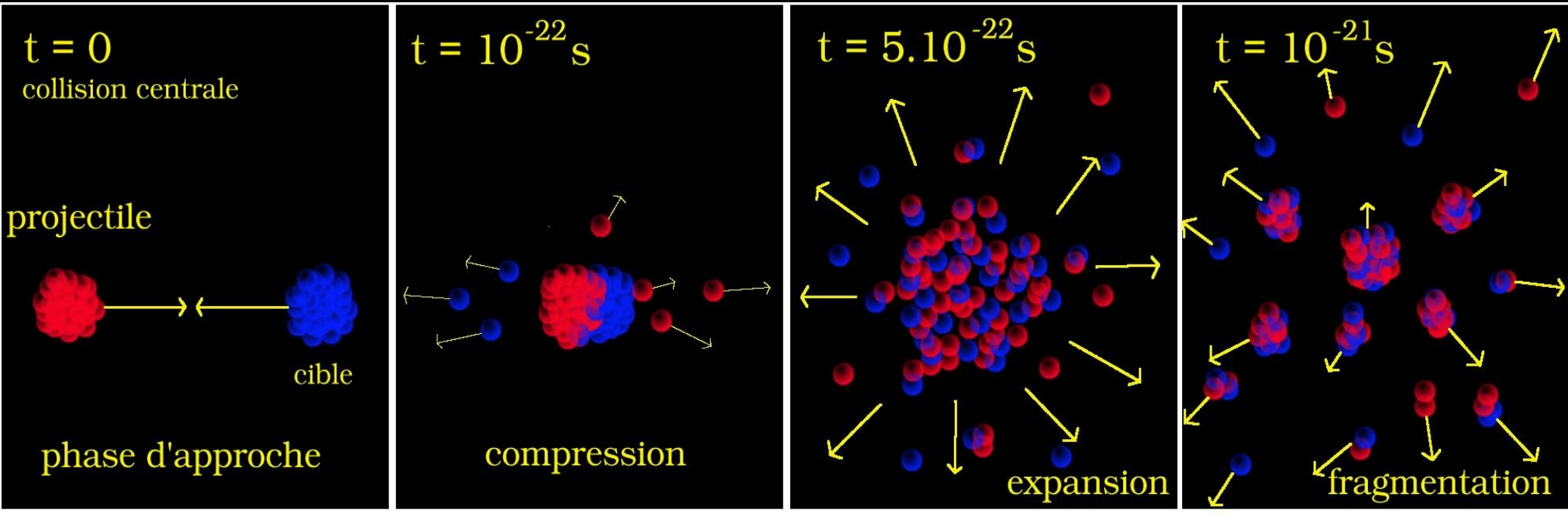
Nuclear Collision Simulation

(Z=54,A=129) on (Z=50,A=119) @ E/A= 50MeV, b=4.0fm
HIPSE model - Phys. Rev. C69, 054604 (2004)
D. Lacroix (GANIL) and D. Durand (LPC Caen)

Simulation done by O. Lopez (lopezo@in2p3.fr)
Details at <http://www.lpc-caen.in2p3.fr>

Central collisions ... **Little Big Bang** !

Central collision (b=0)



Denser
 $\rho / \rho_0 > 1-3$

Hotter
 $T > 5 \text{ MeV}$
 $1 \text{ MeV} = 10^{10} \text{ K} !$

Fragmented
and diluted
 $N > 10-100$



Multifragmentation



Simulation Xe+Sn at 39 MeV/nucleon b=0 fm

Nuclear Collision Simulation

(Z=54,A=129) on (Z=50,A=119) @ E/A= 39MeV, b=0.0fm

HIPSE model - Phys. Rev. C69, 054604 (2004)
D. Lacroix (GANIL) and D. Durand (LPC Caen)

Simulation done by O. Lopez (lopezo@in2p3.fr)
Details at <http://www.lpc-caen.in2p3.fr>

Nuclear Collision Simulation

(Z=54,A=129) on (Z=50,A=119) @ E/A= 39MeV, b=0.0fm

HIPSE model - Phys. Rev. C69, 054604 (2004)
D. Lacroix (GANIL) and D. Durand (LPC Caen)

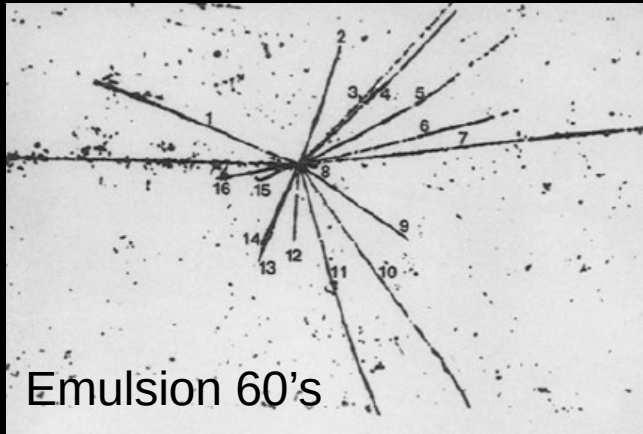
Simulation done by O. Lopez (lopezo@in2p3.fr)
Details at <http://www.lpc-caen.in2p3.fr>

More videos available on this YouTube channel :

<https://www.youtube.com/watch?v=azCjJx6REKg>

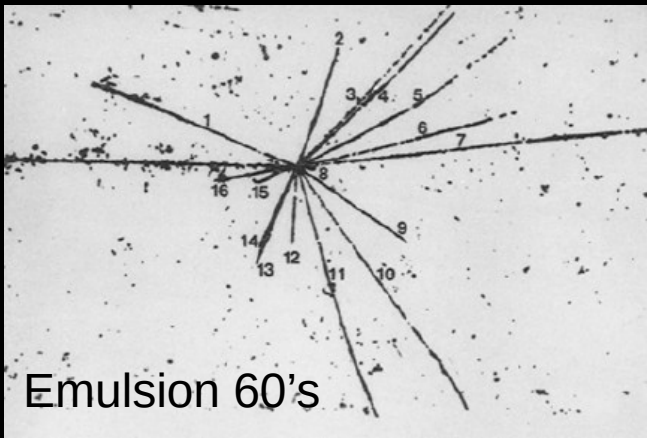


Multifragmentation as Liquid-gas Phase Transition

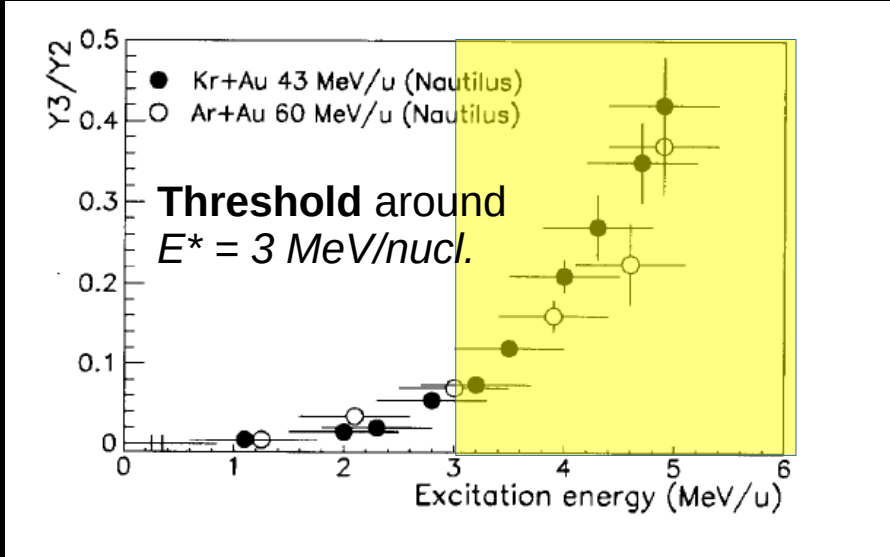
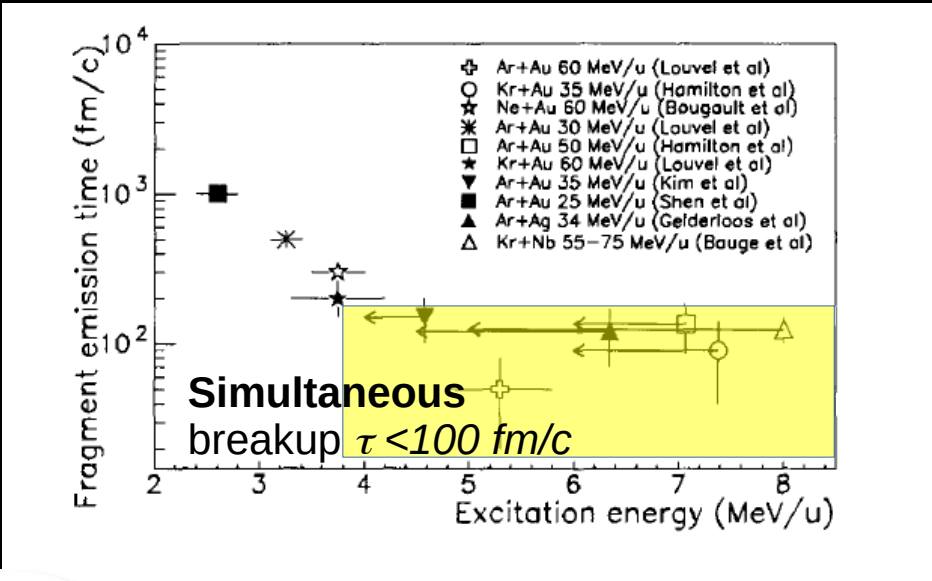
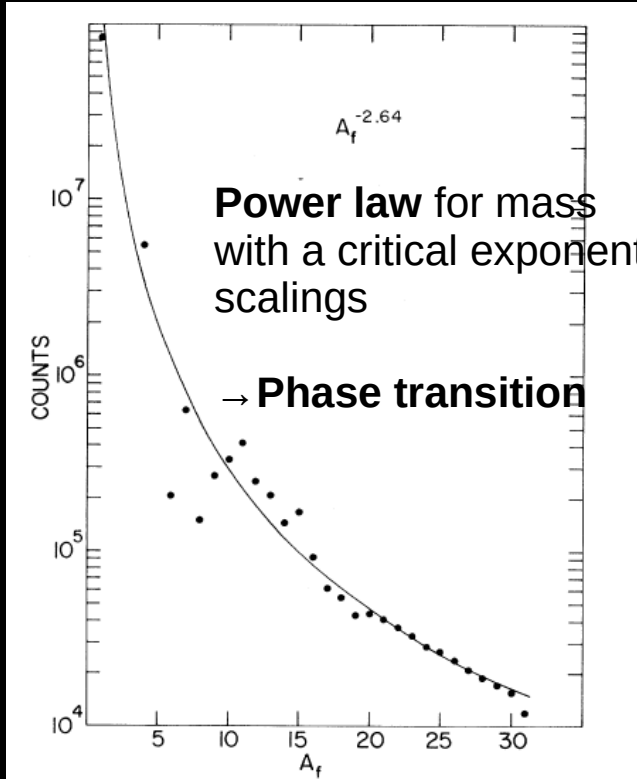


**Breakup reactions with
more than 2 fragments...**

Multifragmentation as Liquid-gas Phase Transition

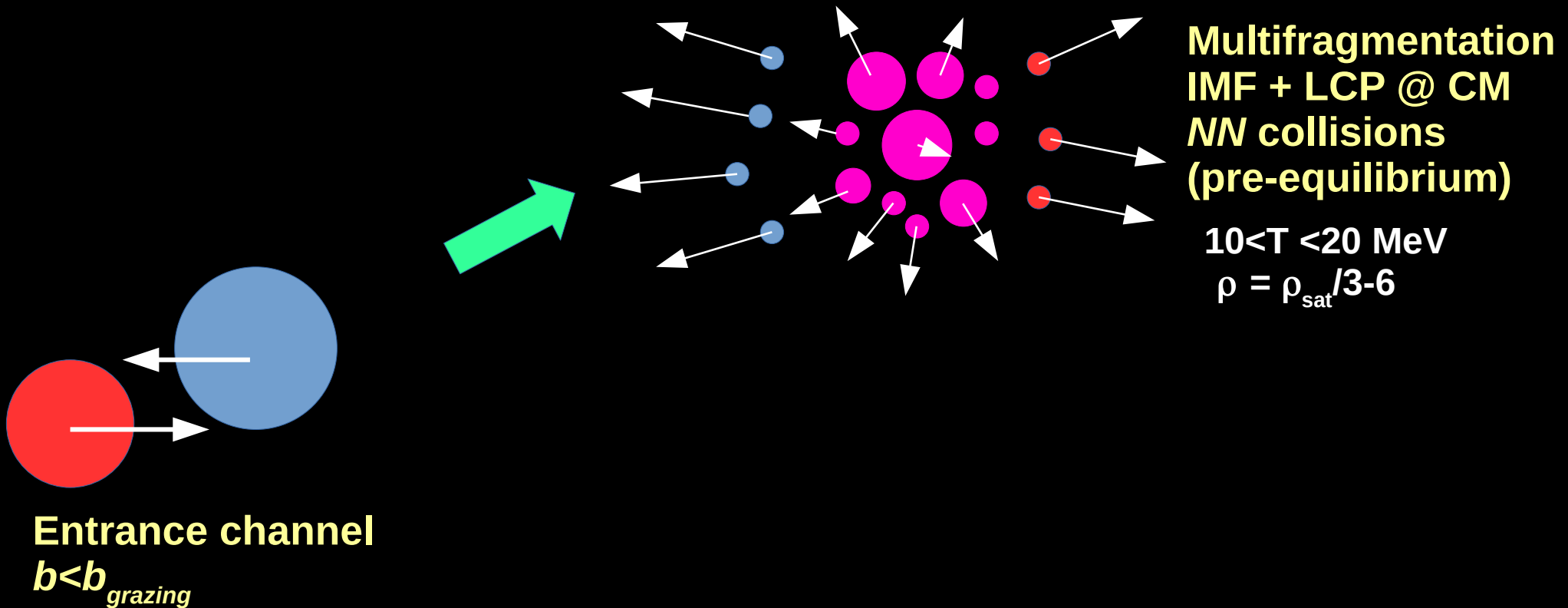


Breakup reactions with more than 2 fragments...



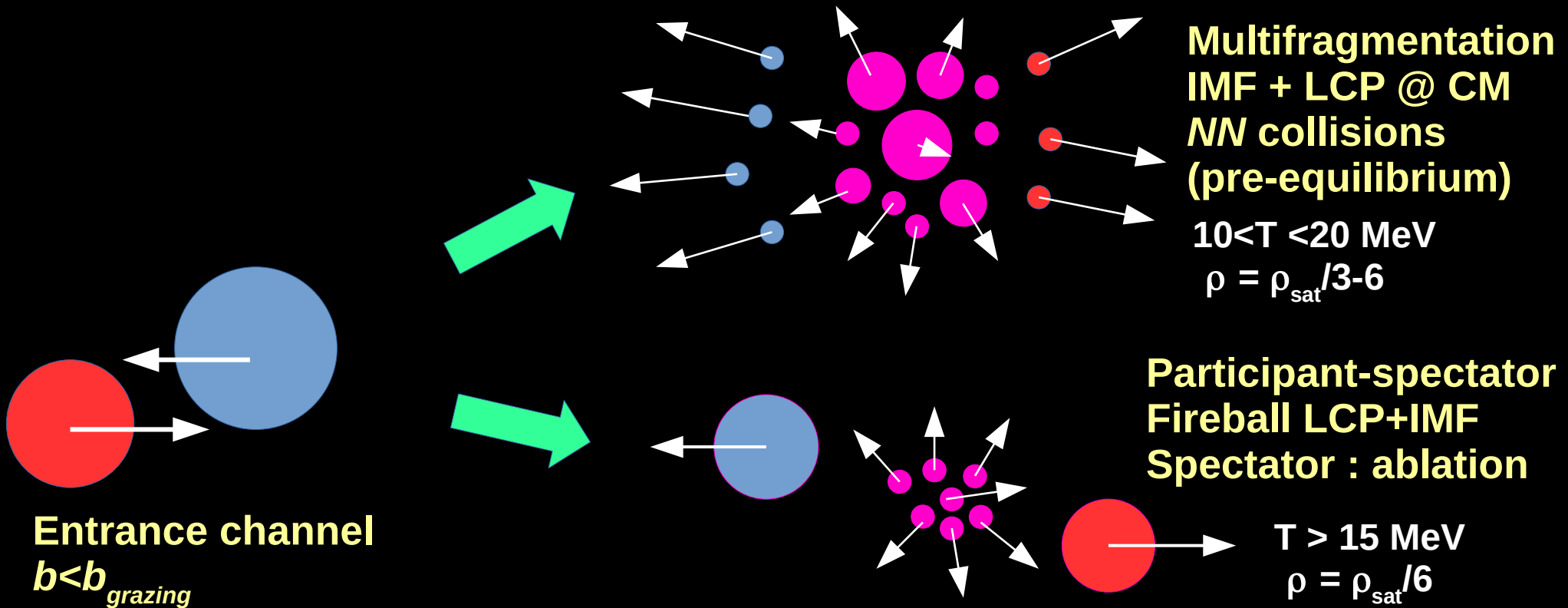
Intermediate energy reaction mechanisms

$40 < E_{inc} < 150 \text{ MeV/nucl.}$



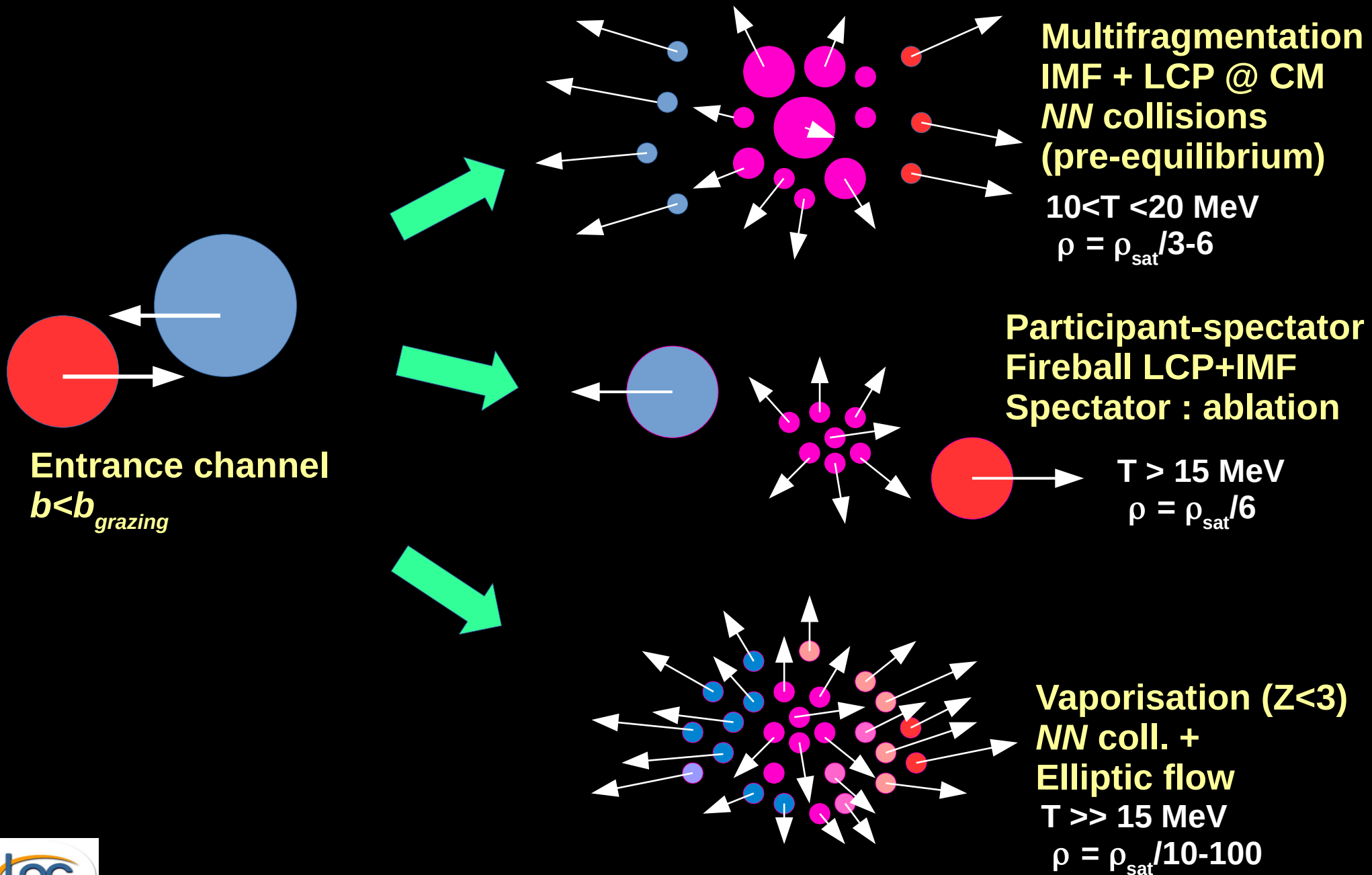
Intermediate energy reaction mechanisms

$40 < E_{inc} < 150 \text{ MeV/nucl.}$



Intermediate energy reaction mechanisms

$40 < E_{inc} < 150 \text{ MeV/nucl.}$

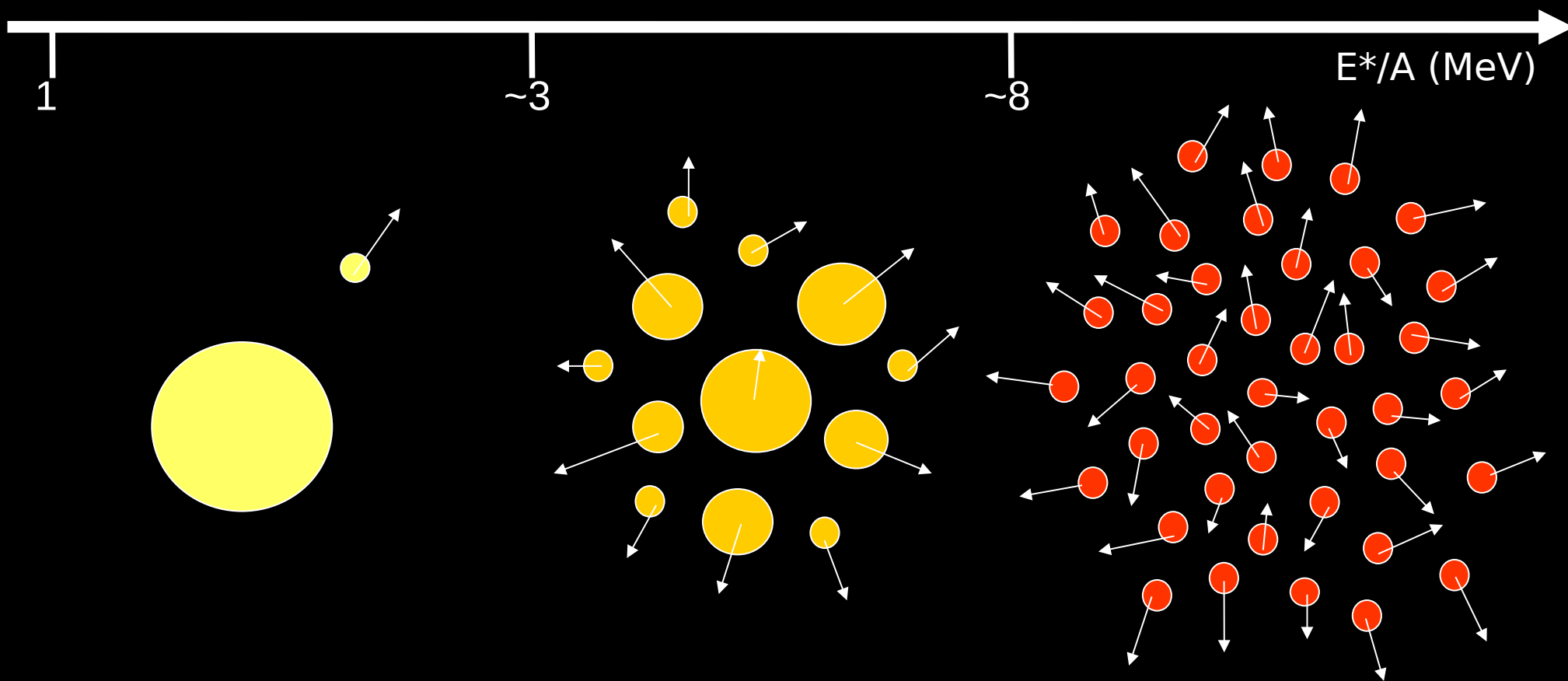


Hot nuclear matter (nuclei) ; from liquid to gas phase

Evaporation

Multifragmentation

Vaporization



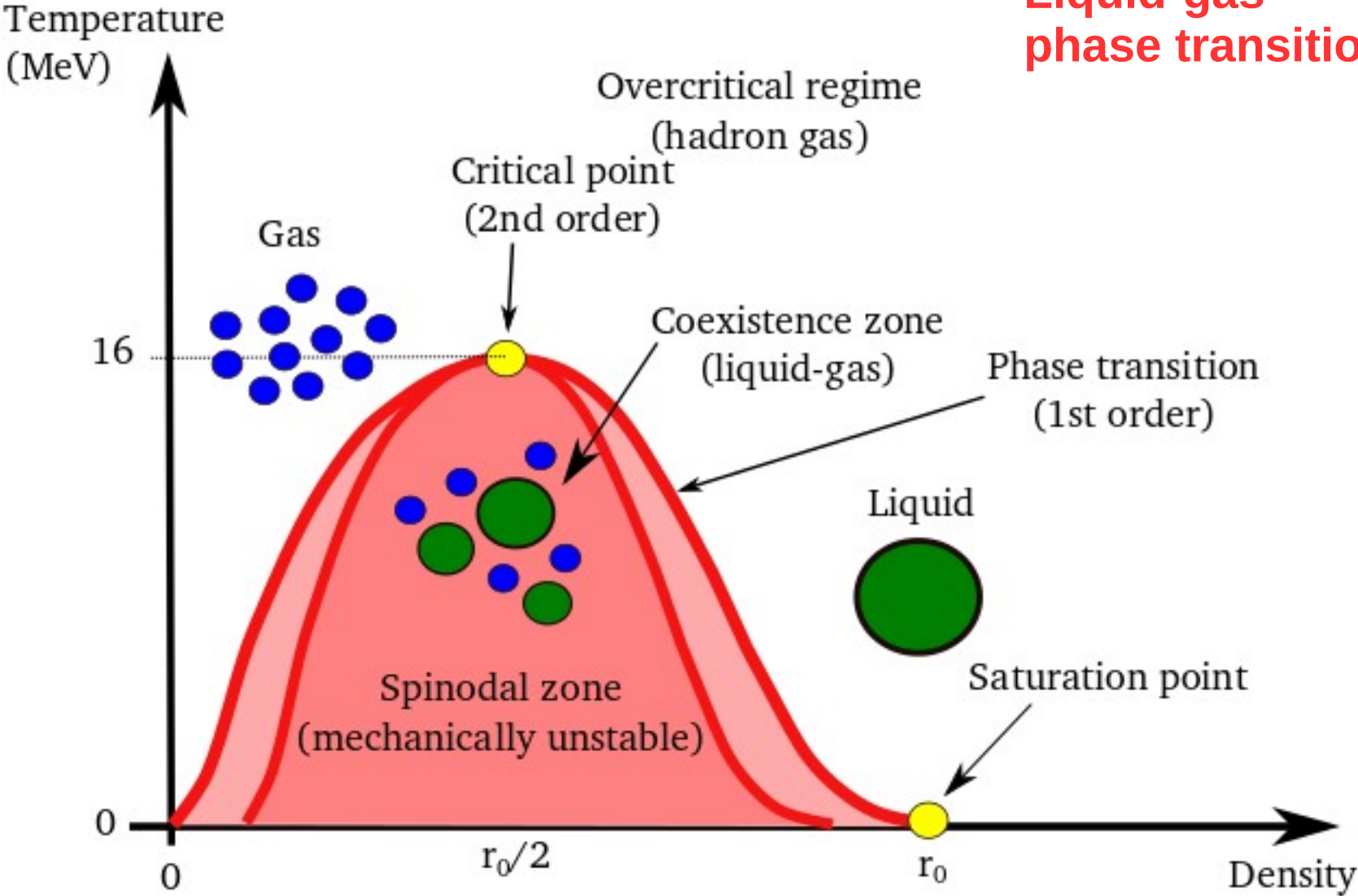
$\rho \sim \rho_{\text{sat}}$
 $T < 5 \text{ MeV}$

$\rho < \rho_{\text{sat}}$
 $T = 5-10 \text{ MeV}$

$\rho \ll \rho_{\text{sat}}$
 $T > 10 \text{ MeV}$

Multifragmentation : Mean-Field density instabilities

Liquid-gas phase transition



Transport properties

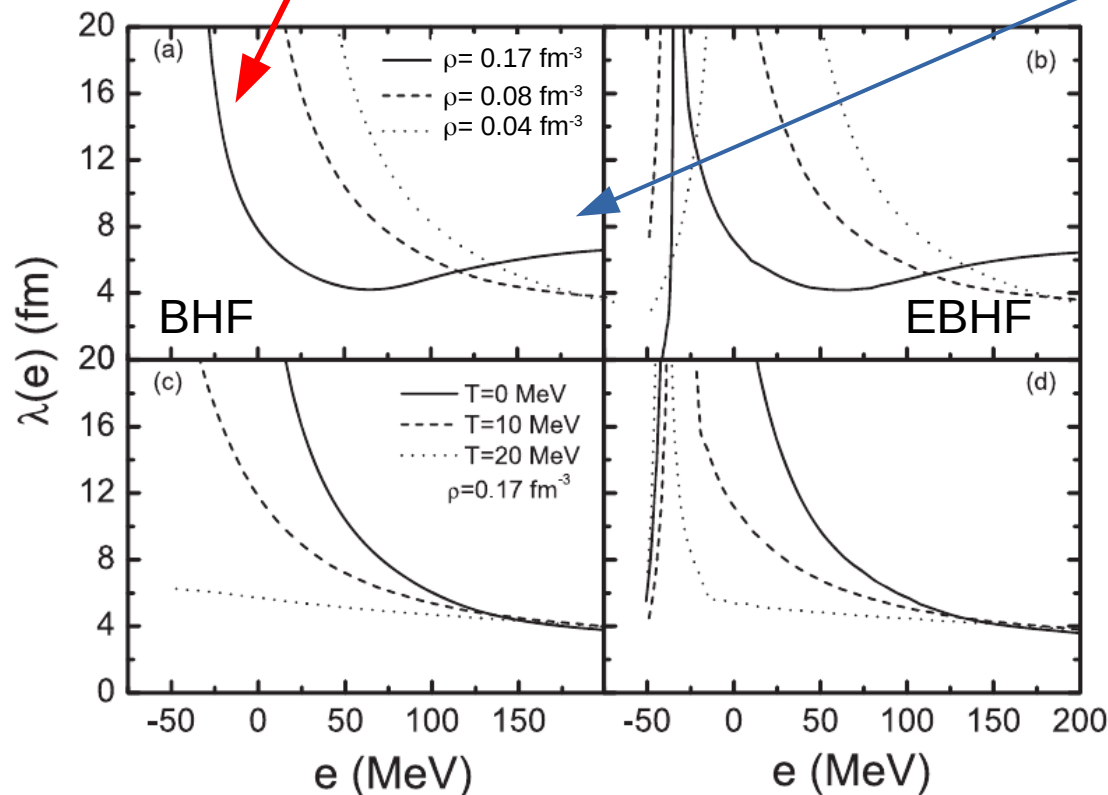
Energy dissipation

Energy dissipation in HIC

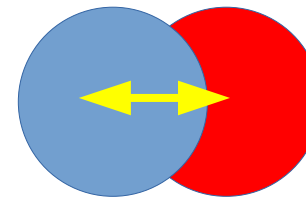
Mean Free Path : 2 phenomena coexist

Mean-Field : 1-body dissipation
 Prominent for $E_{inc} < E_{Fermi}$

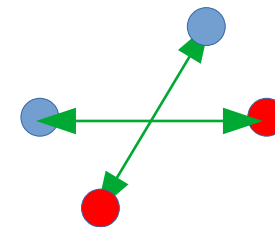
NN collisions : 2-body dissipation
 Increasingly important above E_{Fermi}



$E_{Fermi} \approx 38 \text{ MeV}$



1-body dissipation
 below E_{fermi}
 MF dissipation



2-body dissipation
 above E_{fermi}
 Elastic NN collisions

Role of Pauli blocking and high-order correlations between nucleons (fermions) In-medium effects

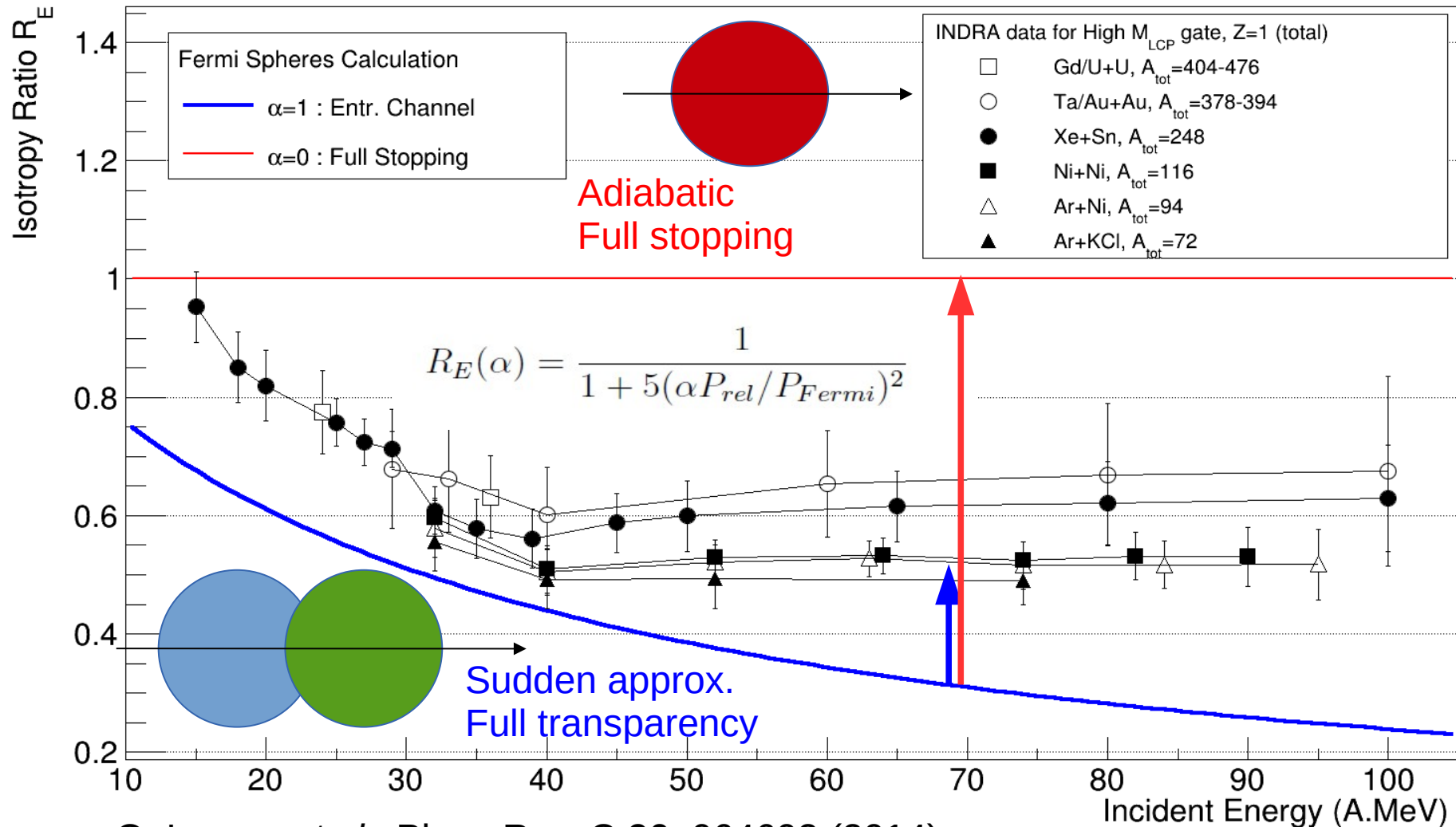
X.J. Bao, *et al.*, J. Phys. G: Nucl. Part. Phys. **41** (2014)

Probing E dissipation : stopping power in central HIC

Isotropy ratio R_E : ratio between **transverse** and **longitudinal** kinetic energies

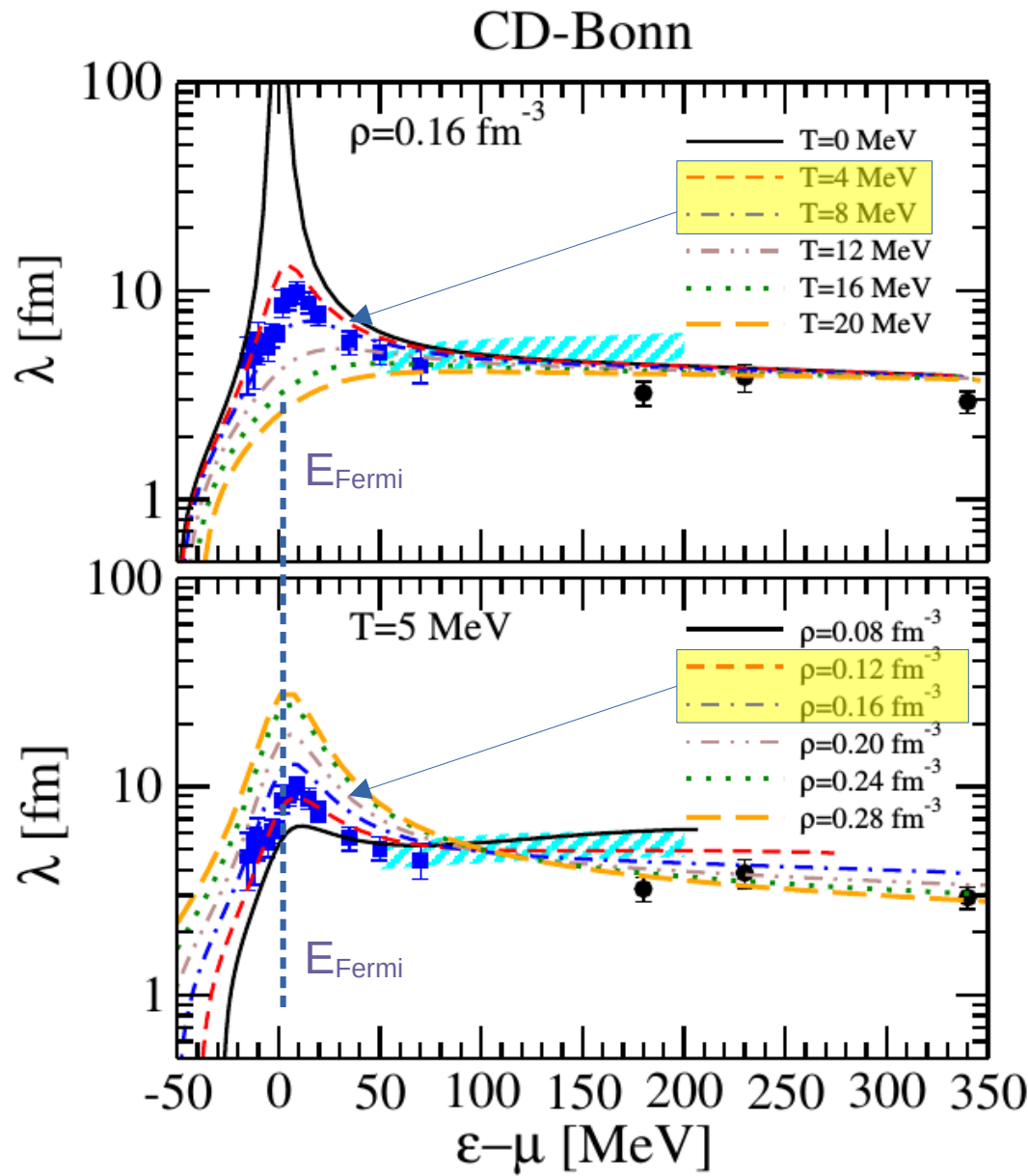
42 (quasi)-symmetric systems, only protons for $\langle R_E \rangle$

Nuclear Stopping



O. Lopez, et al., Phys. Rev. C **90**, 064602 (2014)

Mean free path and EoS



QFT-SCGF + CD-Bonn int.

A. Rios and V. Soma, *PRL* **108**, 012501 (2016)

- Calculations at $\rho = \rho_{\text{sat}}$ for different temperatures

$T = 4-8 \text{ MeV}$

- Calculations at $T = 5 \text{ MeV}$ for different densities

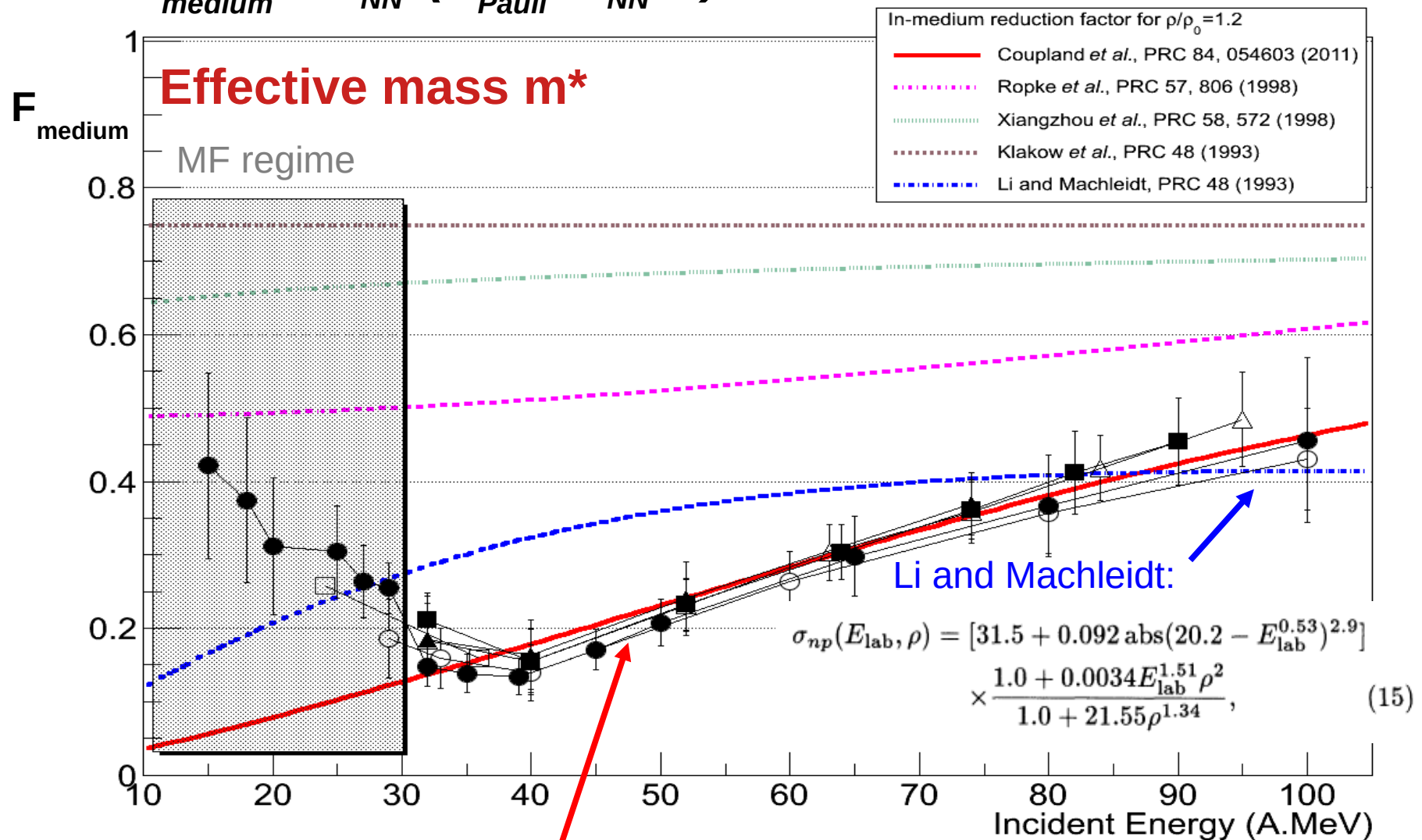
$\rho = 0.8-1.2 \rho_{\text{sat}}$

Enhanced sensitivity for $E \approx E_{\text{Fermi}}$

Quenching factor for σ_{nn}^* in nuclear medium

$$F_{medium} = \sigma_{NN}^* / (P_{Pauli} \cdot \sigma_{NN}^{free})$$

O. Lopez, et al., Phys. Rev. C **90**, 064602 (2014)

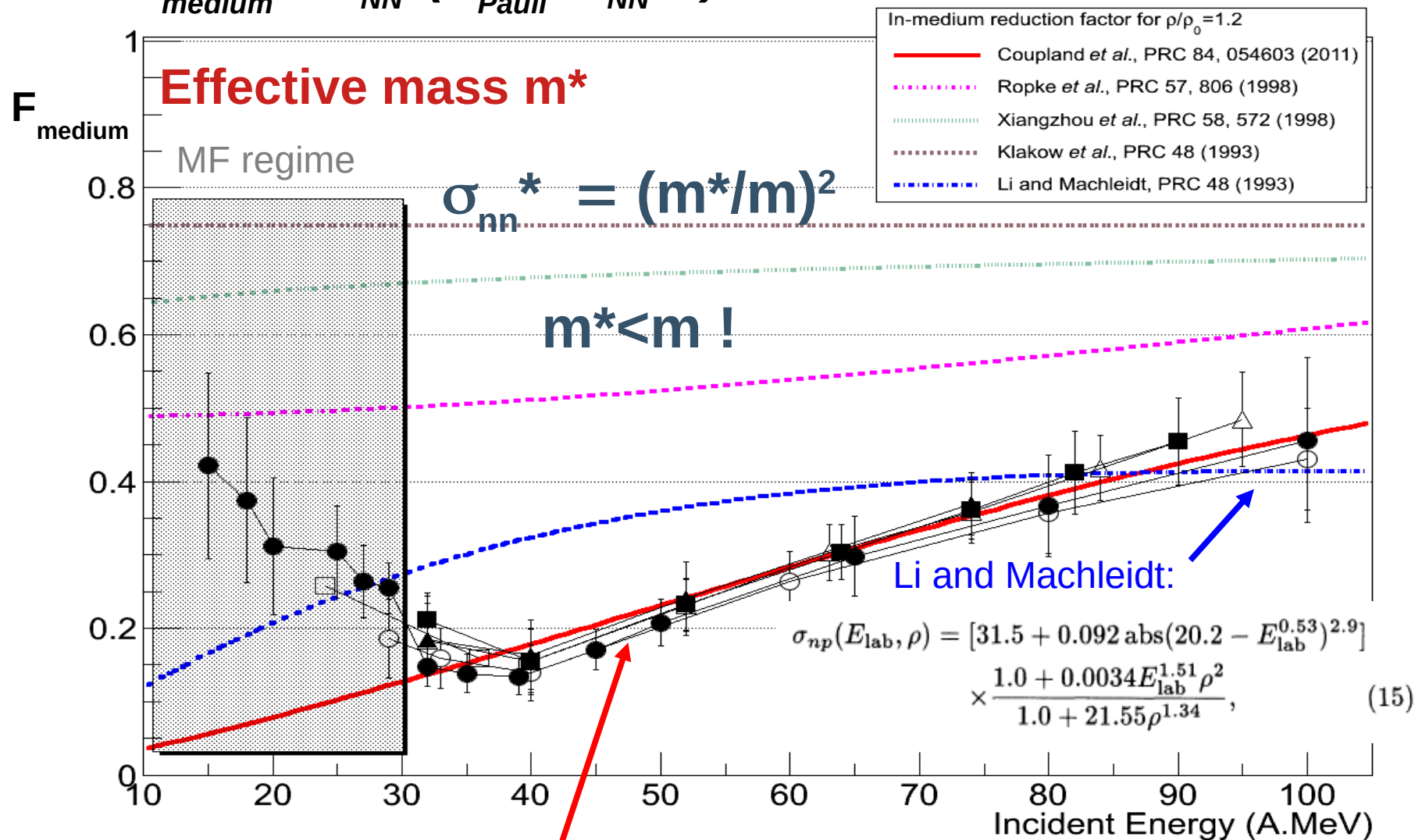


Danielewicz (phenom.): $F = \sigma_0 \tanh(\sigma_{free} / \sigma_0)$, with $\sigma_0(mb) = 8.5/\rho^{2/3}$

Quenching factor for σ_{nn}^* in nuclear medium

$$F_{medium} = \sigma_{NN}^* / (P_{Pauli} \cdot \sigma_{NN}^{free})$$

O. Lopez, et al., Phys. Rev. C **90**, 064602 (2014)



Danielewicz (phenom.): $F = \sigma_0 \tanh(\sigma_{free}/\sigma_0)$, with $\sigma_0(mb) = 8.5/\rho^{2/3}$

Isospin transport

Density Dependence of E_{sym} : experimental probes

Probing EOS at low density and finite temperature

Isospin transport (flux) :

$$j_n - j_p \propto E_{sym}(\rho) \nabla I - I \left(\frac{\partial E_{sym}}{\partial \rho} \right) \nabla \rho$$

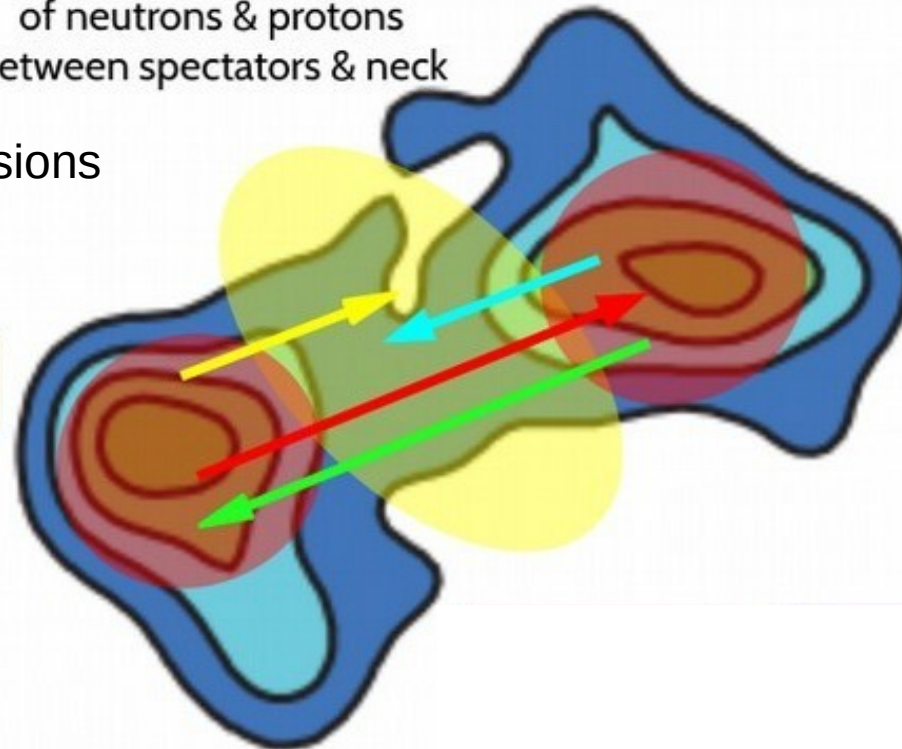
Competing migrations
of neutrons & protons
between spectators & neck

Binary dissipative collisions
around Fermi energy

Neck and QP formation

Competition between

- Diffusion ∇I (QP)
- Migration $\nabla \rho$ (neck)



Density Dependence of E_{sym} : experimental probes

Probing EOS at low density and finite temperature

→ See T. Génard's poster

Isospin transport (flux) :

$$j_n - j_p \propto E_{sym}(\rho) \nabla I - I \left(\frac{\partial E_{sym}}{\partial \rho} \right) \nabla \rho$$

Neck isotopic content

$Z = 1 - 8, A = 1 - 16$ (clusters)

$\rho \sim \rho_{sat}/10, T \gg 0$

Competing migrations
of neutrons & protons
between spectators & neck

Measuring (Z,A) for all
reaction products
at forward angles :

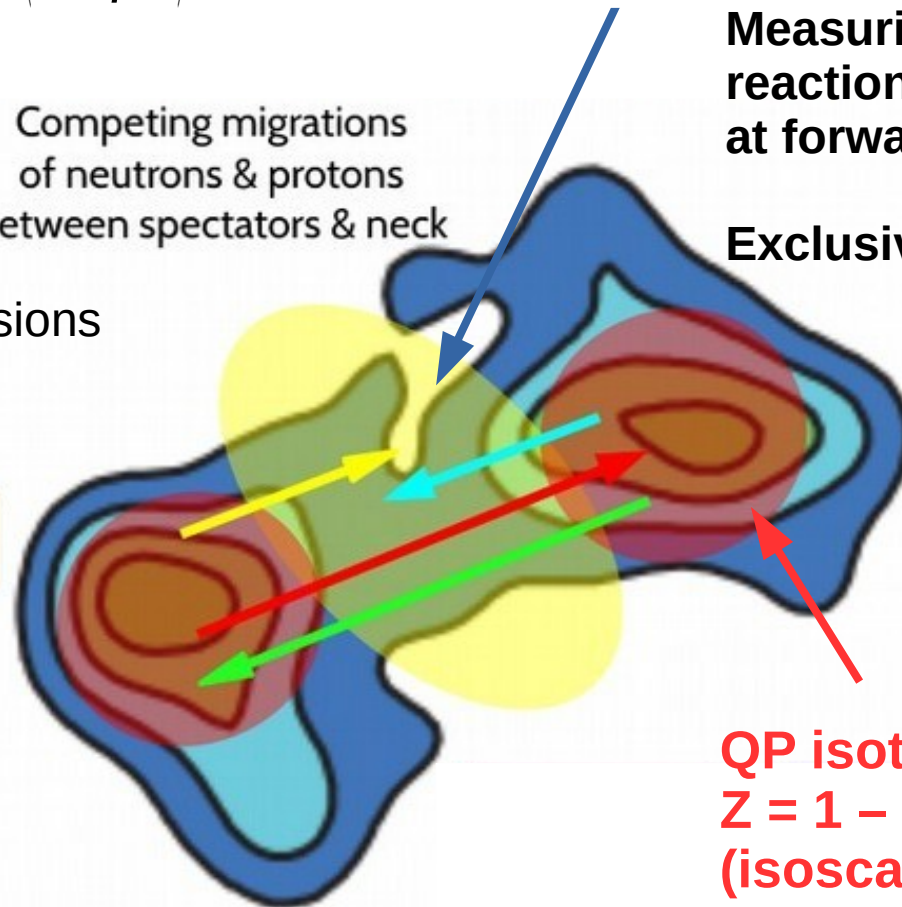
Exclusive events !

Binary dissipative collisions
around Fermi energy

Neck and QP formation

Competition between

- Diffusion ∇I (QP)
- Migration $\nabla \rho$ (neck)

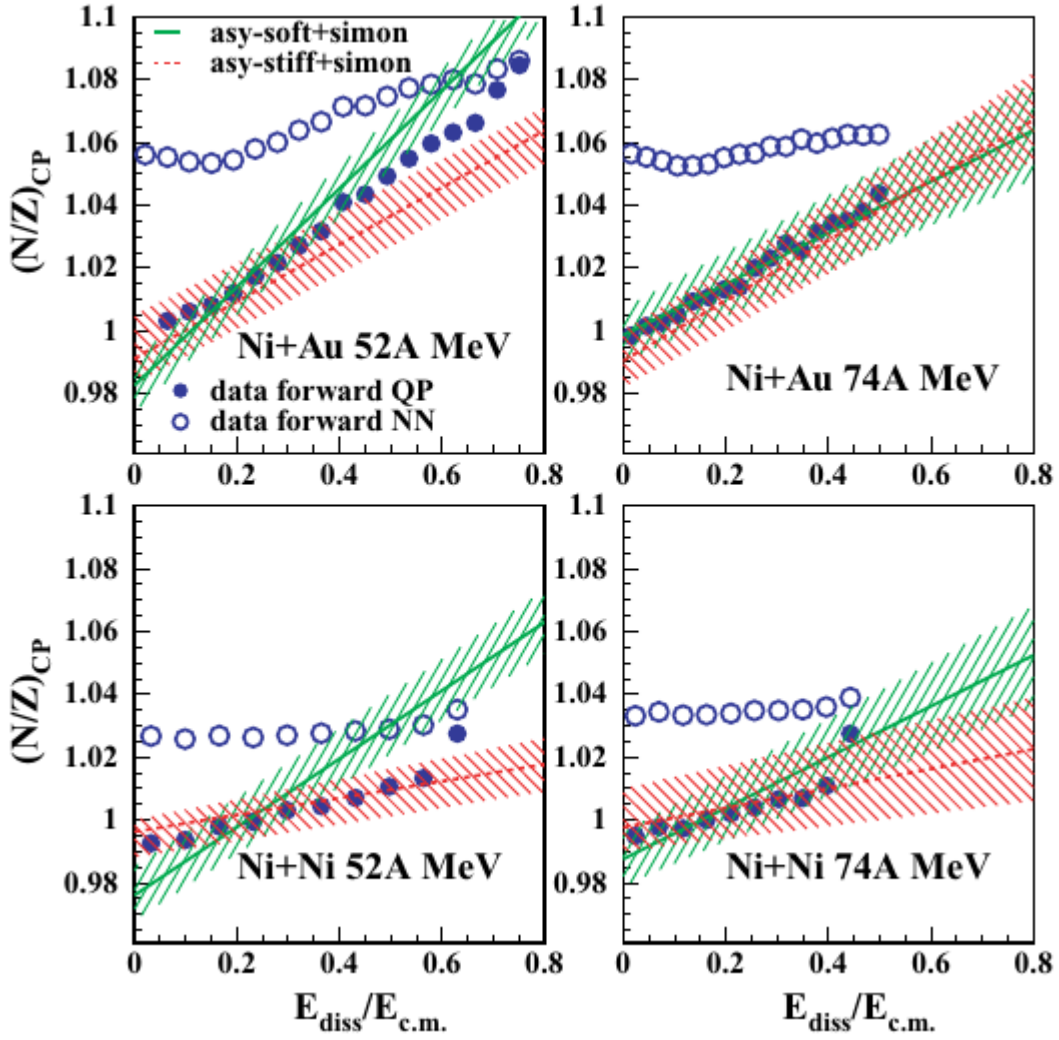


QP isotopic id.
 $Z = 1 - 30, A = 1 - 50$
(isoscaling)
 $\rho \sim \rho_{sat}, T > 0$

Isospin transport for semi-peripheral collisions

Isospin content for Quasi-Projectile

INDRA data, $^{58}\text{Ni}+^{58}\text{Ni}/^{197}\text{Au}$ at $E/A=52,74$ MeV
 BNV simulations at $b=5$ fm



- Quasi-Ni neutron-enrichment as a function of dissipation/centrality
- **Moderately stiff $\gamma=1$** better matches
- Isospin equilibration time:

$$\tau_{eq} = 130 \pm 10 \text{ fm/c}$$

From SMF

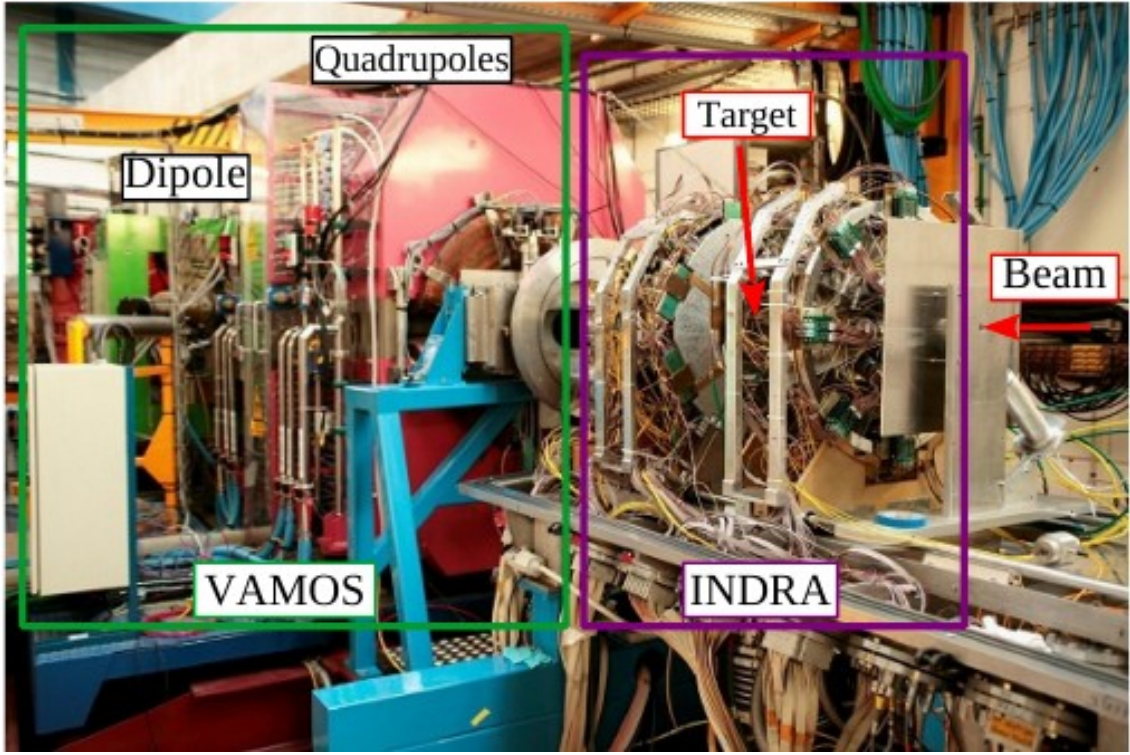
Small sensitivity
Impact parameter mixing

E. Galichet *et al.*, PRC **79**, 064615 (2009)

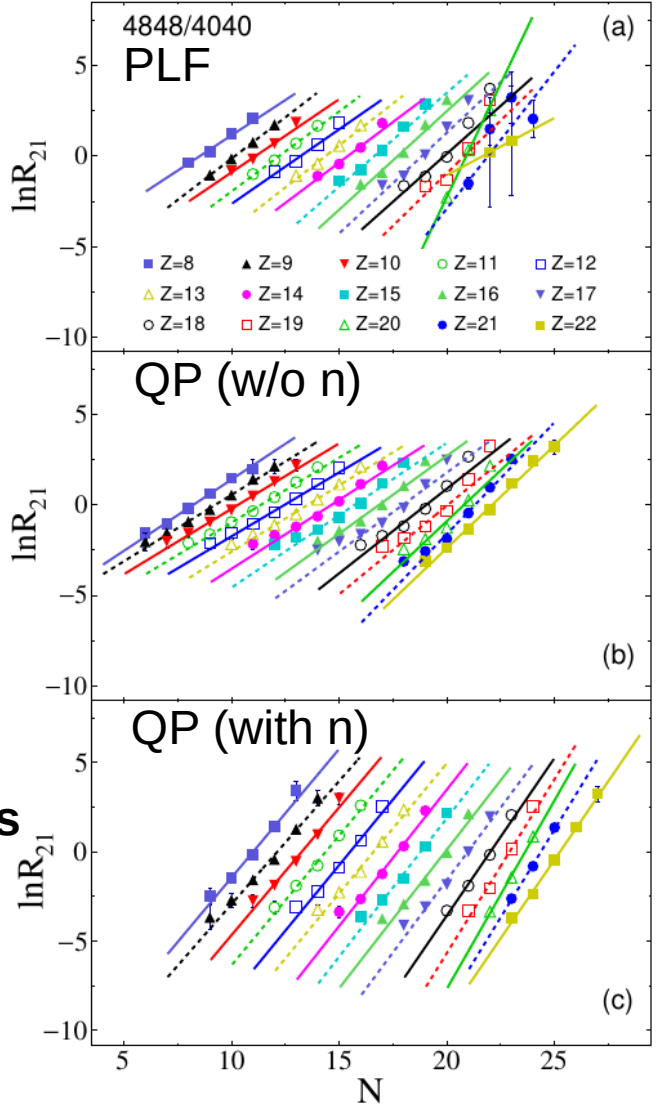


Isospin transport for semi-peripheral collisions

INDRA-VAMOS @ GANIL



Isoscaling $^{48}\text{Ca}+^{48}\text{Ca}$ 35 MeV/nucleon
 $^{40}\text{Ca}+^{40}\text{Ca}$



Importance of QP reconstruction for isoscaling analysis
 Need an event-by-event detection

Isoscaling : yield ratio Y of a given specie (N,Z)

$$R_{21}(N, Z) = \frac{Y_{(2)}(N, Z)}{Y_{(1)}(N, Z)} \propto \exp[\alpha N + \beta Z]$$

Q. Fable et al., Phys. Rev. C **106**, 024605 (2022)



Isospin transport for semi-peripheral collisions

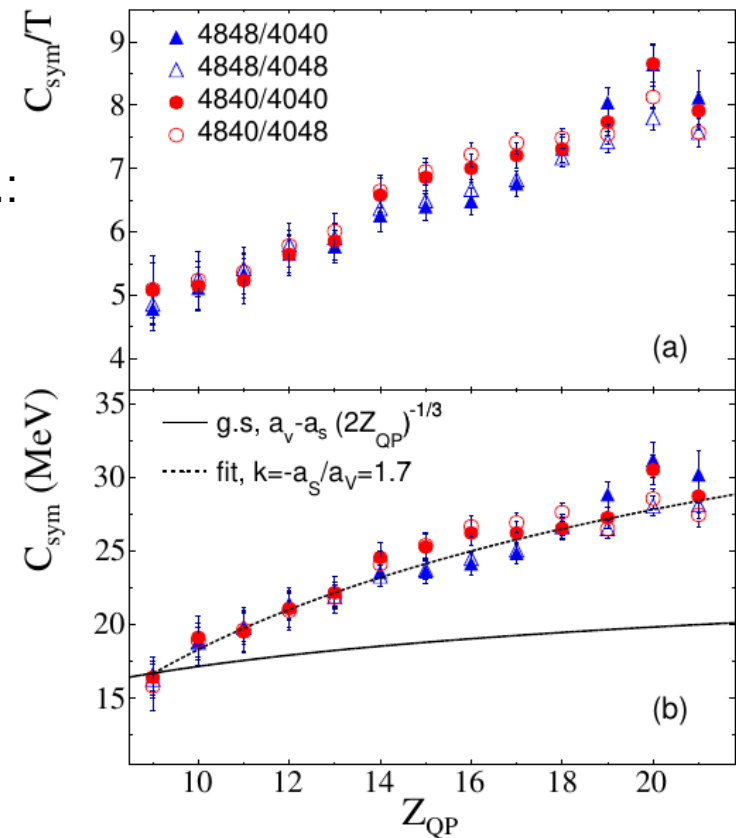
Isoscaling for projectile

Link between isoscaling α parameter to C_{sym} in the fragmentation regime and grand-canonical approx.:

$$\frac{4C_{sym}(Z)}{T} = \frac{\alpha(Z)}{\left(\frac{Z}{\langle A_1(Z) \rangle}\right)^2 - \left(\frac{Z}{\langle A_2(Z) \rangle}\right)^2}$$

- C_{sym} can be obtained from isoscaling analysis
- **AMD** simulations: $\rho / \rho_{sat} = 0.33-0.84$
- Surface-to-volume ratio: $|a_s|/a_v = 1.7$

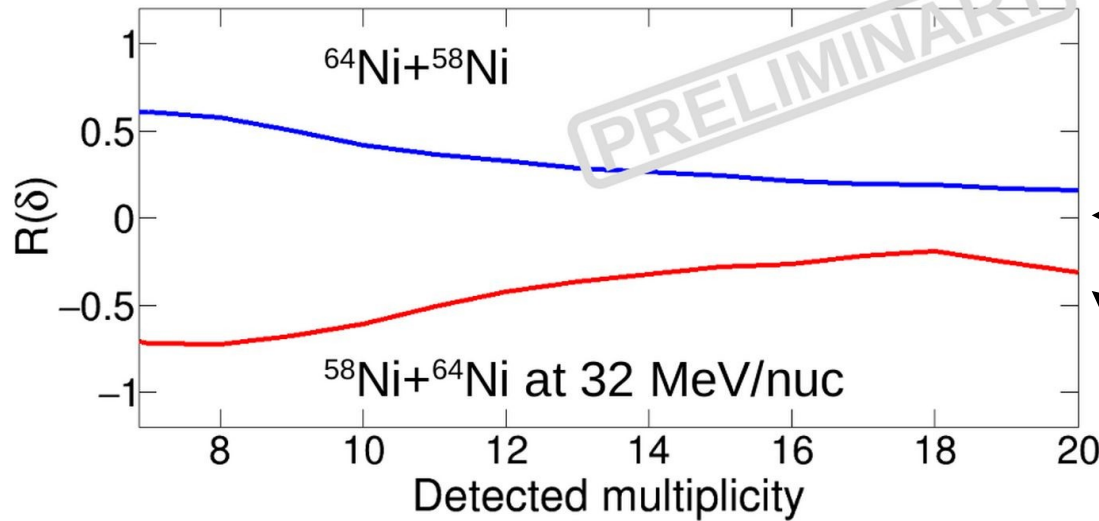
$$C_{sym}(A) = a_v - a_s A^{-1/3}$$



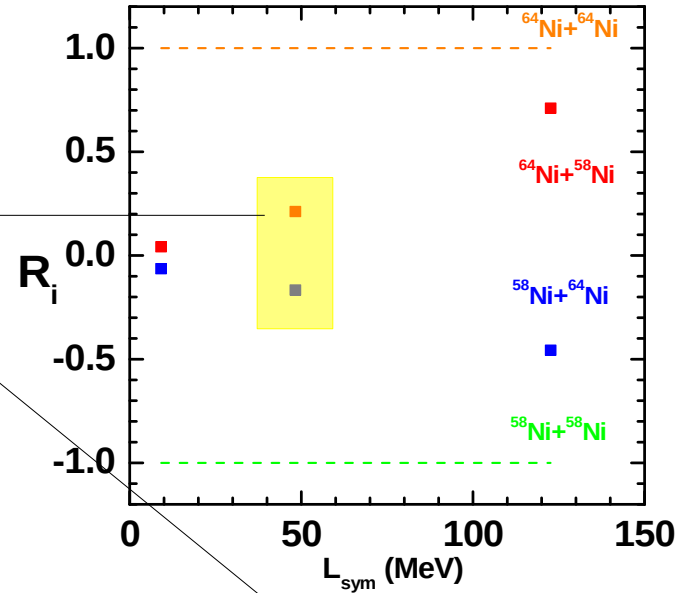
Q. Fable *et al.*, Phys. Rev. C **106**, 024605 (2022)

Strong surface contribution : connected to neutron skin ?

DDSE : toward new probes, isospin imbalance ratio



BUU, $b=3$ fm
S. Mallik, private comm. (2021)

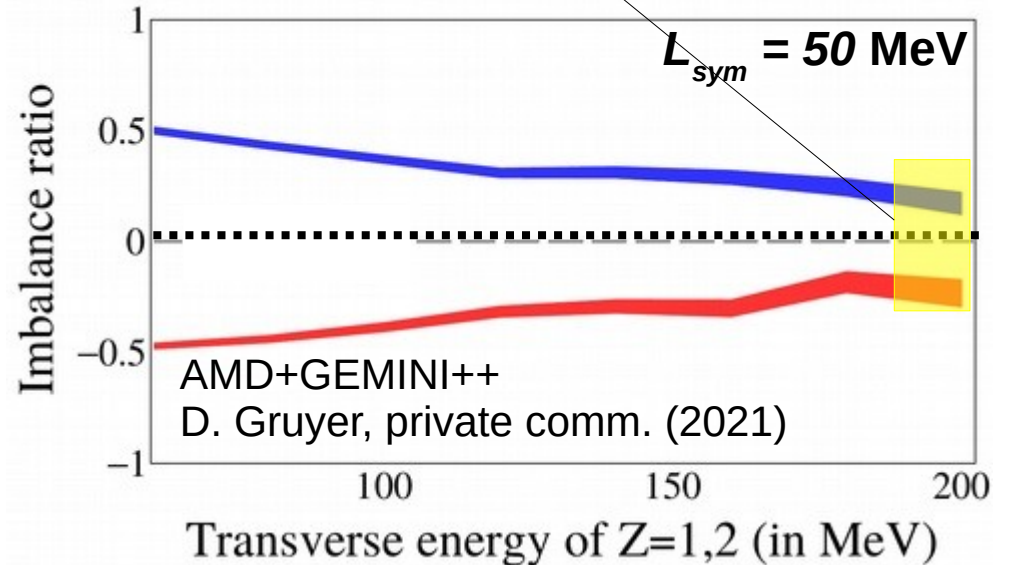


Asy-soft $L_{sym}=50$ MeV better ?

BUT :

Different centrality selections ...

→ See J. Lemarié's poster

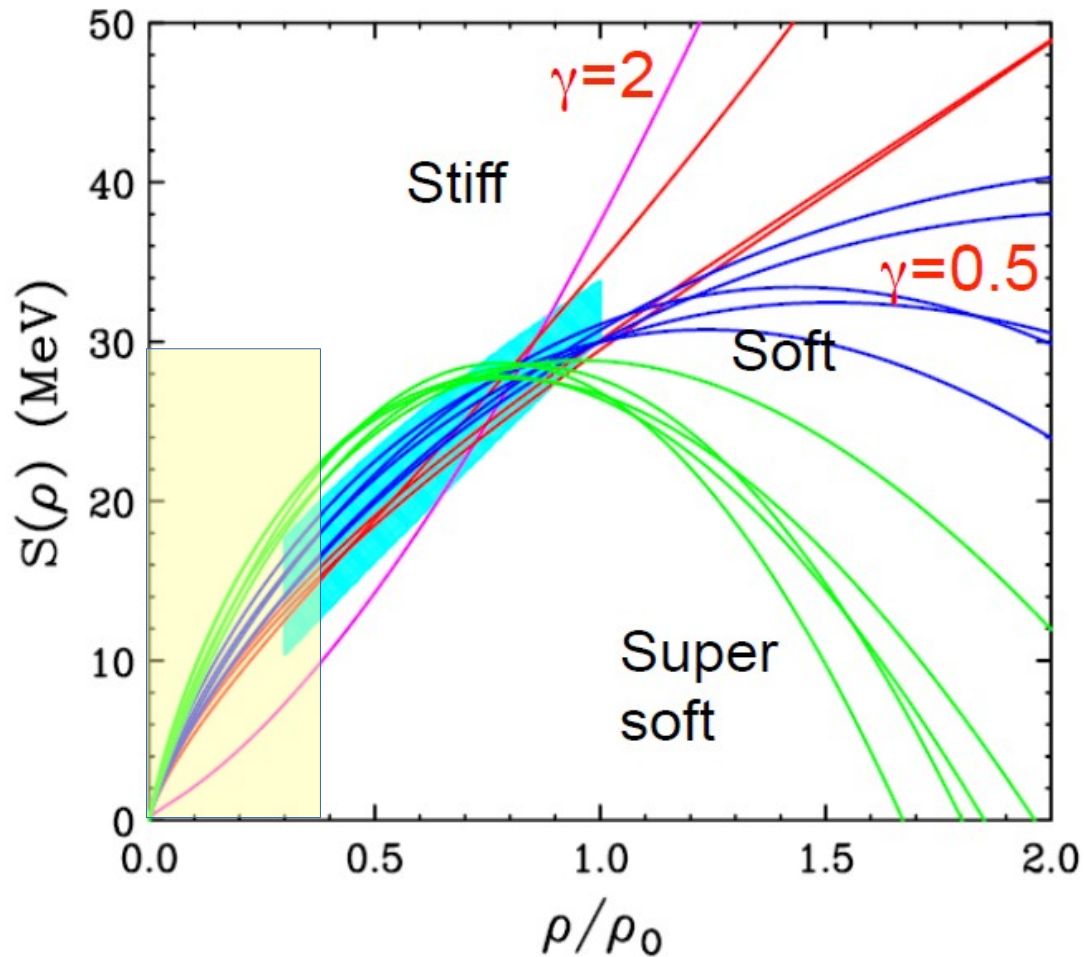


Probing the isovector dependence of EoS

Isospin Physics

Symmetry energy for $\rho \ll \rho_0$

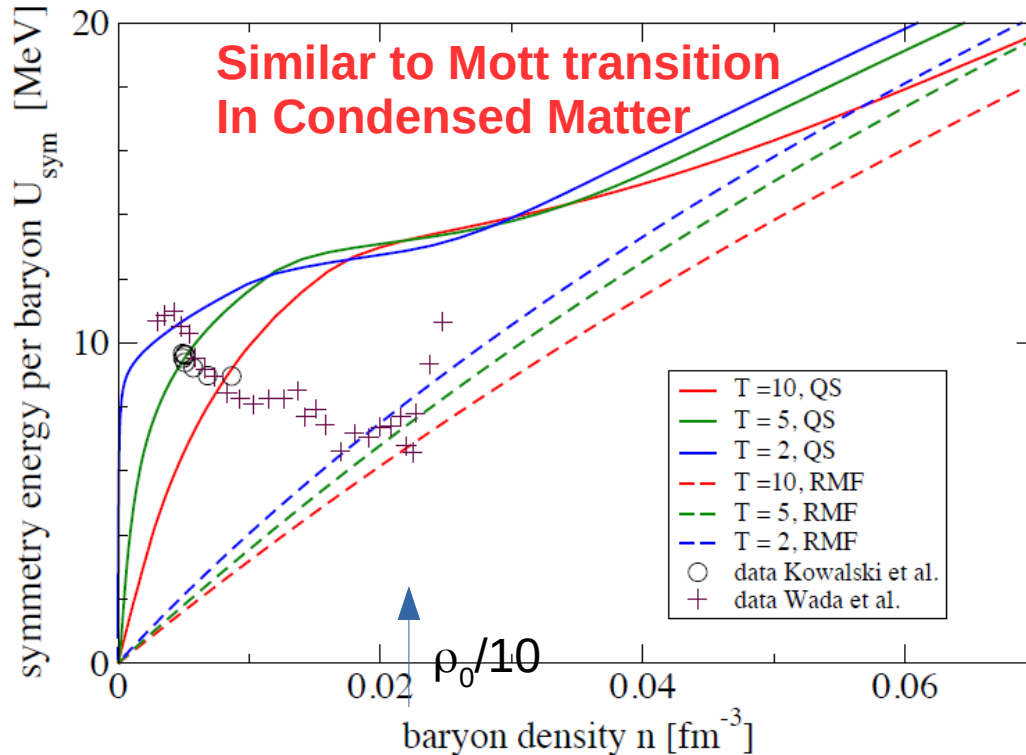
M.B. Tsang, Prog. Part.Nucl.Phys. 66, 400 (2011)
Brown, Phys. Rev. Lett. 85, 5296 (2001)



$$S(\rho) = S_K(\rho/\rho_0)^{2/3} + S_i(\rho/\rho_0)^\gamma$$

Symmetry energy for $\rho \ll \rho_0$

Prediction for the nuclear EOS : symmetry energy at subsaturation density ($\rho < \rho_0/10$) and finite temperature ($T=1-10$ MeV)



Data versus

- Relativistic Mean Field (RMF without cluster)
- Quantum Statistical Model (QSM)

K. Hagel, J.B. Natowitz, G. Röpke
Eur. Phys. Journal A **50** (2014) 39

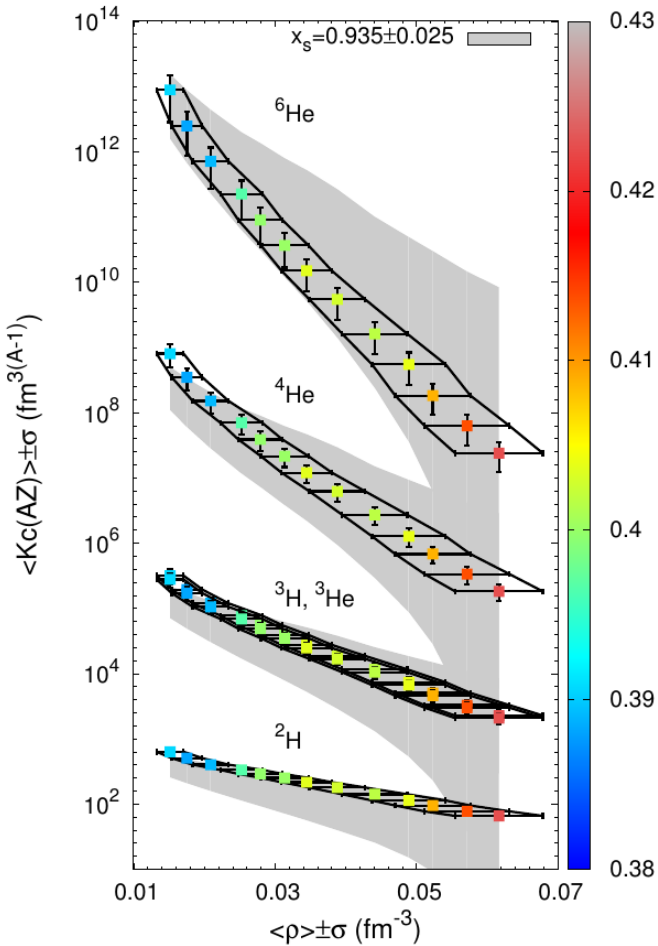
S. Kowalski, *et al.*, PRC **75**, 014601 (2007)
R. Wada, *et al.*, PRC **85**, 064618 (2012)



Relativistic Mean field (no clusters): linear decrease of E_{sym}
QSM : formation of clusters leads to an increase of E_{sym} at (very) low densities

In-medium cluster properties as a function of ρ, T and N/Z

In-medium properties ...



Chemical Equilibrium constants in nuclear medium:

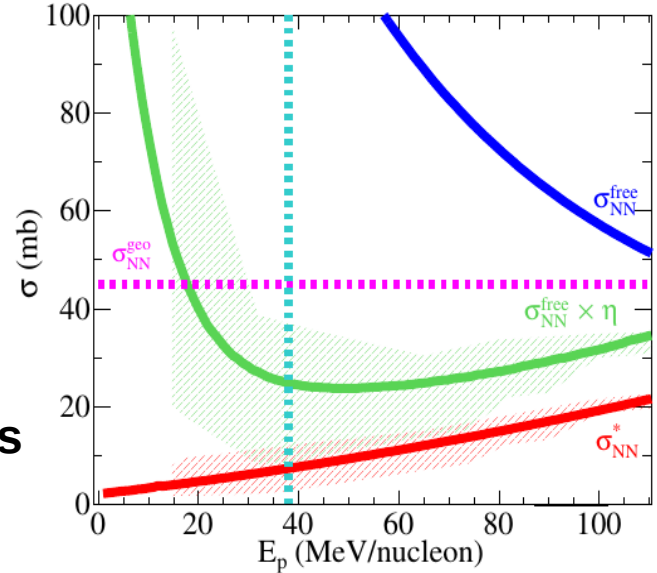
Cluster production at low density

→ **Astrophysics, CCSNe**

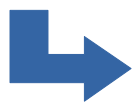
H. Pais, R. Bougault *et al.*, Phys. Rev. Lett. 125, 012701 (2020)
 R. Bougault, E. Bonnet *et al.*, J. Phys. G 47(2), 025103 (2020)
 H. Pais, R. Bougault *et al.*, J. Phys. G 47(10), 025204 (2020)

Experimental determination of σ_{NN}^* :

→ **Transport models, viscosity, effective masses**



M. Henri, O. Lopez *et al.*, Phys. Rev. C **101**, 064622 (2020)



**E818 experiment @ GANIL : ${}^{36}\text{Ar}/{}^{58}\text{Ni} + {}^{58}\text{Ni}$ à 74 MeV/nucléon
 Performed April-May 2022**

→ See A. Rebillard-Soulié's poster

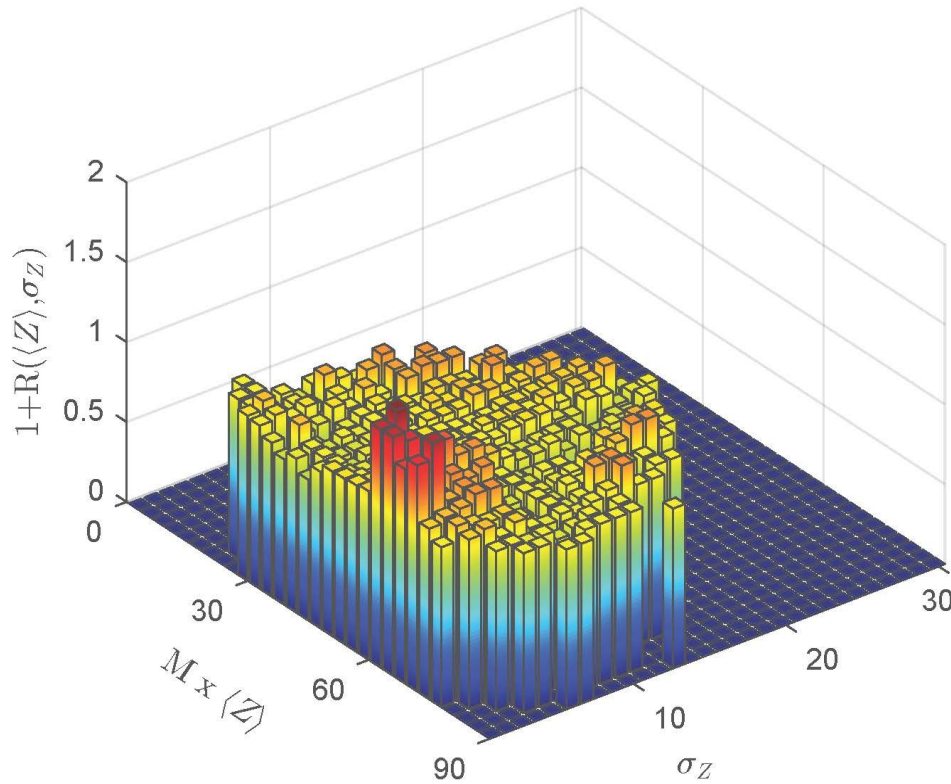


Spinodal decomposition: isoscalar vs isovector instabilities

Same analysis done for *central* events

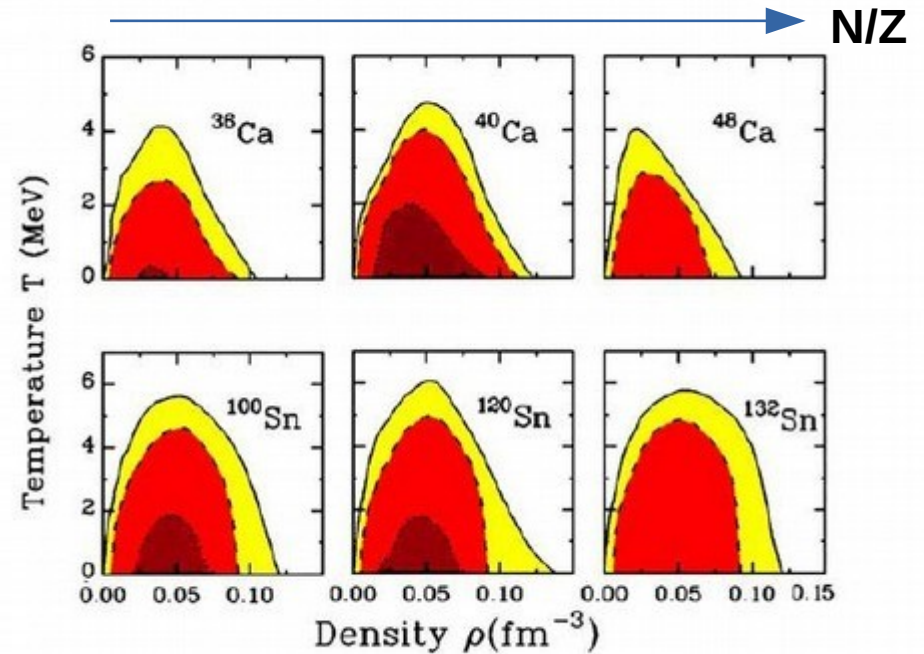
$^{124}\text{Xe} + ^{112}\text{Sn}$ @ 32A,45A MeV
 $^{136}\text{Xe} + ^{124}\text{Sn}$ @ 32A,45A MeV

B. Borderie *et al.*
(INDRA Coll.)
PLB 782 (2018)



Spinodal instabilities are indeed reduced in neutron-rich matter !

Spinodal region is reduced



Better with size correlations (A)

- **Equal-sized** fragments are **over-produced**
- Statistical confidence is **largely enhanced** (10x statistics) to overcome the **5 σ limit** ...

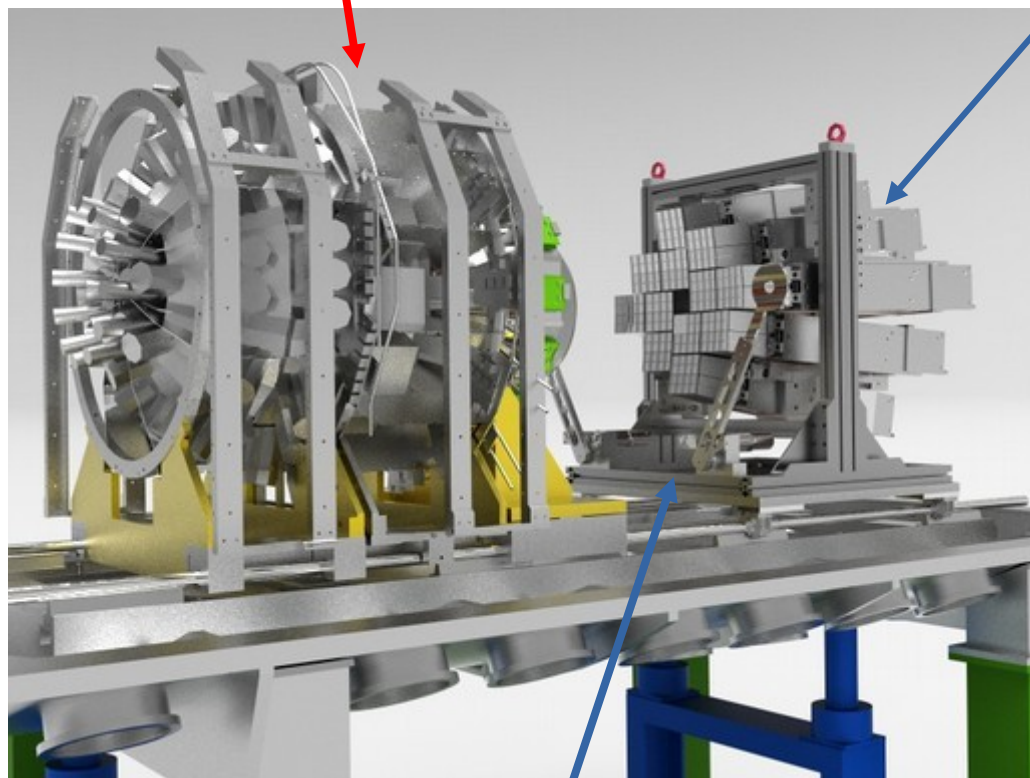
Experimental tools
and
instrumentation

Coupling FAZIA demonstrator with INDRA@GANIL

$^{58/64}\text{Ni} + ^{58/64}\text{Ni}$ @ 32 and 52 MeV/nucl : E789 performed in 2019

INDRA in D5

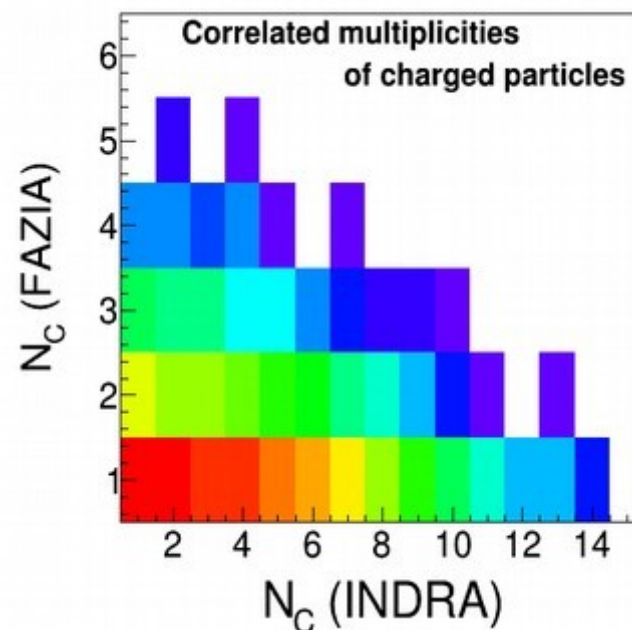
- 240 detection modules (rings 1,2/3,4/5 removed)
- 96 Si-CsI from 16 to 45 deg.
- 144 CsI from 45 to 176 deg.



FAZIA demonstrator: 12 blocks of 16 telescopes
192 High-Quality Si-Si-CsI telescopes
from 2 to 14 deg. + dedicated Full Digital Electronics

FAZIA geom. acceptance 82% (90%)
Granularity x2 as compared to INDRA

Beam Tests in June-July 2018

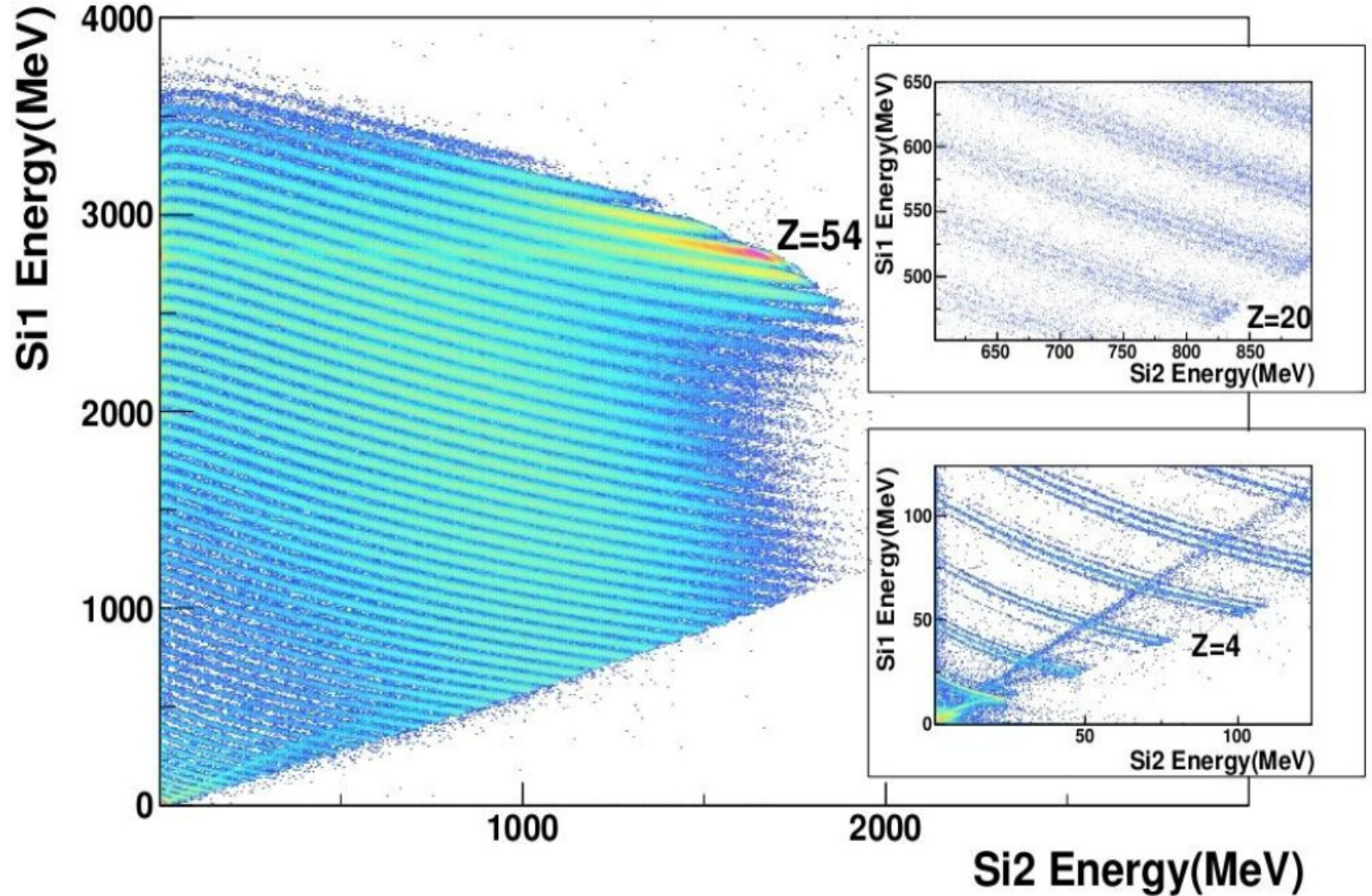
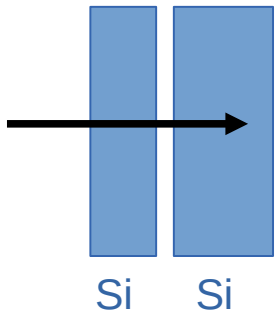


Experiment E789 performed at GANIL
in April-May 2019 :

$^{58/64}\text{Ni} + ^{58/64}\text{Ni}$ @ 32,52 MeV/nucleon

FAZIA : ΔE -E identification

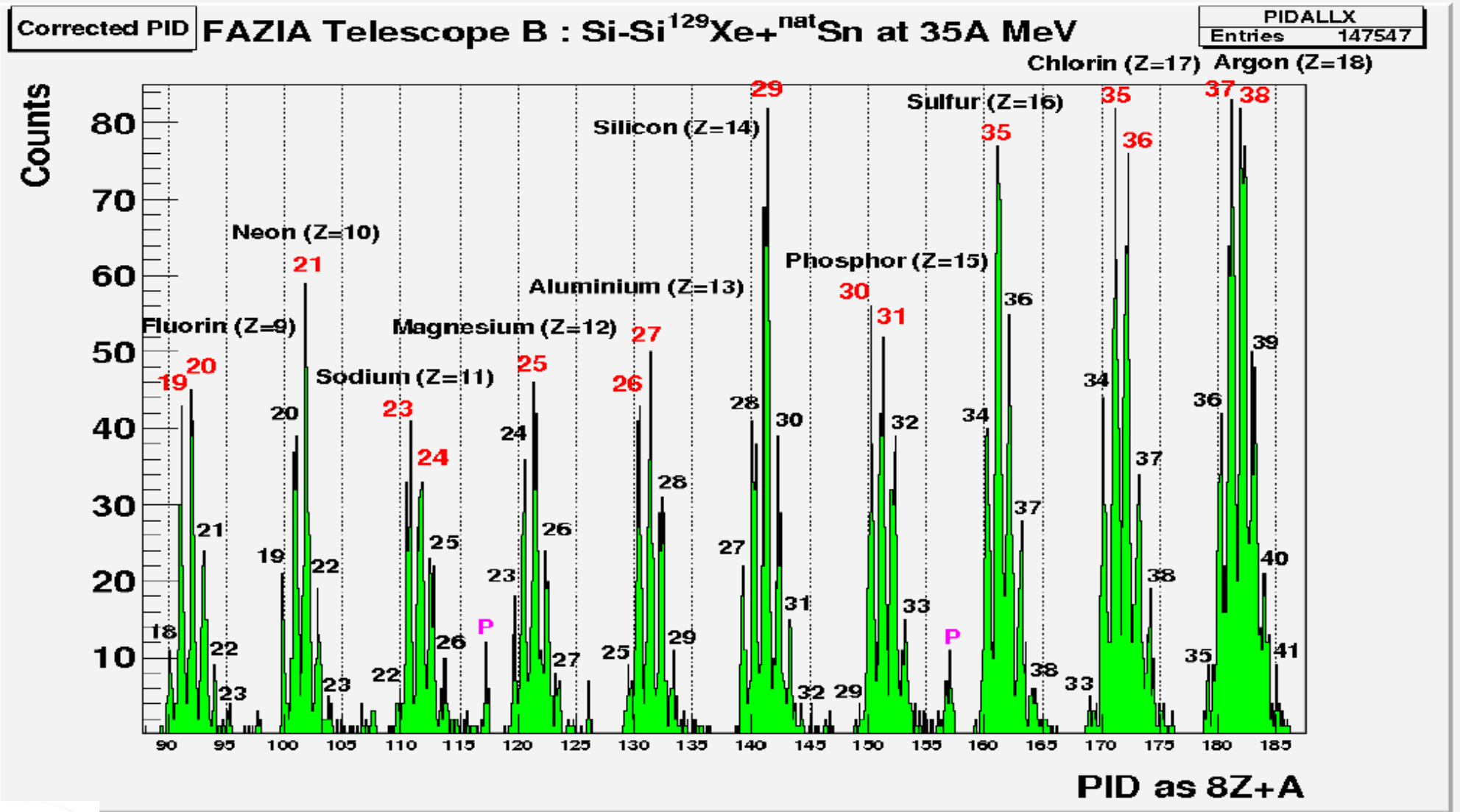
Some results at the end of phase 1: $\Delta E(\text{Si1}) - E(\text{Si2})$



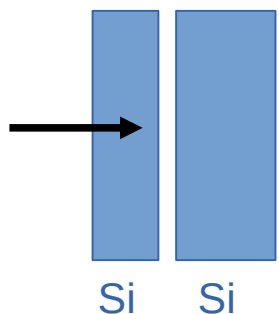
S. Carboni et al., NIMA 664 (2012) 251 Energy = max of shaped signal (trapezoidal filter)

FAZIA improvements for ΔE - E identification

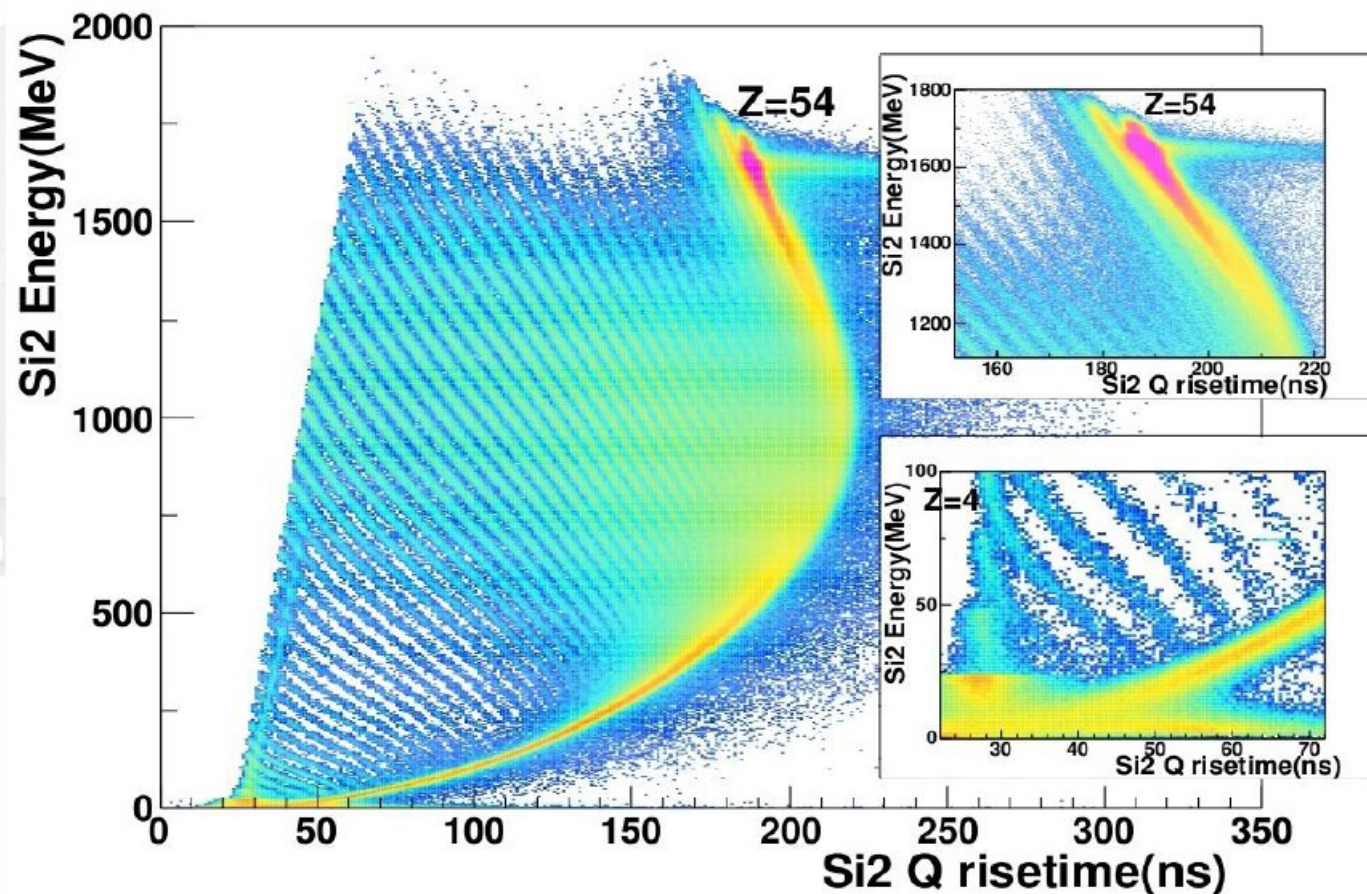
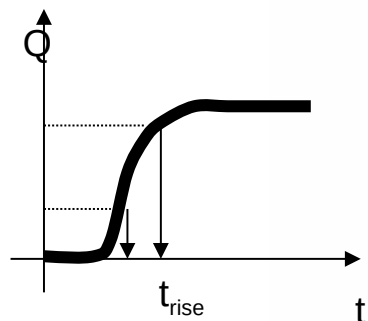
Improving standard E - ΔE identification method up to $Z=25-30$!



FAZIA : Pulse Shape Analysis

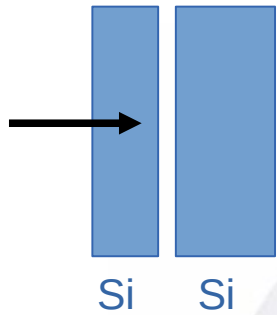


**Some results at the end of phase 1:
Pulse Shape Analysis from E – Charge Rise Time**



S.Carboni et al., NIMA 664 (2012) 251

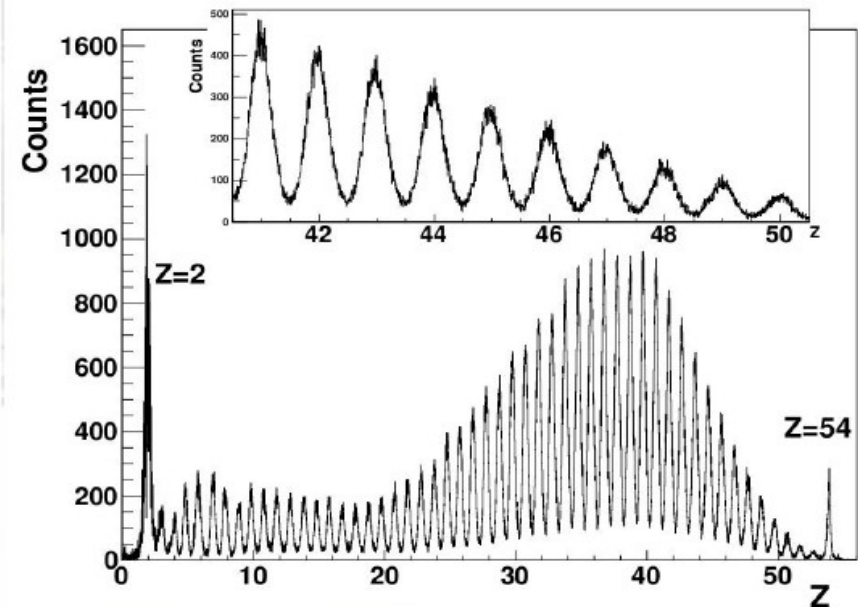
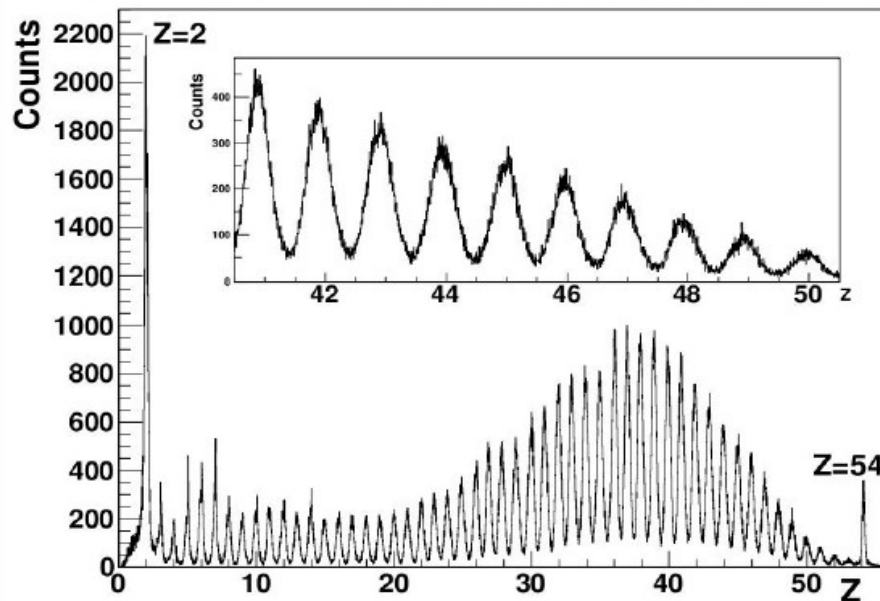
FAZIA : Pulse Shape Analysis



**Some results at the end of phase 1:
Particle Identification from Pulse Shape Analysis**

Energy vs. charge rise time

Energy vs. maximum of current signal

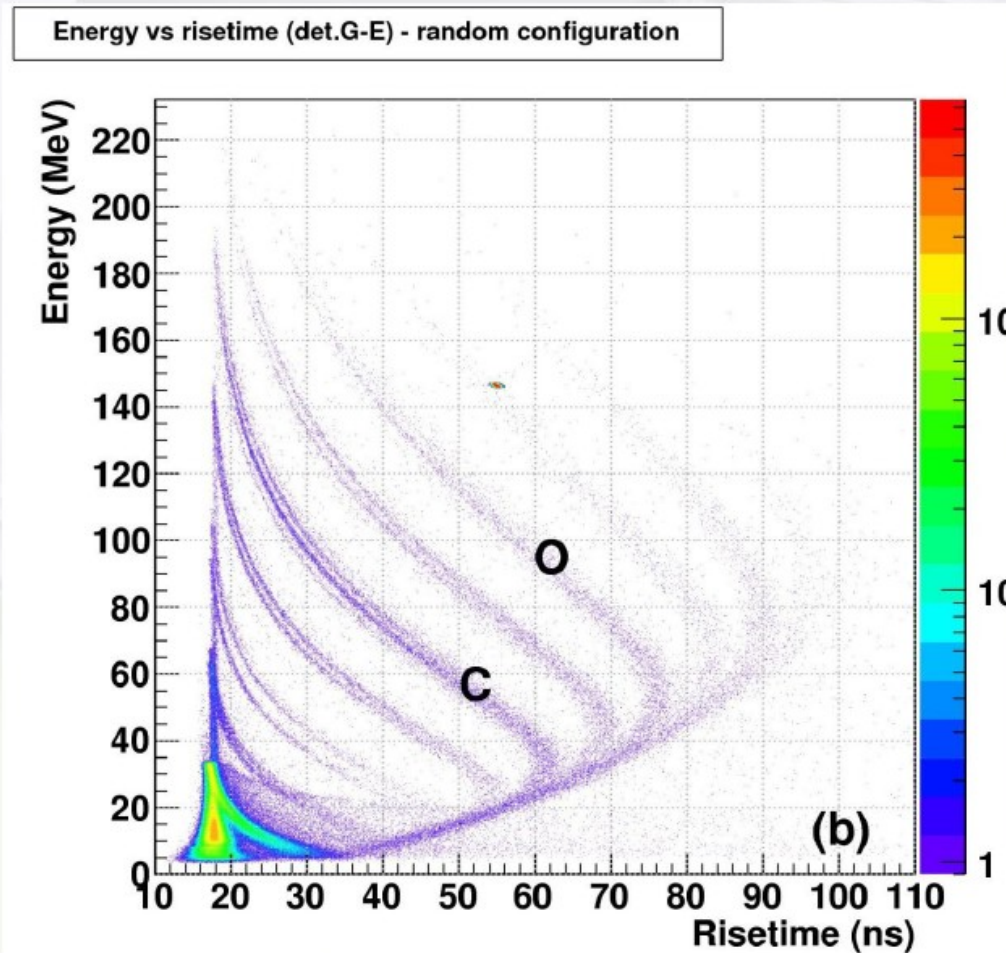
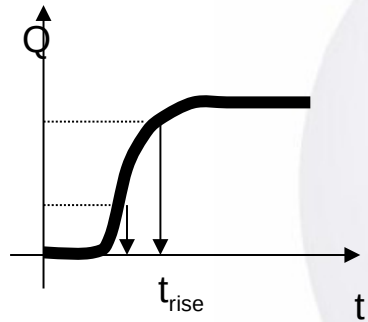


➤ Z identification can be achieved in the **first Silicon** detector

S. Carboni et al., NIMA 664 (2012) 251

FAZIA : Pulse Shape Analysis

Some results at the end of phase 1: Mass resolution from Pulse Shape Analysis Energy vs. charge rise time

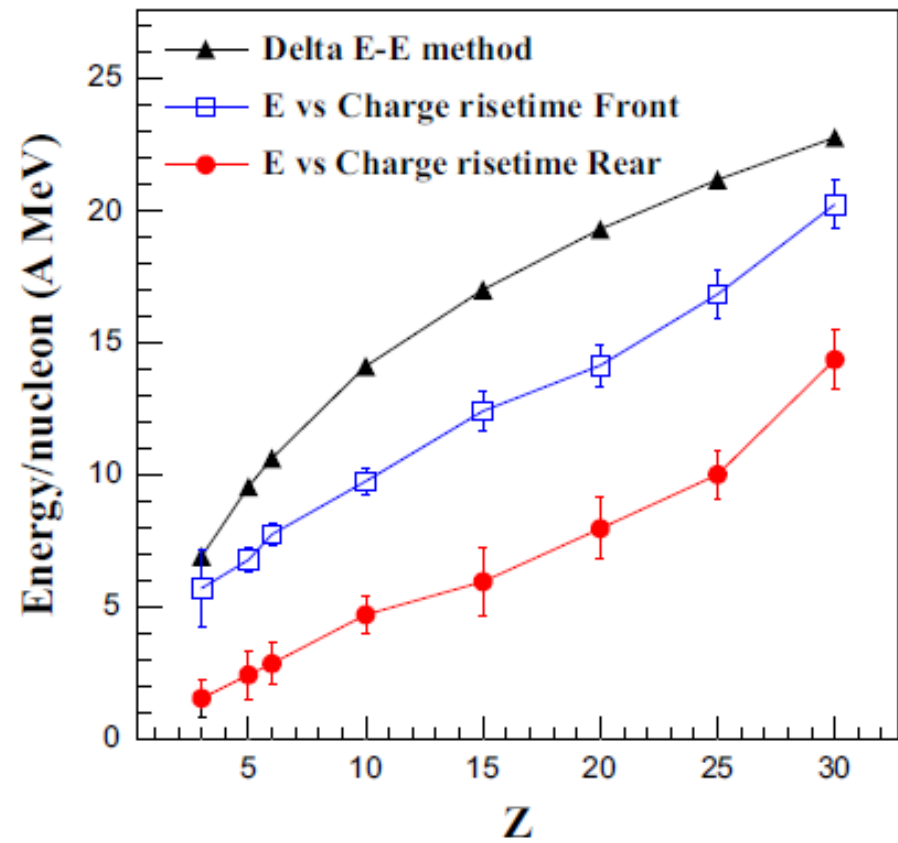
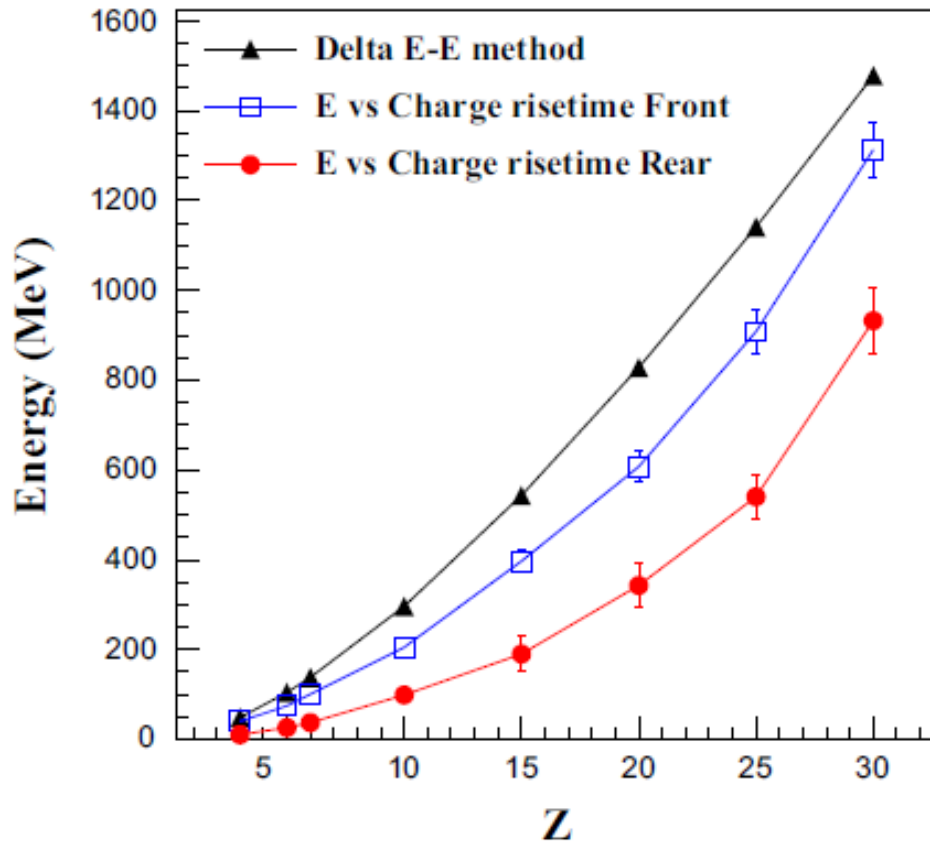


High gain
 ^{32}S beam@473MeV

L.Bardelli et al., NIMA 654 (2011) 272

➤ Isotopic identification for $Z=3-8$

FAZIA : ID thresholds (Z)

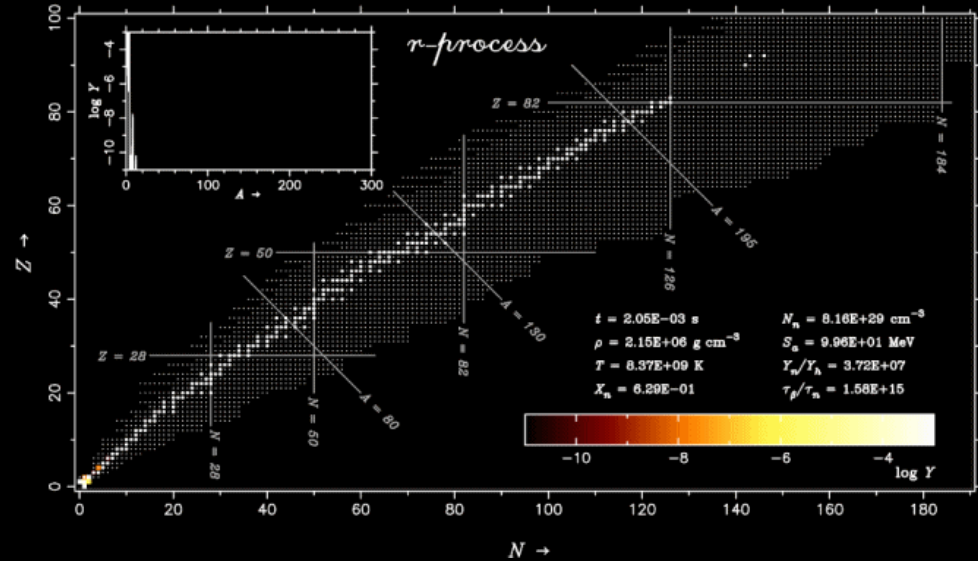
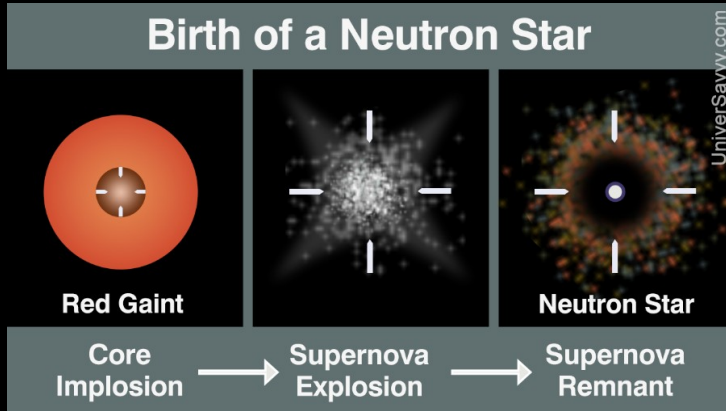


- **Pulse Shape Analysis** lowers significantly the Z (and A) thresholds
- **Rear-side** injection (low Electric Field entrance) is preferred
- « **dead** » range in Silicon is between **30** and **150 μm** for **Z=30**

N. Le Neindre *et al.*, NIM A 701(2013) 145–152

Nuclear EOS in Astrophysics

Neutron Stars (NS) are unique systems for investigating dense nuclear matter !



B.P. Abbott *et al.* (LIGO/VIRGO),
PRL **116**, 061102 (2016)
PRL **119**, 161101 (2017)

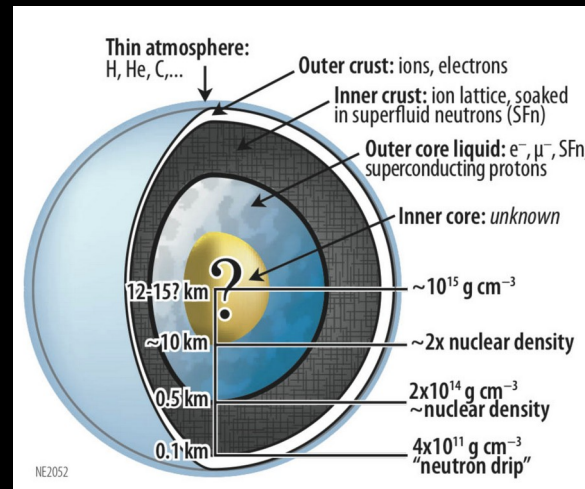
Detection of GW and multi-messenger observables (GW170817) considerably reinforces terrestrial EOS studies

Core Collapses Sne

- EoS (isoscalar/isovector) : shock waves
- E_{sym} : r-process and nucleosynthesis
- Cooling : d-URCA and Neutrinosphere (low density nuclear matter)

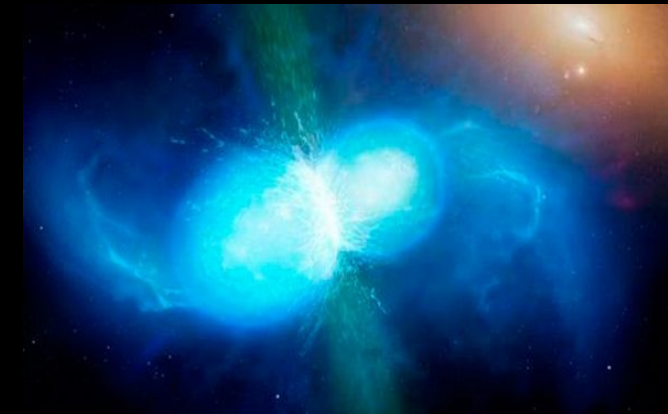
NS structure :

- Crust : pasta phases (frustration/clusters)
- Crust/Core transition: L, K_{sym}
- Core : hyperons (strange matter, QCD)



N. Yunes, M. Coleman Miller, and K. Yagi,
Nature Review Physics **4**, 237 (2022)

NS- NS merger (Kilonova)



Conclusions

Large diversity of reaction mechanisms between 5 – 100 MeV/nucleon

Produce many different nuclear systems :

- in terms of ρ , E^* , T , J , δ
- variety of conditions for the EOS characterization

Allow the production and study of exotic nuclei :

- direct/transfer reactions: probing effective interactions in nuclei, quantum shells
- multi-nucleon transfer and deep inelastic scattering : toward large N/Z excursion
- multifragmentation : phase transitions, order, latent heat and criticality
- complete/incomplete fusion : toward superheavy nuclei

Mimick violent phenomena in Astrophysics of compact objects :

- Core Collapse of Supernovae: CCSNe
- Neutron stars mergers + multi-messenger astrophysics (GW+EM): NS-NS, X-ray bursts
- Stellar and extra-stellar nucleosynthesis: r-, p-,s-processes

Investigate EOS at low density and phase transitions in strongly corr. systems :

- EOS at low densities
- Density and Isospin Instabilities: LG coexistence regions, spinodal decomposition
- finite (nuclei) vs infinite (NS): finite-size effects

Some references

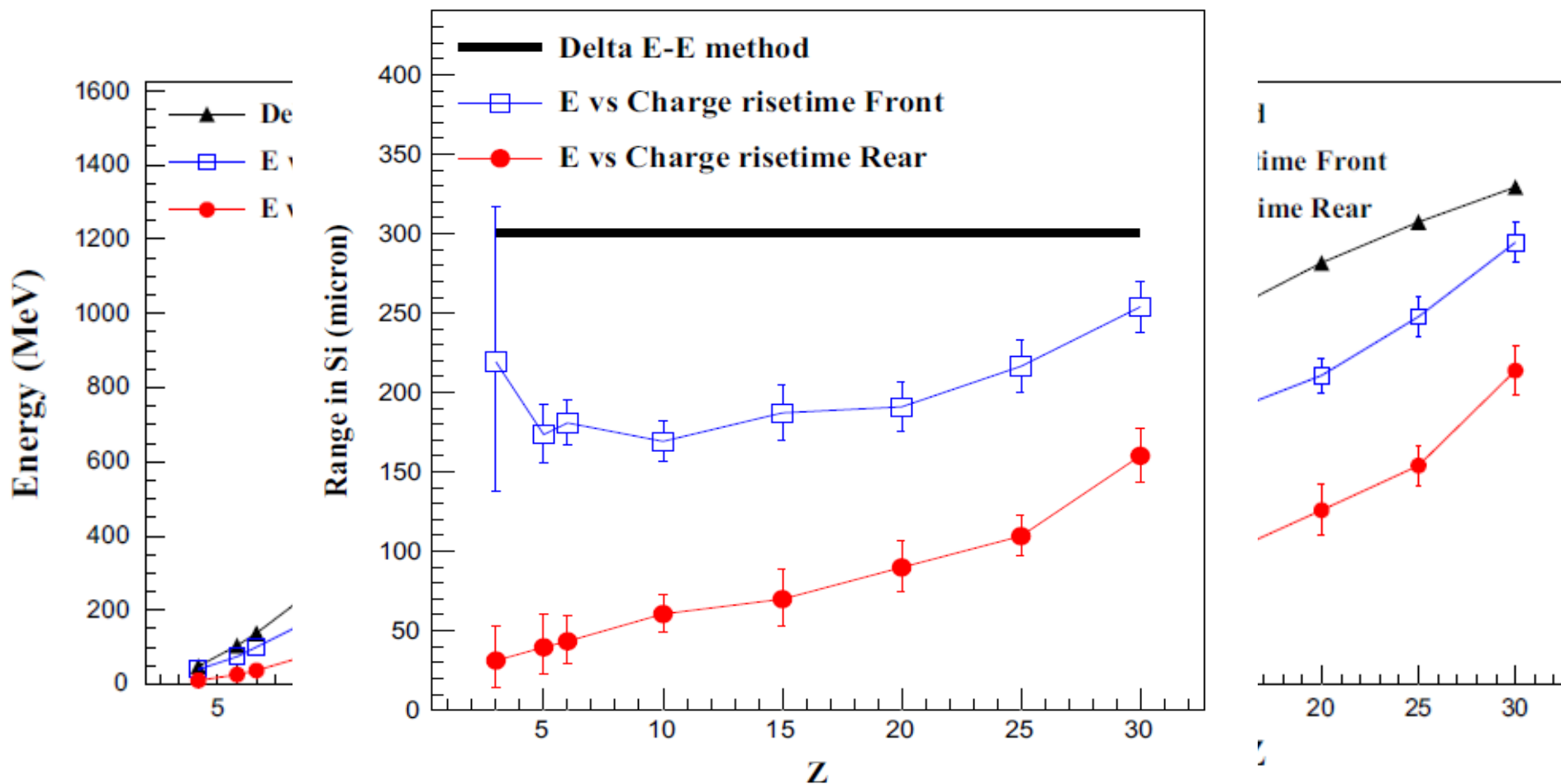
- D. Durand, B. Tamain, and E. Suraud, *Nuclear Dynamics in the Nucleonic Regime* (Institute of Physics), New York, 2001
- F. Gulminelli, W. Trautmann, S. J. Yennello, and Ph. Chomaz, *Dynamics and thermodynamics with nuclear degrees of freedom*, Eur. Phys. J. A 30, 1 (2006).
- Ph. Chomaz, M. Colonna, and J. Randrup, *Mean-Field instabilities in the Fermi energy regime*, Phys. Rep. 389, 263 (2004)
- B. Borderie *et al.*, Prog. in Part. Sci. and Nucl. Phys. 61, 551 (2008)
- R. Bougault *et al.* (FAZIA Collaboration) Eur. Phys. J. A 50 (2014) 47

More infos and also scientific outreach contents :

<https://www.lpc-caen.in2p3.fr/en/lpc-caen/>



FAZIA : ID thresholds (Z)

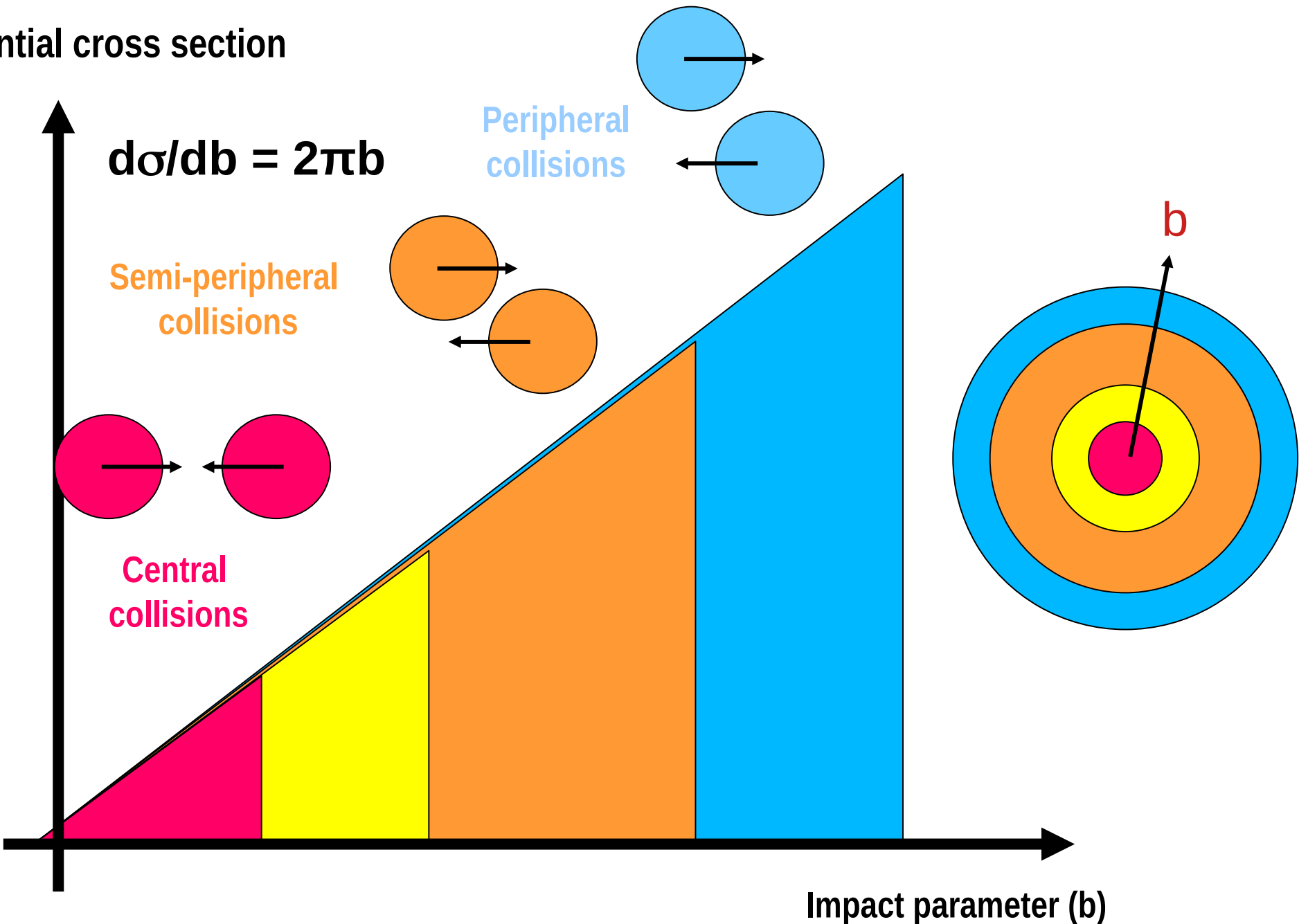


- **Pulse Shape Analysis** lowers significantly the Z (and A) thresholds
- **Rear-side** injection (low Electric Field entrance) is preferred
- **Dead layer** in Silicon is between **30** and **150 μm** for **Z=30**

N. Le Neindre *et al.*, NIM A 701(2013) 145–152

Nuclear reactions : playing darts ...

Differential cross section



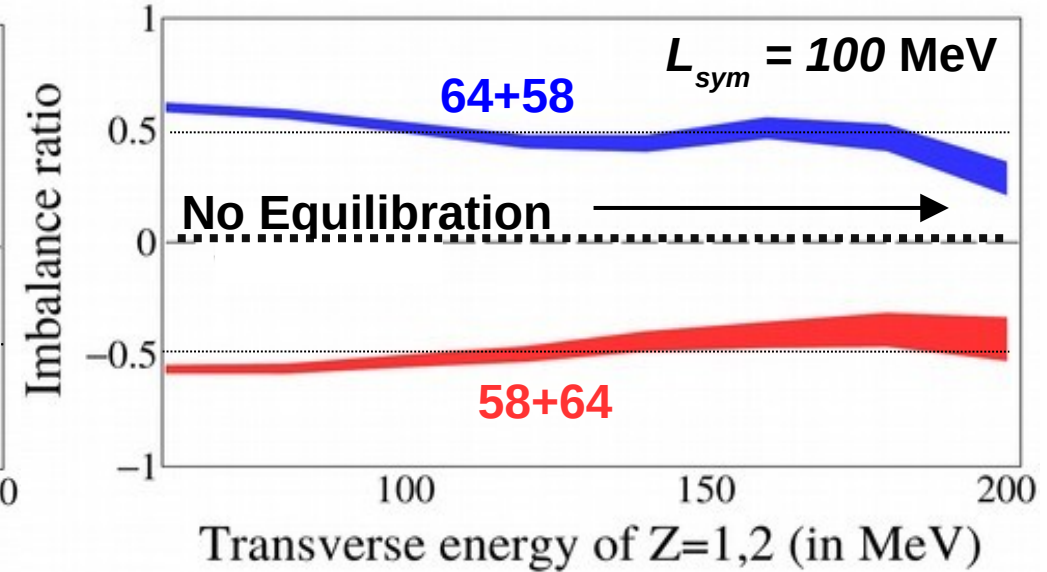
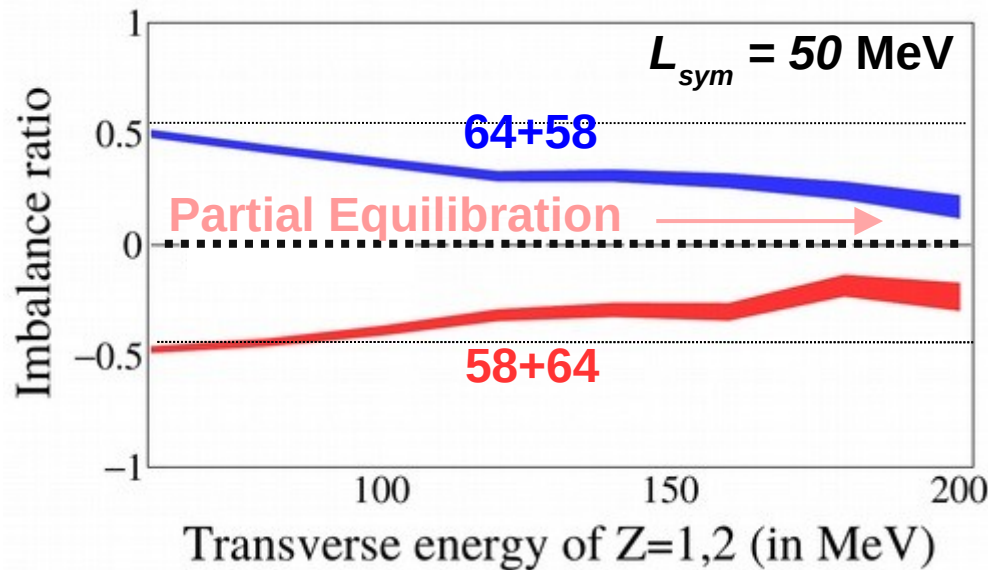
DDSE: toward new probes, isospin imbalance ratio

AMD+GEMINI++ filtered simulations : 2.10^6 events

Imbalance ratio R for $\delta_{PLF} = (N_{PLF} - Z_{PLF})/A_{PLF}$

$$R_x = (2X - X_1 - X_2)/(X_1 - X_2)$$

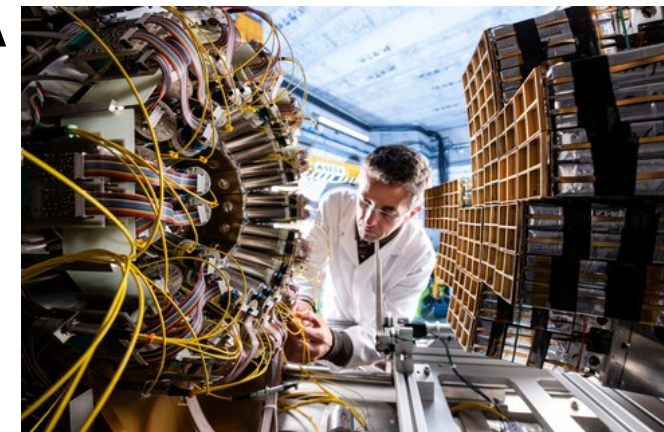
$^{58,64}\text{Ni} + ^{58,64}\text{Ni}$ @ 32A MeV



Transverse energy of Z=1,2 : measured by INDRA
N/Z of PLF : measured by FAZIA

E789 : results coming soon !

→ See J. Lemarié's poster



End of lecture II

Nucleosynthesis

Abundance
of elements
in the Universe

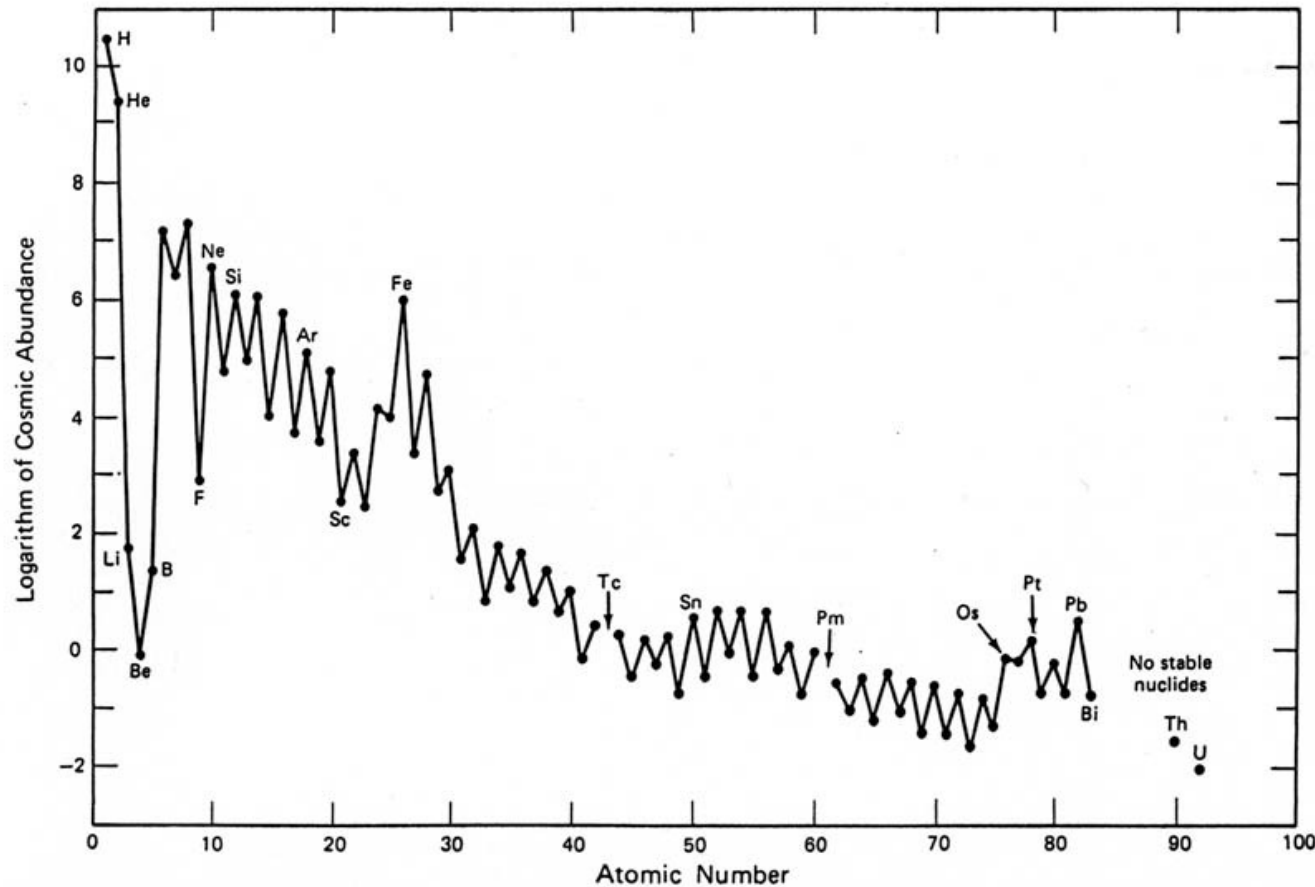


Figure 2.4 Plot of the abundances of the elements in the solar system versus their atomic number. The abundances are expressed as the logarithm of the number of atoms of each element relative to 10^6 atoms of silicon. (Data are listed in Table 2.2 after Anders and Ebihara, 1982.)

Nucleosynthesis : different origins

Abundance of elements in the Universe

Primordial Hydrogen (Big Bang)
Z=1

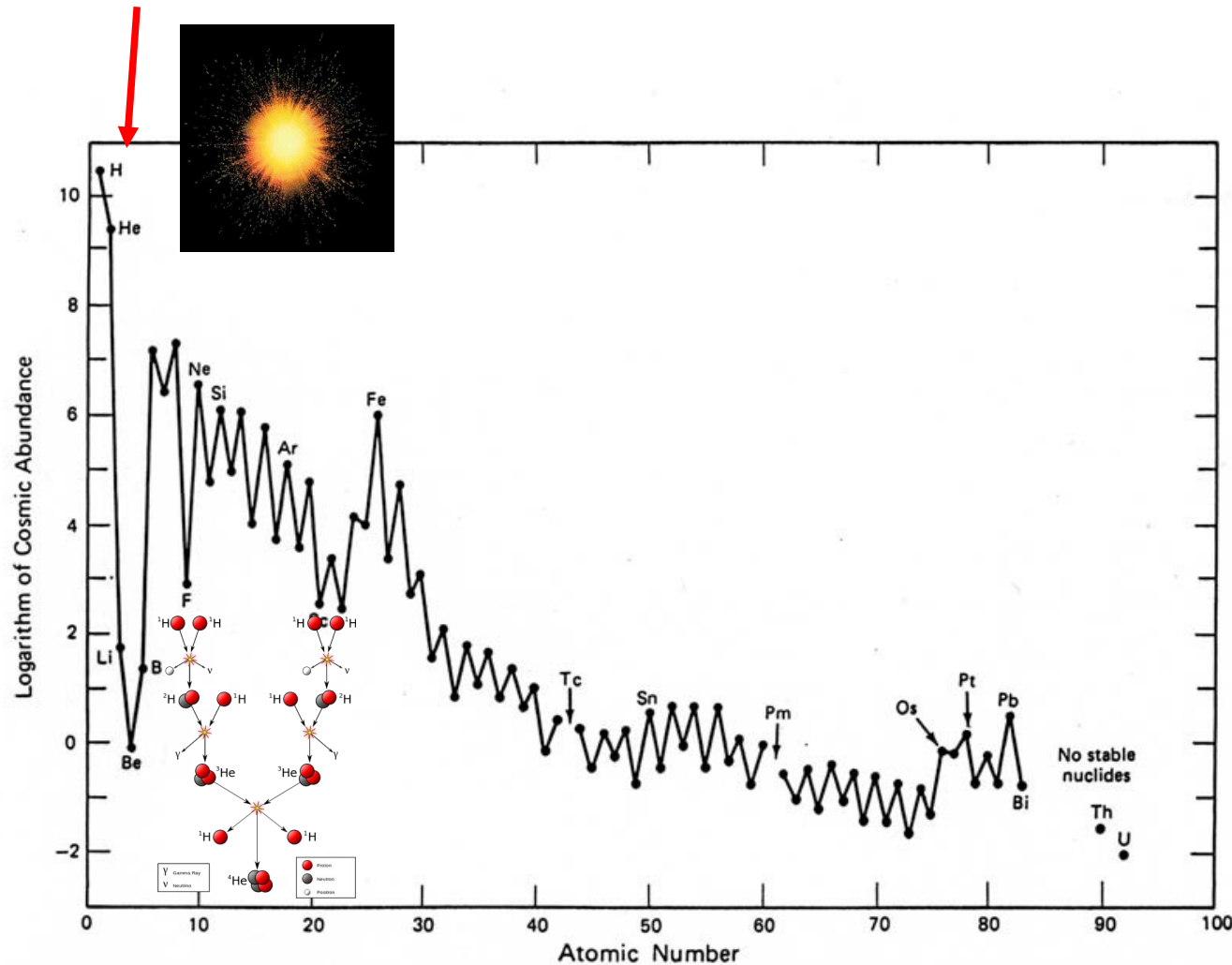


Figure 2.4 Plot of the abundances of the elements in the solar system versus their atomic number. The abundances are expressed as the logarithm of the number of atoms of each element relative to 10^6 atoms of silicon. (Data are listed in Table 2.2 after Anders and Ebihara, 1982.)

Nucleosynthesis : different origins

Abundance of elements in the Universe

Primordial Hydrogen (Big Bang)
Z=1

Stellar synthesis
Z=2-26

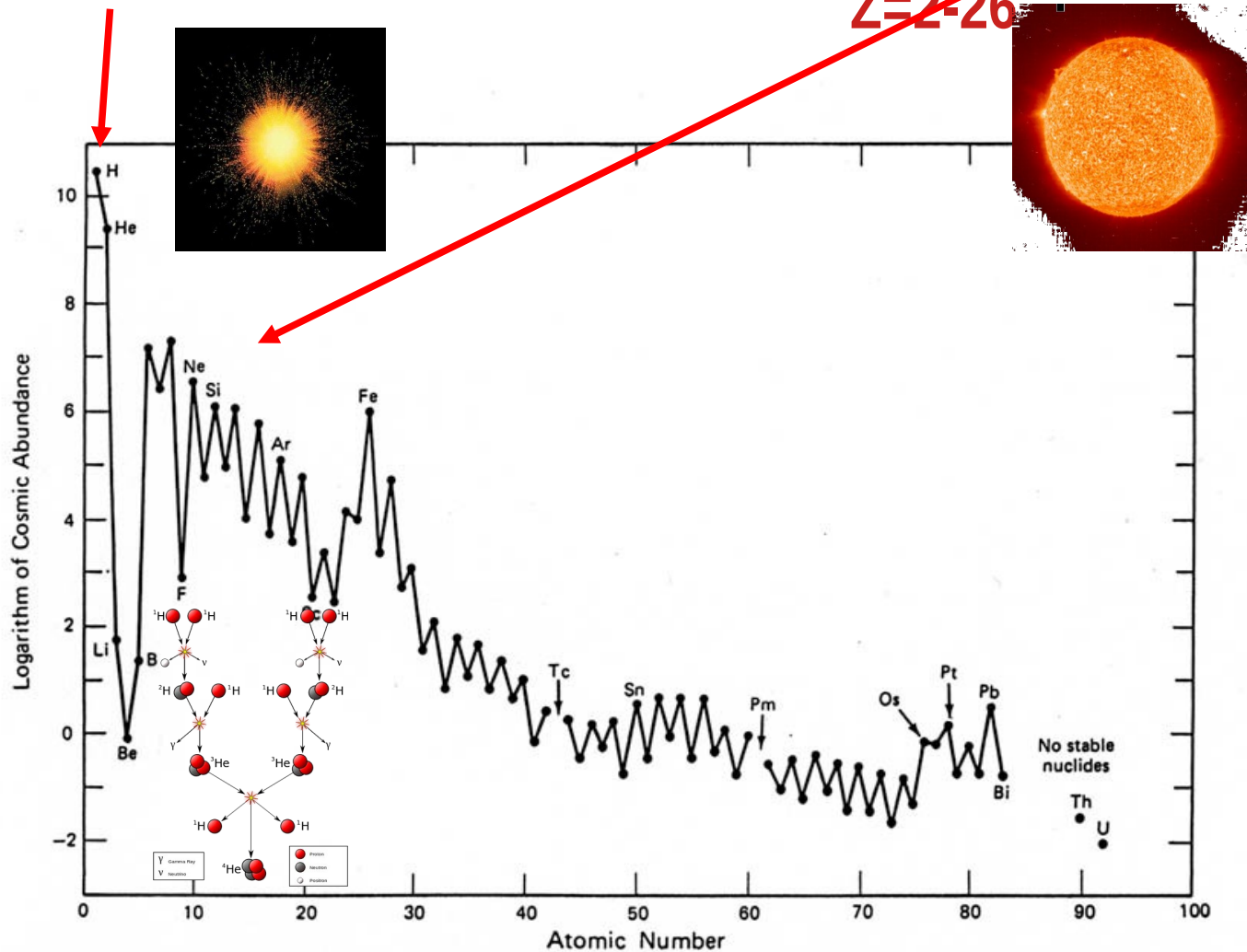


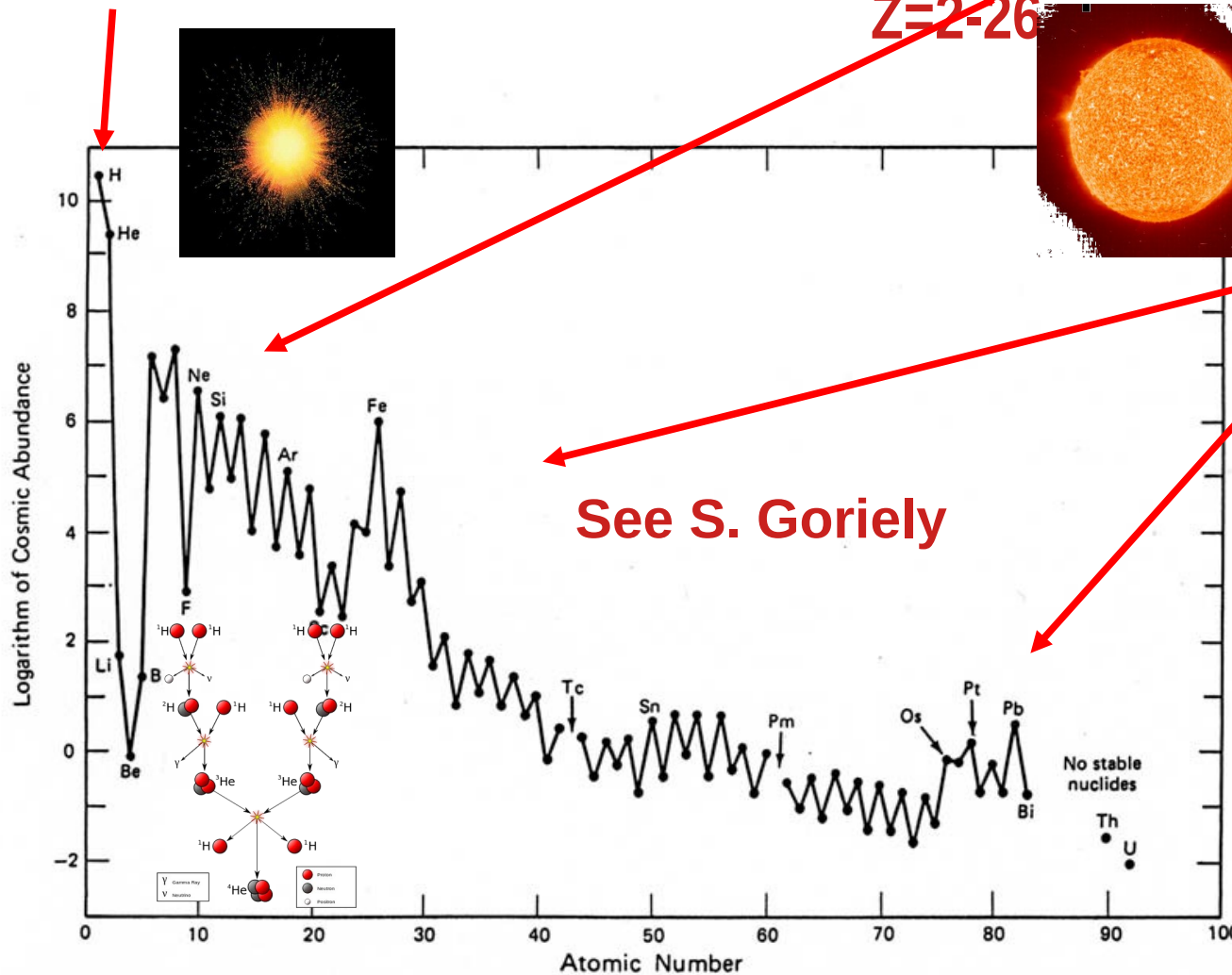
Figure 2.4 Plot of the abundances of the elements in the solar system versus their atomic number. The abundances are expressed as the logarithm of the number of atoms of each element relative to 10^6 atoms of silicon. (Data are listed in Table 2.2 after Anders and Ebihara, 1982.)

Nucleosynthesis : different origins

Abundance of elements in the Universe

Primordial Hydrogen (Big Bang)
Z=1

Stellar synthesis
Z=2-26



See S. Goriely

Extra-stellar processes
r/s/p-processes
in supernovae
and NS-NS
mergers
Z>26



Figure 2.4 Plot of the abundances of the elements in the solar system versus their atomic number. The abundances are expressed as the logarithm of the number of atoms of each element relative to 10^6 atoms of silicon. (Data are listed in Table 2.2 after Anders and Ebihara, 1982.)

Novae & Supernovae

$E=10^{44}$ J , $L \times 10^{10}$!!



Nova Monocerotis V838, Licorne
May - December 2002
Hubble Telescope (NASA)

$E = 10^{38}$ J , $L \times 1000$!



Crab Nebula (M1) - 1054
Hubble Telescope (NASA)